UNIVERSITÀ DEGLI STUDI DI MILANO

Ph.D. in Pharmacological Biomolecular Sciences, Experimental and Clinical

XXXV cycle

Department of Pharmacological and Biomolecular Sciences

Heterogeneity of latency establishment in different human CD4+ T cell subsets stimulated with Interleukin-15

SSD BIO/19

Giacomo Maria Butta

Matricola: R12608

Ph.D. Tutor: Raffaele De Francesco

Ph.D. Co-Tutor: Lara Manganaro

Ph.D. School coordinator: Giuseppe Danilo Norata

UNIVERSITÀ DEGLI STUDI DI MILANO

A.Y. 2021/2022

4 8 15 16 23 42

English Abstract

The Human Immunodeficiency Virus (HIV) integrates its genome into the host DNA and persists for the lifetime of the infected cell. Even in the presence of an efficacious Highly Active Anti-Retroviral Therapy (HAART) treatment, a pool of latently infected cells persists and reactivates to produce viral particles if antiretroviral therapies are stopped or discontinued. This so-called latent reservoir is established mainly in CD4+ T memory ad naïve cells early during infection under conditions that are still not well defined. CD4+ T memory lymphocytes are highly heterogeneous and comprise both effector and long-lived subsets. This study aimed to analyze HIV latency establishment at the subset level in *ex vivo* primary CD4+ T cells stimulated with Interleukin-15 (IL-15) to mimic the pathophysiological conditions of the *in vivo* establishment during the early phases of infection. To do that, we used the dual-reporter virus HIV-GKO, which bears two different fluorescent reporters, one under the control of the HIV-LTR promoter and one under the control of a constitutive cellular promoter thus allowing the discrimination between transcriptionally silent infected cells and transcriptionally active infected cells. We demonstrated that HIV preferentially infects the more differentiated Central Memory (T_{CM}), Transitional Memory (T_{TM}) and Effector Memory (T_{EM}) subsets. However, the less differentiated naïve and Stem-Cell Memory (T_{SCM}) subsets were enriched in latency, suggesting that the rare infection of these compartments likely ends in a transcriptionally silent integrated provirus. This phenotype was independent of differential expression of the positive transcription elongation factor b (P-TEFb) components Cyclin T1 and phospho/Cyclin-dependent kinase 9 (P/CDK9). When we analyzed the cellular distribution of the nuclear factor kappa-light-chain-enhancer of activated B cells (NF-κB) transcription factor, which is important for HIV expression, we observed that nuclear levels of NF-κB were lower in naïve compared to the other memory subsets, thus partially explaining the higher propensity of this subset to harbor a

silent provirus. On the other hand, T_{SCM} displayed NF-κB nuclear levels comparable to the other memory subsets, suggesting that other factors are responsible for the latency enrichment in this subset.

Italian Abstract

HIV integra il suo genoma nel DNA della cellula ospite, persistendo indefinitamente. Il DNA virale integrato (provirus) rimane silente in una frazione di cellule infettate, portando ad un'infezione latente. Questo reservoir è in grado di persistere anche durante la terapia antiretrovirale e di riattivarsi per produrre particelle virali qualora la terapia venisse interrotta. Il reservoir latente si forma nelle prime fasi dell'infezione acuta ed è rappresentato per la maggior parte da linfociti CD4+ naïve e di memoria. Questa popolazione altamente eterogenea è composta sia da subsets poco differenziati con caratteristiche staminali, sia da compartimenti effettori con una vita media breve, ed è considerata uno degli ostacoli verso una cura all'infezione da HIV. Lo studio descritto in questa tesi ha come obiettivo quello di analizzare la formazione del reservoir latente in *ex vivo* nei vari subsets di linfociti CD4+ stimolati con IL-15, una citochina upregolata durante la fase acuta dell'infezione. Per discriminare cellule latenti e produttive, abbiamo utilizzato un virus dual-reporter chiamato HIV-GKO che codifica per un fluoroforo sotto il controllo di un promotore cellulare ed uno sotto il controllo del promotore virale LTR. I dati raccolti dimostrano come HIV infetta principalmente i subsets di memoria più differenziati T_{CM}, T_{TM} e $T_{EM,}$ mentre le naïve e le T_{SCM} si dimostrano largamente refrattarie all'infezione. Ciononostante, questi due subset meno differenziati, se infettati, tendono a sviluppare un'infezione latente data dall'assenza di attività trascrizionale provirale. Questo fenotipo non è causato da un'espressione differente del complesso trascrizionale P-TEFb composto da Ciclina T1 e P/CDK9. Al contrario, analizzando la localizzazione di NF-κB, il subset di naïve ha dimostrato di avere livelli nucleari del fattore trascrizionale più bassi se comparati con quelli registrati nei subsets di memoria, suggerendo come la scarsa disponibilità di NF-κB potrebbe spiegare la propensità di questo subset ad ospitare un'infezione latente. Le T_{SCM}, invece, hanno mostrato livelli di NF-κB nucleare

comparabili a quelli degli altri subsets di memoria, suggerendo come la tendenza alla latenza in questo subset debba essere spiegata da altri fattori.

Summary

Chapter 1 – Introduction

The Human Immunodeficiency Virus

The Human Immunodeficiency Virus (HIV) is a member of the *Retroviridae* family and *Lentivirus* genus. It is the etiological agent of acquired immunodeficiency syndrome (AIDS), a condition characterized by the progressive loss of CD4+ T lymphocytes. These cells play a pivotal role in orchestrating the immune response against pathogens. If not treated, the loss of CD4+ T cells causes severe immunodeficiency and the host succumbs to opportunistic infections. The HIV pandemic is one of our time's defining public health crises: worldwide more than 38 million people live with HIV/AIDS[1].

This condition was first described in 1981 by a team of US clinicians who reported the occurrence of rare *Pneumocystis* pneumonia (PCP) in five young gay men living in Los Angeles. Soon after the publication in the *Morbidity and Mortality Weekly Report*, other opportunistic infection observations were reported in New York City, San Francisco and Atlanta, raising concerns about the spread of a new infectious disease[2].

Since its discovery, HIV has infected more than 80 million people and until the development and introduction of the highly active antiretroviral therapy (HAART) in 1995, AIDS was the major cause of death in the USA for men aged 25-44[3]. Since then, the high efficacy of HAART has drastically reduced AIDS-related deaths globally and the therapy availability has reached 70% of People Living with HIV (PWHIV), that adhere to the therapy daily.

The *Lentivirus* genus consists of two different, but closely related HIV viral species: HIV-1 and HIV-2. HIV-1 is the cause of most infections worldwide and has spread to all five continents. HIV-1 is further classified into four groups (M, N, O and P) that emerged from four different spillover events from apes (chimpanzees and

gorillas) to humans[4]. Only the HIV-1 group M has spread globally and has evolved rapidly to produce many different subtypes (defined by the letters A, B, C, D, F, G, H, J and K). The first HIV-1 isolate was obtained at the Institute Pasteur in Paris in 1983[5]. HIV-2 has been discovered in 1986 and is the product of at least nine spillover events from sooty mangabeys Simian Immunodeficiency viruses (SIVs)[6,7]. HIV-2 is endemic in West Africa, has a reduced pathogenicity and is believed to infect less than 1 million individuals in this area[8]. Although the virion structure is almost identical for both viruses, the nucleotide and amino acid homology is 60% for the *gag* and *pol* genes and less than 40% for *env* and the accessory protein genes[9]. The main difference in the genome of the viruses is the lack of the *vpu* gene in HIV-2, which is replaced by *vpx*. Of note, *vpu* and *vpx* have different functions during infection: while vpu main function is the counteraction of the restriction factor BST2/tetherin, vpx overcomes SAMHD1 restriction allowing efficient HIV-2 infection of dendritic cells and macrophages[10–13].Of note, HIV-1 will be the focus of all the experiments and discussions in this manuscript.

Both HIV-1 and HIV-2 are the product of zoonotic events from wild African non-human primates' SIVs. Throughout the 20th century, a series of events took place to favor the spread of HIV-1 into the human population. Economic, political and societal changes have contributed to the migration of the virus from the spillover areas in Africa to Haiti, the United States of America (USA) and the rest of the world. Phylogenomic analysis performed on archival infected blood samples dated the most recent common ancestor of HIV-1 group M around 1920 in the area of what is now Kinshasa (Leopoldville at the time), Democratic Republic of Congo, where the highest genomic diversity has been recorded[14]. The cross-species events instead took probably place in the Southeastern part of Cameroon, where hunting of SIV-infected primates was common. The virus then escaped from Africa and arrived in Haiti in the late 1960s. Molecular clock analysis of the *env* gene then confirmed the

circulation of the virus in the USA for all of the 1970s, until AIDS was recognized in 1981[15].

After 40 years of intense scientific research and many life-changing improvements in the quality of living of PWHIV (of note, Highly Active Anti-Retroviral Therapy, HAART), there is still no vaccine for the infection nor a complete cure (so-called "sterilizing"). Only three individuals have been declared free from HIV virus. All these remarkable cases are ART-treated patients (known as the Berlin, London and Düsseldorf patients) who developed acute myeloid leukemia and underwent an allogenic CCR5Δ32/Δ32 hematopoietic stem cell transplantation (HSCT)[16–19], followed by HAART interruption and no viral rebounds. The transplanted cells lack a functional CCR5 coreceptor used by HIV-1 to enter cells, conferring resistance to HIV-1. This procedure is highly invasive and relies on *in vivo* T cell depletion and graft-versus-host disease prophylaxis using immunosuppressive agents in the recipient patient. For these reasons, it is currently deployed for a small group of PWHIV who develop leukemia. Nevertheless, HIV can be controlled by modern antiretroviral regimens or, in some rare cases, by the immune system (elite controllers). HAART inhibits the active replication of the virus by blocking multiple steps of its life cycle. However, it demands complete adherence for the rest of the life, and most importantly it does not eradicate the virus from an infected individual. If a patient withdrawals from therapy, the viral replication restarts and the viral population is refueled in a couple of weeks[20]. The levels of viral RNA in the blood (viremia), below detectable levels under HAART therapy, rise to pre-HAART levels. There is an agreement in defining the source of viral rebound in latently infected cells that host an intact integrated replication-competent HIV in their chromosome without actively producing viral progeny[21,22]. A percentage of these latently infected cells, by reactivating HIV transcription, is the source of newly produced virions and, therefore, the rise of viremia. These cells, called globally "reservoir", are the main obstacle to a sterilizing cure. More feasible strategies,

rather than HSCT, are under investigation to eliminate the reservoir and achieve a scalable sterilizing cure. “Shock and Kill” or “Block and Lock” pharmacological approaches reflect opposite approaches pursued in HIV research to tackle the reservoir[23,24]. The first relies on classes of drugs able to reactivate the silenced HIV provirus (Latency reversing gents, LRA, shock phase) followed by immune clearance of the reactivated cell (kill), while the second acts to prevent latency reactivation using Latency Promoting Agents (LPA, block phase) and induce silencing of the provirus (lock). Both these antithetical procedures rely on the understanding of the reservoir, which has become one of the prioritized objects of study in the HIV field[25–27]. Understanding the molecular mechanism of the biology and dynamics of the latent infection has been set as a pivotal goal for the future[28]. If the global effort of the scientific community will succeed in the development of a concrete solution to the HIV/AIDS infection, that commitment will have surely passed through the understanding and tackling of the silent reservoir.

The HIV impact on our society has been such profound that it has become the most studied microorganism in scientific research. Large investments and global efforts in the rush to find a cure for HIV/AIDS have produced technological innovations that have brought development and discoveries in many fields different from virology. In 2022, after three years of the COVID-19 pandemic, the United Nations’ program for AIDS (UNAIDS) has reached out for a call of efforts to improve global attention to control the spread of the HIV/AIDS pandemic. In these years of overlapping crises, investments in fighting AIDS have shrunk and HAART availability has become even more unequal in many regions of the world. In the last year, 1.5 million HIV new infections were registered. This number is 1 million higher than what is expected to be by the UN’s global targets if the epidemic shall see and end by 2030[1].

HIV-1 transmission and pathogenesis

HIV-1 is a human blood-borne virus and it is present in several body fluids such as blood, semen, vaginal secretions and breast milk[29]. Its transmission occurs through unprotected sex, sharing needles, blood transfusion or organ transplant from infected individuals. It can also be transmitted vertically from mother to child during pregnancy and birth. 80% of adults become infected through mucosal exposure, while the remaining 20% are infected through percutaneous or intravenous inoculations[30].

Immediately after infection, HIV-1 replicates in the mucosal and submucosal tissues. HIV-1 has a tropism for cells that express the CD4 receptor and a coreceptor that can be the C-C chemokine receptor type 5 (CCR5) or the C-X-C chemokine receptor type 4 (CXCR4) coreceptor. Activated CD4+ T lymphocytes are the most susceptible cells and sustain the active replication of HIV-1. The average half-life of these infected cells is 2 days and implies a continuous and sustained viral production and a rapid turnover of activated CD4+ T lymphocytes[31]. In addition, also monocytes, macrophages and dendritic cells (DC) express variable levels of CD4 and thus can be infected. Of these, DCs play an important role during the mucosal transmission of the infection and the subsequent viral dissemination through the lymphatic system. These professional antigen-presenting cells (APC) can uptake the virions through the mannose-binding C-type lectin domain of a type II membrane protein called DC-SIGN without sustaining the active replication[32,33]. Virions are retained in an infectious state and delivered from infected mucosa to lymph nodes where they are presented to resident CD4+ T cells, a process known as *trans-infection*[34].

When HIV-1 transmission occurs, only a few genetic variants are selected and can spread in the recipient host. Mucosal environment and immune pressures of the recipient individual favor the transmission of CCR5 tropic strains, which are for this reason the transmitted/founder virus (T/F virus)[35]. Although the R5 strain's selective

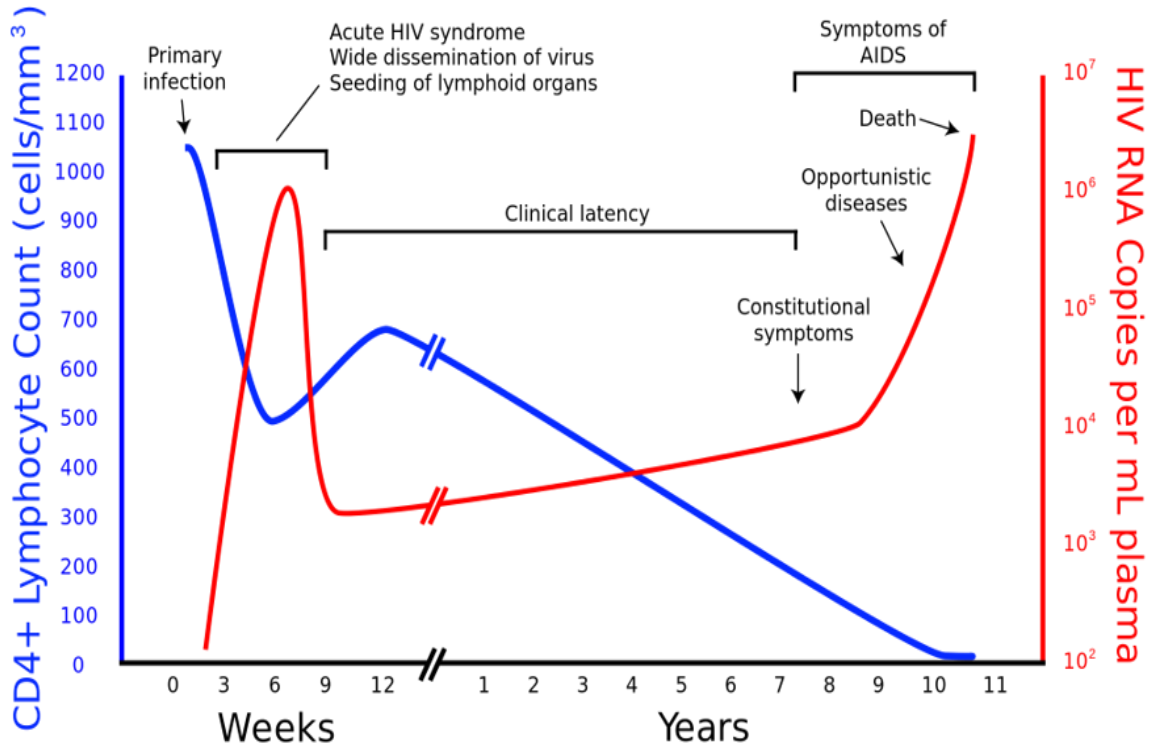

Figure 1 *HIV/AIDS disease progression. Typical progression of an untreated HIV infection. A healthy adult has a CD4+ T cell count ranging from 500 to 1200 cells per µl. During the acute phase of HIV infection, this number drops (blue line) because of viral replication in CD4+ T cells and subsequent HIV-mediated death. As replication occurs, HIV RNA is detectable in the bloodstream (red line) and reaches a peak during the acute phase. When the adaptive immune system reaches partial control of the infection, the chronic phase of the infection starts. A steady-state level of viremia is established and the CD4+ count slowly decreases until it declines to <200 cells/µl. At this point, HIV-associated immunodeficiency increases the risk of Kaposi Sarcoma, pneumonia, meningitis, tuberculosis, certain lymphomas and invasive cervical cancer. Image from https://commons.wikimedia.org/w/index.php?curid=15383502, author: Sigve Holmen*

advantages are not fully understood, it is believed that the high expression of the CCR5 co-receptors in resident CD4+ T lymphocytes in the mucosal tissues is one of the main reasons that favor the R5-tropic viruses.

If the virus successfully establishes in the new host, it migrates from the mucosa to the lymphoid system and the bloodstream in approximately 10 days. At this time, viral mRNA levels can be detected (Figure 1). Before this period, named "eclipse phase", it is not possible to detect HIV-1 in the plasma. Laboratory staging of the infection has been characterized deeply and relies on the subsequent detection of viral RNA (Fiebig stage I, as early as 10 days post-infection), p24 antigen (stage II) and HIV-1-specific antibodies (stage III and IV)[36]. During the first weeks of infection, the virus grows exponentially and antibodies against the pathogen can be detected after 30 days, when seroconversion is completed (stages III and IV). Flu-like

symptoms such as fever, headache, chills, and rashes can develop in the infected individual during this phase. However, symptoms do not always develop and there is no sign to predict the infection apart to be tested.

The infection phase characterized by possible symptoms, sustained viral replication and appearance of viral markers in the bloodstream is called "acute phase" and can last up to three months from the initial infection[37]. After this period, the immune system is partially able to control the infection reaching a host-pathogen equilibrium. Virus replication in the bloodstream sets to a level called set-point equal to the number of viral particles detected in the blood (viremia)[38].

In the acute phase, the infection reaches susceptible cells in the majority of the body's districts: lymph nodes, gut-associated lymphoid tissue (GALT), central nervous system (CNS), lungs, bone marrow, spleen and genital tract. Particularly, districts such as lymph nodes and the genital tract become "sanctuaries" for the virus. In some individuals, HAART penetration in these districts is sub-optimal and immune clearance is weak, resulting in a favorable environment for the virus to replicate[39]. In the early phase of the acute infection, some cells develop a latent infection and can persist in a quiescent state hosting the virus and hiding it from the immune system and HAART therapy. These cells form the silent "reservoir" and do not express viral proteins or produce new particles. Still not fully understood, this pool of cells drives the resurgence of infection if the antiretroviral regimen is stopped and is one of the major obstacles in the resolution of the infection[22].

Even though the immune system controls the infection, it is not able to eradicate it and the infection develops a chronic phase characterized by persistent inflammation and a progressive loss in the CD4+ T cells. Eventually, after several years of chronic infection, a severe immunodeficiency caused by a CD4 count <200 cells/μl leads to AIDS symptoms (Figure 1). The sub-optimal and pathological conditions of the immune system increase the risk of opportunistic infections such as pneumonia, meningitis, tuberculosis and the development of rare tumors.

Treatments such as the Highly active antiretroviral therapy (HAART) are nowadays available to control HIV infection. HAART is one of the most significant life-changing medical treatments developed by modern medicine. Until the late-1980s, HIV-infected individuals were treated only for opportunistic infection to minimize AIDS symptoms as no specific drugs targeting HIV replication were available. In 1987, AZT (azidothymidine or Zidovudine) was the first FDA-approved drug for HIV/AIDS treatment. The medication was first described in 1964 as an antineoplastic drug but was discharged for its severe side effects. Once its potential as antiretroviral was discovered, AZT was prescribed as a monotherapy for individuals affected by HIV infection. Between 1987 and 1992, this monotherapy was set as the normal regimen for the treatment of infection. Unfortunately, it became soon clear that the monotherapy regimen was only a temporary solution as HIV rapidly evolved resistance to AZT and new drugs were necessary to control the infection. Thanks to intense basic and clinical research, many different new molecules were approved for HIV medication and the golden standard for HIV+ individuals became a cocktail of different antiretrovirals named HAART. The advent of HAART rapidly changed the landscape of treatments for all HIV+ individuals. The drugs that compose this combination were targeting different viral enzymes and steps of the life cycle. The result was a dramatic suppression of the viral replication and HIV plasma levels below the limits of detections of available instruments, resulting in a strong reconstitution of the immune system in most patients[40].

The main reason for the need for a combination of drugs lies in the resistance that most patients were developing to AZT monotherapy[41,42]. AZT, a thymidine analog belonging to the nucleoside analog reverse-transcriptase inhibitors (NRTI) class of drugs, works by mimicking the naturally available deoxythymidine triphosphate (one of the four deoxynucleotide triphosphates available for DNA synthesis, dNTPs) that the viral reverse transcriptase enzyme uses to reverse transcribe the

viral RNA to DNA. Instead of being functional to the new DNA strand, AZT lacks the 3' hydroxyl group and acts as a chain terminator resulting in the abortion of the newly synthesized nucleic acid. The synthesis of every new molecule with AZT instead of the correct thymidine results truncated[43].

After an initial benefit, where AZT was blocking the reverse transcription of the viral RNA, variants of the reverse transcriptase enzyme able to selectively excide AZT from the DNA incorporation emerged during the course of the infection, resulting in a loss of function of the treatment[41]. The problem was solved by developing new classes of antiretroviral targeting other steps and enzymes of the virus and using them in combination. The chances to develop a simultaneous resistance to more than one drug were incredibly lower.

Until 2022, FDA has approved more than thirty antiretroviral drugs[44], which are used in combination with HAART depending on the nature and progression of the infection. After more than two decades of availability, HAART continues to be highly efficient in blocking new rounds of infection, protecting uninfected cells from the virus and controlling viremia. In 2019, a pilot study named PARTNER gathered enough data to conclude that an HIV+ individual that responds optimally to the therapy and thus has no viremia, is not able to transmit the virus[45]. Under the equation U = U (undetectable equals untransmissible), another step forward in the quality of life of PWHIV has been made.

HIV-1 structure and genome

HIV-1 is an enveloped virus, meaning that it is characterized by a phospholipid bilayer that protects and separates the viral content from the external environment. The entire particle (virion) is ~100nm in diameter. The phospholipid membrane is acquired from the infected cell and becomes part of the virion in the last stages of the life cycle when newly produced particles bud off from the cell. The lipid membrane is embedded with two viral glycoproteins that mediate HIV-1 tropism

for the human CD4 receptor: gp120 (SU, surface) and gp41 (TM, transmembrane), cleaved by a host protease from the gp160 precursor. Each spike glycoprotein is formed by a trimer of gp120 and a trimer of gp41 that non-covalently bind together[46]. Highly glycosylated, viral spikes are difficult to be targeted by antibodies produced by the immune response or by immunotherapies. On the inner side of the lipid membrane, the matrix protein MA/p17 trimers form an inner shell[47].

Enclosed in the viral membrane, a proteinic core structure (capsid) houses the RNA genome and delivers it through the cell cytoplasm. The structure is a fullerene and made of ~250 hexamers and 12 pentamers of a single protein named p24 (also CA, capsid protein) that spontaneously assembles[48]. Each p24 monomer is made of two protein domains linked by a flexible region that enables multiple folding possibilities. Each N-terminal domain binds to another monomer to form hexamer structures or, less frequently, pentameric rings[49,50] and each C-terminal domain binds to neighboring rings to form the characteristic asymmetric shape of the capsid. In addition to the genome, the nucleocapsid protein p7 and copies of viral enzymes are enclosed in the capsid: protease (PR) that cleaves HIV-1 polyproteins during virion maturation, reverse transcriptase (RT) that reverse transcribes the RNA genome into double-stranded DNA (dsDNA) and integrase (IN) that nicks the host chromosome and inserts the viral DNA to become part of the infected cell genome.

Inside the capsid, two copies of a (+) single-stranded RNA (ssRNA) approximately 10 kb long represent the HIV-1 genome. The ssRNA molecule is the template for the synthesis of the viral dsDNA that is integrated into the host genome by IN. The expression of the integrated viral DNA (provirus) is tightly dependent on the signals present in two regions that flank the provirus named LTRs (Long terminal Repeats), which serve as viral promoters. The provirus acts as a cellular gene, exploiting the cell's transcriptional machinery to transcribe mRNA and the replication machinery to be replicated along with the host genome.

All retroviral genomes encode for three main polyproteins: Gag ("group-specific antigen", structural proteins), Pol (viral enzymes) and Env (membrane glycoproteins). However, lentiviral genomes are more complex. They encode for several other proteins that modulate infectivity, replication and interactions with the host molecular defenses.

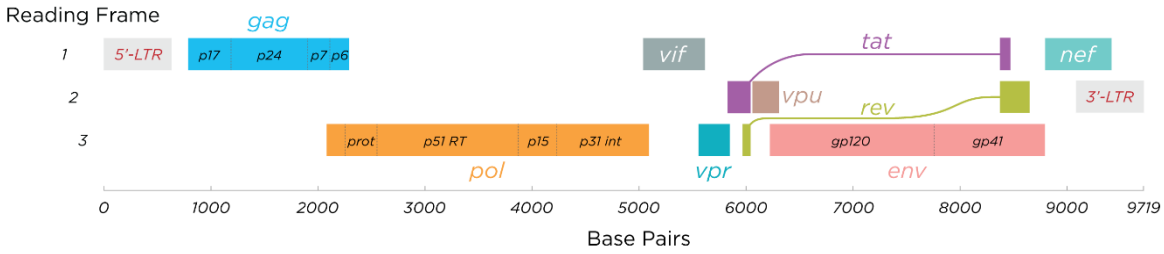

Figure 2 *HIV-1 genome representation. The viral genome is organized into 9 ORFs divided into three different reading frames. The 5' LTR acts as the viral promoter for the encoding of viral proteins, divided into structural proteins (Gag, Pol, Env), regulatory proteins (Tat and Rev), and accessory proteins (Nef, Vpr, Vpu, Vif). Image from https://en.wikipedia.org/wiki/Structure_and_genome_of_HIV1/media/File:HIV-genome.png, author: Thomas Splettstoesser (www.scistyle.com)*

In particular, the HIV-1 genome is made of 9 genes on three separate reading frames that encode for 15 mature proteins (Figure 2). *Gag*, positioned at the 5' end of the genome and mainly transcribed singularly, encodes for a polyprotein named p55. This precursor is cleaved by the viral protease to form all the structural proteins: p17 (matrix MA), p24 (capsid CA), p7 (nucleocapsid NC), p6 (budding protein) and two spacer proteins (SP1, SP2). Once every 20 transcripts, a programmed -1 frameshift occurs and the proviral transcription continues towards the *pol* gene, which provides the three viral enzymes PR, RT and IN. The two genes overlap by 205-241 nucleotides and lie in different reading frames[51]. However, when the frameshift occurs, *pol* is also transcribed and translated as a single polyprotein with *gag* (Gag-Pol polyprotein) that is cleaved by the viral protease PR to produce the structural proteins and the viral enzymes.

Env gene is positioned towards the 3' end of the genome, downstream *gag* and *pol* genes. *Env* encodes the proteins that decorate the viral envelope, gp120 and gp41. These molecules are responsible for the recognition, attachment, and fusion of susceptible cells. The precursor gp160 is cleaved by the cellular protease furin to

form gp120 and gp41 heterodimers that interact to form the mature Env trimer glycoprotein. The two subunits are non-covalently bound and shedding of gp120 has been shown to form inactive envelope glycoproteins made solely by membrane-bound gp41[52]. Furthermore, inefficient furin cleavage of gp160 can lead to the release of mature virions carrying non-functional gp160 glycoproteins rather than the mature gp120/gp41 cleaved subunits. Perhaps the most important feature of the Env protein is its high glycosylation, which represents 50% of its total mass[53]. The N-linked glycans form a shield to the underlying viral protein and protect it from immune surveillance.

In addition to the three main proteins, Tat (Transactivator of transcription, p16 and p14) and Rev (Regulator of virion, p19) are the regulatory proteins encoded in the early steps of HIV DNA transcription. Tat ensures the elongation of transcription in the early phases, while Rev is responsible for the nuclear export of late transcripts. The role of these two proteins is essential for the efficient transcription and translation of viral proteins.

In the HIV-1 genome, other four accessory proteins are encoded: Vif (Viral infectivity factor), Nef (Negative regulatory factor), Vpr (Viral protein r) and Vpu (Viral protein u). In immortalized cell lines, none of these accessory proteins are needed for viral replication[54]. However, these proteins are important for many different aspects of *in vivo* replication. Vif is a 23-kDa protein known to overcome the antiviral activity of APOBEC3G by mediating its polyubiquitination and subsequently its proteasomal degradation[55]. APOBEC3G is a cellular cytidine deaminase that is encapsulated in newly produced virions and induces G to A hypermutations in newly synthesized viral DNA. Vif-defective virions incorporate APOBEC3G that interferes with the next round of reverse transcription and affects both genome stability and viral fitness. The Nef protein is believed to be indispensable for HIV-1 replication *in vivo*. It downmodulates many surface receptors essential for the immune system's function. The best-known physiological

activity of Nef is the downregulation of both the CD4 receptor and the major histocompatibility class I (MHC I) complexes. The proposed benefit of CD4 downregulation is the enhancement of viral particle release caused by the prevention of the viral envelope sequestration mediated by the CD4 itself[56]. By binding to the CD4 cytoplasmic tail, Nef induces the CD4 internalization and subsequent degradation. Similarly, a Nef-mediated disruption of the MHC I would avoid viral antigen presentation and subsequent CD8+ T cell-mediated clearance for an HIV-1-infected cell[57,58]. In addition, Nef is known to counteract the action of the restriction factors SERINC3/SERINC5 by avoiding their incorporation into the virions[59–61]. The serine incorporator protein family (SERINC1-5) members are multiple-transmembrane-segment proteins that incorporate serine into the structures of cell membranes and thus facilitating the biosynthesis of serine-derived lipids[62]. SERINC3/5 can be incorporated into nascent virions, and when Nef is absent they cause fusogenic impairment of HIV-1 particles[60,61]. Vpr is present in the preintegration complex (PIC) and was believed to play an important role in the nuclear import of viral DNA. However, subsequent studies suggested that Vpr causes cell cycle arrest in the G2 phase[63].

It is still unclear why a G2 phase arrest is beneficial for the virus. Some studies suggested that it increases the viral yield while others propose that G2/M arrest is the result of the activation of the structure-specific endonuclease (SSE) regulator SLX4 complex (SLX4com) recruited by Vpr to escape from innate immune sensing [64,65]. Vpu, a 16-kDa membrane phosphoprotein, has long been known to play a crucial role in virion release and its absence impairs viral budding[66]. Moreover, the molecular mechanism has been disclosed and shreds of evidence suggest that Vpu counteracts the cellular factor tetherin/BST2 that physiologically mediates the retentions of virions on the cell surface[10].

HIV-1 life cycle

Every virus relies on a cell to complete its life cycle. As obliged intracellular parasites, viruses are not able to perform all the chemical reactions needed to replicate their genome. For this reason, the cell's transcriptional and translational machinery is harnessed by the virus. The totality of steps in between viral attachment to the cell membrane and the release of new virions is called the life cycle. The viral particle needs to attach and enter a susceptible cell through the recognition of a receptor on the cell's surface. Once inside, the virus parasites the cell's machinery to replicate its genome, produce mRNAs and translate them into proteins using the cell's ribosomes. The cycle is concluded when new viral particles are released outside the infected cell (Figure 3).

Entry and reverse transcription

To start its cycle, HIV-1 virions need to adhere to the cell surface of a permissive cell. Env nonspecifically interacts with negatively charged cell-surface heparan sulfate proteoglycans or more specifically with the α4β7 integrin[67,68]. These interactions likely increase the efficiency of attachment by bringing the extracellular gp120 Env subunit into close contact with the primary CD4 receptor. CD4 is a 55 kDa type I integral membrane protein consisting of four extracellular immunoglobulin-like domains (D1-D4), a transmembrane region and a short cytoplasmic tail. Physiologically, it stabilizes the interaction between the MHC-II molecule of an APC and the T cell receptor during antigen presentation. The CD4 molecule is expressed on the cell surface of about 60% of circulating T-lymphocytes, on T-cell precursors, macrophages, monocytes and dendritic cells. The gp120 attachment to CD4 induces a series of rearrangements in the gp120 that enable the subsequent interaction with the CCR5 or CXCR4 co-receptor. This second step induces even more drastic conformational changes in Env that bring to the exposure of the fusion peptide buried into the N-terminal portion of the gp41 transmembrane glycoprotein. The two membranes, viral and cellular, are mechanically approached

by the changes in the gp41 until they fuse. This pH-independent fusion entry at the plasma membrane is thought to be the major route for HIV-1 entry[69,70]. Nonetheless, endocytosis is also recognized as a possible mode for entry[71].

If the CD4 tropism is shared by all HIV-1 and 2 lineages, the choice of the co-receptor used by different HIV-1 strains can rely on either the CCR5 or the CXCR4. The gp120 sequence is highly variable and the less conserved domains, called hypervariable loops, are exposed at the surface of the glycoprotein where they bind to the CD4 receptor and CCR5/CXCR4. Specific mutations in the third hypervariable loop V3 of gp120 determine the tropism towards one of the two possible co-receptors[72]: when CCR5 is the co-receptor recognized by the viral gp120, the strain is called R5 tropic, when the co-receptor is the CXCR4, the strain will be named X4 tropic. R5 strains are the T/F viruses and can be isolated during the course of the natural infection, while X4 or dual-tropic R5X4 strains emerge in ~ 50% of late stages of infection, when the immune system is impaired[73].

The need for a co-receptor to properly infect a cell for HIV profoundly impacts its infectivity. A polymorphism in the CCR5 gene consisting of a 32-base-pair deletion in the CCR5 gene (CCR5-Δ32 mutation) which causes the production of a non-functional receptor was shown to confer resistance to HIV infection if present in homozygosis[74]. The allele frequency shows a North-South cline in the European and Asiatic geographic regions, ranging from 16% in Northern Europe to 4% in Greece. The homozygosis condition has been detected in the 0.16-2.5% of European descendants[75].

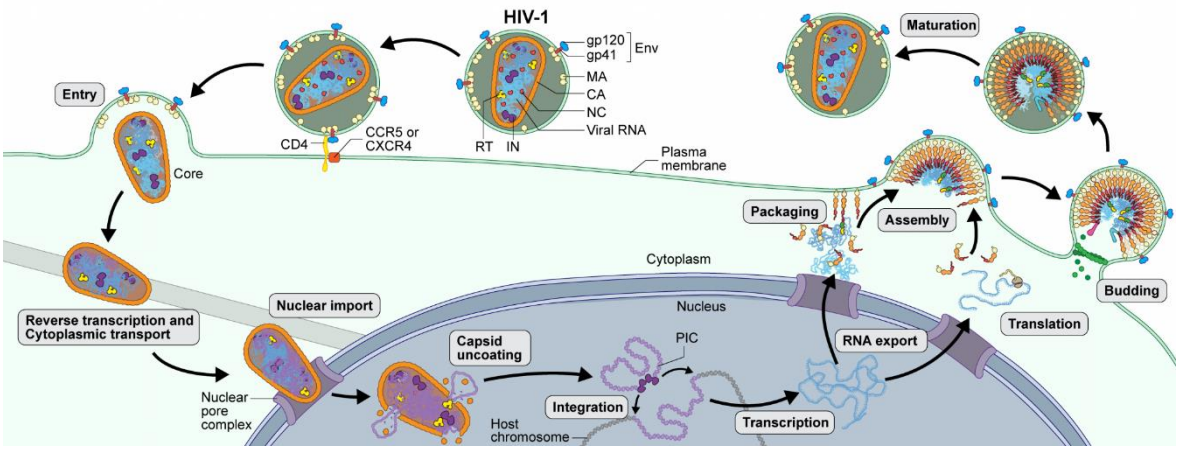

Figure 3 *Schematic representation of the HIV life cycle. HIV enters a susceptible cell via CD4 receptor and either CCR5 or CXCR4 co-receptors through interactions with the viral envelope glycoproteins (gp41 and gp120). After fusion, viral RNA inside the capsid is retrotranscribed to dsDNA by the viral RT while imported into the nucleus through nuclear pore complexes. Here, dsDNA forms a complex within the viral IN and other cellular factors named the preintegration complex (PIC). Viral dsDNA is integrated (provirus) into the host genome, where it can be actively transcribing mRNA or lay quiescent indefinitely. An active infection leads to the formation of new viral particles that bud off from the cell and can start a new round of infection. Image from https://scienceofhiv.org/wp/life-cycle/*

Once fusion has occurred, the viral capsid is released in the host cell and transported towards the nucleus through interactions with microtubules-based motor proteins. The RT enzyme readily starts the retrotranscription of the genomic ssRNA to dsDNA (Figure 3). RT is an RNA-dependent DNA polymerase shared by all retroviruses that can synthesize dsDNA from an RNA template. 50 to 100 RT molecules are present in the mature virion that infects a new cell. RT catalyzes the dsDNA production as soon as the viral capsid becomes permeable to the deoxynucleotides (dNTPs) present in the cell. Conversion of the ssRNA to dsDNA requires two template exchanges promoted by annealing of the viral ends, called R, which are direct repeats. RT first synthesizes the complementary (-) DNA strand starting near the 5′ end of the viral RNA genome, adding dNTPs. RT uses as a primer a cellular tRNA carried inside the virion, hybridized in a specific sequence called the primer binding site (pbs). The first template switch occurs at the 5′ end of the genome, where the newly synthesized (-) DNA is complementary and hybridizes with the viral 3′ end of the viral RNA genome. After this transfer, the (-) strand DNA synthesis can continue while a specific RT domain called RNase H acts as an endonuclease and degrades the RNA template. A purine-rich sequence (ppt)

of 13-15 nucleotides is resistant to RNase H activity and serves as a primer for the synthesis of the (+) strand DNA. (+) strand DNA synthesis continues until it reaches the pbs site with the tRNA annealed on the (-) strand, where the second template exchange occurs. Here DNA ends are juxtaposed by annealing at the complementary PBS sequences to mediate the template exchange and allow the DNA synthesis to continue. The final product is a linear, blunt-end dsDNA with long terminal repeats (LTRs) at both ends called provirus that will be integrated into the host genome by the viral IN.

During the RT reaction, cellular dNTPs must be available for RT to synthesize new DNA. Capsid should then be degraded before the RT activity or be permeable to small molecules such as dNTPs. It was once believed that capsid released all its content in the cytoplasm by disassembling after viral fusion and that only subviral complexes could be found inside the nucleus, given that the diameter of the nuclear pore complex (NPC) channel is inferior than the viral capsid dimensions[76]. In the last years, growing evidences suggest that capsid persists intact, or almost, for a longer period without completely dissolving in the cytoplasm[77,78], travelling from the cell periphery to the NPC along microtubule networks[79]. In addition, several pieces of evidence point out not only the presence of capsid inside the nucleus but also its active role in the docking process to the NPC and integration[80].

HIV-1 integration

The RT reaction product is a linear-blunt-dsDNA that can be integrated into the host genome by the viral IN (Figure 3). This feature allows the virus to protect its genome and propagate it along with the cell's divisions. When the infected cell duplicates, daughter cells will inherit the viral provirus in its site of integration. Reverse transcription mediated by the RT enzyme starts in the cytoplasm inside the viral capsid, but completes only inside the nuclear environment[81]. Early RT products have been recorded as early as 30 minutes after infection, while late RT products and viral cDNA are largely located inside the nucleus[77,80,82].

A remarkable property specific to lentiviruses is their ability to infect non-dividing cells, implying that subviral complexes must be guided through the intact nuclear membrane[83]. Once in proximity to the nuclear membrane, the viral capsid passes through the NPCs[84,85], that are the nuclear membrane's highly selective channels composed of various nucleoporins (Nups). This active transport is facilitated by the activity of transportins such as the identified β-karyopherin Transportin-1 (TRN-1) and interaction between viral CA and phenylalanine-glycine repeats (FG) found in multiple Nups[86,87]. TRN-1 has been shown to directly bind to the cyclophilin A (CypA)-binding loop of CA and trigger capsid uncoating and nuclear import, while two specific Nups (NUP358 and NUP153) have been shown to bind to CA and mediate NPC docking and subsequently its exiting from the nuclear basket[88,89]. NUP358 is located in the cytoplasmic part of the NPC and forms cytoplasmic fibrils that directly interact with HIV-1 CA through the C-terminal cyclophilin homology domain (CycH), thus facilitating the income capsid docking[90,91]. NUP153 is part of the NPC's nuclear basket and interacts with CA through its C-terminal portion, favoring the last stage of capsid nuclear import[92,93]. Knockdowns of other Nups, such as NUP214 and NUP98, resulted in an HIV-1 low infectivity phenotype but their participation in HIV-1 nuclear translocation was not confirmed[88].

Viral RNA is completely reverse transcribed to dsDNA in the nuclear environment[81]. Here, the dsDNA is joined with many other viral and cellular proteins to form the nuclear preintegration complex (PIC). PIC is a nucleoprotein complex composed of viral enzymes (RT, IN), viral proteins (CA, Vpr, MA, NC), viral dsDNA and several host proteins (BAF, LEDGF/p75, LAP2a)[94]. The main player of the PIC complex is the viral protein Integrase (IN). This enzyme is encoded by the 3' end of the *pol* gene. IN is ⌾ 300 aa long and consists of three structurally and functionally distinct domains: an N-terminal zinc-binding domain (NTD) that contributes to oligomerization, the conserved core domain (CCD) with catalytic and DNA-binding activity, and the C-terminal DNA-binding domain (CTD) that binds

host DNA non-specifically[95]. It is known that IN functions as a multimer bound to the DNA viral termini creating a complex known as the Intasome.

The generally accepted model for the integration process can be divided into three distinct reactions: 3′ processing, strand transfer and repair. During the first step of the integration process, 2 terminal nucleotides (NN) are removed from the 3′ends of the retrotranscribed viral DNA by IN, thus exposing the conserved CA_{OH} dinucleotides at the 3′ viral end of each strand. Processing can take place only with completely retrotranscribed substrates and thus avoids the integration of viral DNA with defective ends[96]. In proximity to the host DNA at the site of integration, the strand transfer reaction takes place: the processed and chemically reactive 3′ ends of the viral DNA attack a pair of phosphodiester bonds in the host genome. During joining, IN catalyzes a single-strand nick in both strands of the cell's DNA where the viral 3′ end CA_{OH} can join. Subsequently, a gap between the 5′ viral ends and the sites of chromosomal cuts is repaired by duplicating the cell DNA sequence. This string of base pairs is 5-nucleotides long in the case of HIV-1 but can vary depending on the retrovirus. A single-strand nick is generally sensed by the cell as damage to be repaired. So, it is believed that the DNA-damage response machinery is activated at the site of integration to fill the 5-nucleotides gap and rebuild the double-stranded continuum. This final step is likely to be mediated by cellular proteins and concludes the integration process[97].

HIV-1 takes advantage of many host factors to drive complete and efficient viral integration. To prevent autointegration of RT-produced viral dsDNA, the PIC complex includes the barrier-to-autointegration host protein (BAF). Components of this conserved protein family are capable of binding and compacting DNA, preventing a reaction between the two ends of the viral DNA that would be detrimental to the viral life cycle[98,99].

Host factors are also essential to guide the PIC to the site of integration before the joining reaction. Complexes such as the nuclear protein Lens epithelium-derived

growth factor/p75 (LEDGF/p75, also known as PSIP1) and the cellular protein polyadenylation specificity factor subunit 6 (CPSF6) are proteins that bind both the PIC subunits and the cellular DNA, tethering directly or indirectly the two substrates. The present model suggests that the viral dsDNA imported into the nucleus is still associated with CA viral proteins through the C-terminus of IN. Capsid proteins are also bound to CPSF6, which is normally located in regions of genes actively transcribed by RNA pol II[100]. This interaction brings the viral PIC into proximity to gene-dense regions where it binds to LEDGF/p75 complex[101,102]. The ability of this latter to bind both IN and nucleosomes efficiently tethers PIC to the site of integration, where IN catalyzes the joining reaction. In addition, IN is also post-translationally modified by cellular enzymes to control its stability and function[103,104].

The integration process is not site-specific. However, it has been demonstrated that retroviruses integrate at preferential sites[105–108]. Indeed, retroviruses integrate preferentially within the promoters of active genes, while lentiviruses integrate preferentially within introns of active genes[109]. Furthermore, a set of genes denominated recurrent integration genes (RIG) has been reported to be a preferred target for integration in different experimental models and datasets. These RIGs were identified both in patients and in *in vitro* HIV-1 infections of cell lines, primary PBMCs and CD4+ T cells[110,111]. The common feature was the localization in the outer shell of the nucleus in specific chromosomal regions, meaning that also chromatin organization and nuclear topology could act as a major determinant for the site of integration[112]. In addition, these observations have highlighted that HIV-1 strongly disfavors heterochromatic regions in the outer nuclear shell or transcriptionally active ones in inaccessible interior regions while favoring outer, euchromatin regions close to the NPC. Moreover, cellular factors and their localization in the nucleus influence as well the viral integration site. Tandem knock-out of LEDGF/p75 and CPSF6 decreased integration, confirming a role for both in a

probable two-way process where CPSF6 first guides the PIC to active regions and then LEDGF/p75 tethers the complex to gene bodies[100]. As a resume, a concrete body of works supports that both the LEDGF/p75 association with chromatin active regions and the CPFS6 proximity to RNA pol II directs in these permissive areas the proviral integration.

HIV-1 DNA transcription

The integrated provirus has two identical long terminal repeats (LTRs) sequences at the 5' end and 3' end of its genome, composed by the U3, R and U5 regions. While the 3' LTR is not normally functional as a promoter, the 5' LTR acts as the RNA pol II promoter[113]. Once integrated, HIV-1 proviral transcription starts at the U3/R junction of the 5' LTR. Its activity is under the control of many layers of both genetic and epigenetic factors, from the site of integration to the local chromatin environment and transcription factors (TFs) availability. This plethora of aspects concurs to define whether the 5' LTR is transcriptionally active or silent, leading to an active or latent infection[114]. The 5' LTR is functionally divided into 4 domains: the modulatory region (from nt -455 to nt -104), the enhancer (from nt -109 to nt -79), the core promoter (from nt -78 to nt -1) and the leader region (from nt +1 to nt +188). The U3/R junction coincides with the transcription start site (TSS) and the nt +1 is conventionally the first TSS nucleotide. All these functional domains contain *cis*-regulatory elements recognized by multiple constitutive and inducible TFs.

HIV-1 transcription can be induced by a variety of stimuli, such as T cell-receptor ligation, cytokines including IL-1β, TNF-α and mitogens[115–117]. Such stimuli ultimately induce HIV-1 transcription by the induction of TFs availability. Of more than 50 TFs reported to bind to the 5' HIV-1 LTR sequence, only a few are critical for the regulation of proviral transcription *in vivo*[118]: these include NF-κB, Sp1 and TATA-box binding protein. The key player of HIV-1 transcription is the viral protein Tat. While enzymes like RT and IN are present in the virion, Tat must be produced by the infected cell. Early in the viral infection, fully spliced mRNAs

encoding for Tat, Rev and Nef are produced, even though at a very low rate and translated into proteins. Tat protein is imported back to the nucleus where dramatically increases the LTR-driven transcription by binding to a unique viral RNA sequence named TAR (trans-activating response element) found in the 5′ end of the immature viral transcript[119]. TAR is a 59-residue stem-loop secondary structure present in the viral RNA leading sequence and extending from position +1 to +60 in the HIV-1 LTR. In the absence of Tat, most transcripts block at this point. By binding to the TAR sequence, Tat can interact with different cellular cofactors. The current model theorizes that Tat sharply increases levels of transcription by stimulating a specific TAK protein kinase (Tat-associated kinase) known to be CDK9 (cyclin-dependent kinase 9), which in turn hyper-phosphorylates the carboxyl-terminal domain (CTD) of the large subunit of the RNA polymerase II (RNA pol II)[120,121]. These molecular events clear the promoter area and mediate the transcription elongation process. CDK9 is the catalytic subunit of the multiprotein complex P-TEFb (Positive Transcription Elongation Factor)[122–124]. This cyclin-dependent kinase is involved in gene transcription and promotes the synthesis of new mRNA by transitioning RNA pol II into productive elongation. In addition to CDK9, P-TEFb also contains a cyclin subunit made by one of the several cyclins present in the cell. Of this highly conserved protein family, cyclin T1 is the one that tightly associates with CDK9 and is responsible for the binding to Tat[125].

The central role of Tat in transcription elongation is such pivotal that HIV-1 transcription is generally divided into a first "Tat-dependent" phase and a second "Tat-independent" phase. In the absence of Tat, almost 90% of initiated transcripts terminate prematurely at position +55 to +59, at the TAR hairpin site. In the presence of Tat, 99% of the transcripts are fully completed and processed by the spliceosome machinery (Figure 3)[126]. For its essential role in HIV-1 transcription, Tat has also attracted considerable attention in the study of latency. Evidence indicates that enough quantities of exogenous Tat could counteract HIV-1 latency establishment

by sustaining an active proviral transcription. In Jurkat cells, a study demonstrated that cells stably expressing Tat presented fewer latently infected cells compared to cells that did not express Tat[127].

Even after the transcription enhancement led by Tat activity, unspliced or partially spliced transcripts are mainly degraded in the nucleus of the cell. The export of these intron-containing transcripts must be mediated by Rev, which is produced from another fully spliced mRNA. Rev protein interacts with the highly structured RNA element RRE (Rev responsive element) present within the *env*-coding region. The interaction between Rev and the RRE stem-loop RNA structure increases the nuclear export of longer transcripts such as the partially spliced and the unspliced transcripts. By continuously being shuttled between the nucleus and the cytoplasm, Rev can mediate the export of the envelope proteins transcripts, structural protein transcripts that carry the information for the Gag and Gag-pol polyproteins and the RNA templates that will represent the genome of the new viral particles. It has been demonstrated that a minimum threshold quantity of Rev is required to efficiently export long viral transcripts and only its efficient activity leads to partially spliced and unspliced transcripts abundance in the cytoplasm[128].

NF-κB pathway in HIV-1 transcription

NF-κB (nuclear factor kappa-light-chain enhancer of activated B cells) and NFAT (nuclear factor of activated T cells) are two of the TFs known to play a key role in HIV-1 transcription and can bind to overlapping binding sites in the 5′ LTR[129–131]. In resting cells, both complexes are sequestered in the cell cytoplasm, and thus unable to promote HIV-1 transcription. However, they are translocated into the nucleus in response to activating stimuli[132]. Specifically, NF-κB is a family of evolutionary conserved TFs involved in a wide variety of cellular processes. Its inducibility following stimulation with bacterial lipopolysaccharide (LPS) was first described in precursors of B cells in 1986[133]. Since then, NF-κB presence has been found in most mammalian cells and virtually in all human tissues. These protein complexes are

inducible by different stimuli and bind gene promoters controlling their transcription. Many human genes involved in the inflammation process present specific NF-κB binding sites in their promoters/enhancers regions[134]. Dysregulation in the NF-κB localization, expression and activity is linked to autoimmune diseases, viral infections and cell proliferation[132]. HIV-1 transcription initiation is heavily regulated by the nuclear availability of NF-κB and the scarcity of nuclear NF-κB creates a low permissive environment for the HIV-1 LTR activity, supporting HIV-1 latency[135,136].

Five proteins have been described to be part of the NF-κB family: p65 (RelA), RelB, c-Rel, p105/p50 (NF-κB1), and p100/p52 (NF-κB2)[137]. These monomers interact with each other and usually dimer to become transcriptionally active homo-heterodimeric complexes. The monomer's N-terminal region has a conserved 300aa-long Rel homology domain (RHD) specific for DNA binding, dimerization and inhibitory proteins interactions. Specifically, crystal structures of p50 homo and p50/p65 heterodimer bound to DNA demonstrated that the RHD N-terminal domain is responsible for the binding to the NF-κB consensus decameric sequence 5'-GGGRNNYYCC-3', while the RHD C-terminal region is involved in the dimerization and the inhibitory protein interactions[138]. Of all the possible monomer combinations, only a few have been described with the most abundant form being p50/p65[137]. In addition, the NF-κB family can be divided into two sub-groups based on the transactivation potential. Only RelA, RelB and c-Rel contain the C-terminal transactivation domain (TAD) which confers the transcription enhancement activity. Processed p50 and p52 lack TAD and have been found to repress κB-dependent transcription, probably by preventing other NF-κB TAD-containing dimers to bind to decameric sequences[139].

In most unstimulated cells, NF-κB complexes are sequestered in the cell cytoplasm in an inactive state, bound together at the RHD C-terminal regions with the inhibitory IκB proteins[132]. These act as repressors of the system and mediate the NF-

κB cytoplasm abundance through the ubiquitin/proteasome degradation pathway. In response to a variety of stimuli including cytokines, bacterial and viral pathogens and stress-inducing agents[140], two molecular cascades are known to dissociate NF-κB dimers from the IκB inhibitory proteins and promote the nuclear import of the active TF: canonical and non-canonical (or alternative). Both rely on the IκB kinase (IKK) activity.

The canonical cascade starts with the pathogen-associated molecular patterns (PAMPs) receptors, TNF receptor (TNFR) superfamily members or T/B cell receptor (TCR or BCR) that bind with their ligand molecule and integrate the signal inside the cell, causing the activation of IKK. Once activated, the IKKβ subunit of IKK catalyzes the serine residues phosphorylation in the signal-responsive region (SRR) of IκB and its subsequent polyubiquitination/degradation. Without any more impediments, NF-κB dimers are then translocated to the nucleus. The alternative pathway, called non-canonical, acts specifically by processing the NF-κB2 precursor protein, p100. It is induced by specific ligands of the TNFR superfamily members such as LTβR, BAFFR, CD40 and RANK[141,142]. Once the external signal has been internalized, the NF-κB inducing kinase NIK phosphonates the alpha IKK subunit (IKKα) which in turn phosphorylates p100 at the C-terminal region. The inactive p100 form is only partially degraded and so processed to p52, which is imported into the nucleus as a p52/RelB dimer. As a result of both pathways, nuclear NF-κB binds to the NF-κB binding sites found in many cellular genes and the enhancer region of the 5′ LTR, modulating the initiation of proviral transcription.

Assembly, release and maturation

After the transcription and translation of all the viral proteins, trafficking to the plasma membrane is necessary for the assembly and release of newly produced viral particles. All the necessary information for retroviral particle assembly resides in the Gag polypeptide. In the absence of other viral proteins, Gag alone can assemble to form extracellular virus-like particles[143]. Gag polyprotein interacts with

the dimeric viral genomic RNA, multimerizes and anchors to the inner leaflet of the plasma membrane through the myristoyl group of the MA domain[144]. At this site, the nascent particles start to assemble, and all the viral components are packed radially. Meanwhile, the Env polyprotein is co-translationally glycosylated in the ER and transported to the Golgi apparatus where the gp160 precursor is cleaved by furin or furin-like proteases into the functional gp120 and gp41 subunits and subsequently directed to the plasma membrane. Here, the assembling particles bud from the cell incorporating the viral glycoproteins expressed at the plasma membrane. Two copies of the genomic RNA are encapsidated, linked at their 5' end through the dimer linkage site[145]. The virion is now released in the external environment in an immature and not infectious form. Once outside the cell environment, the viral protease PR starts to cleave in between Gag and GagPol polyprotein to trigger the particle maturation leading to the generation of mature infectious viral particles (Figure 3)[146].

Immunology of HIV-1 latency

HIV-1 reservoir

More than 25 years after the discovery of HAART, complete eradication of HIV-1 from an infected individual has not yet been achieved, except few notable cases[16,17]. Although the therapy durably suppresses viral replication, it fails to eradicate the virus from the host and interruption of HAART leads to rapid viral rebound, usually within a few weeks from therapy withdrawal. Furthermore, many people are unable to achieve long-term viral suppression[147]. During the first years of HAART implementation, optimistic previsions estimated the complete viral eradication within 2-3 years of optimal HAART treatment[148]. However, in 1995 a latent form of HIV-1 infection was demonstrated in resting CD4+ T cells isolated from the blood of infected individuals with an ongoing active infection[21]. These rare cells, collectively named the latent reservoir, harbored integrated HIV-1 genomes

and did not produce any viral particles while resting but could do so upon a stimulation. After this first evidence, latently infected cells were found also in HAART patients who had no clinically detectable viremia. The half-life of these cells was estimated to be approximately 44 months[149], implying that previous evaluations were imprecise and that HAART would have never been curative. The longitudinal analysis then demonstrated that the eradication of the reservoir would require a period of more than 60 years of HAART[150,151]. Sequence analysis revealed that the majority of transcriptionally silent proviruses were defective and unable to generate infectious particles due to large deletion within the genome[152]. However, a very low percentage of these cells (1 every 10^6 resting CD4+ T cells) harbor replication-competent silenced provirus that upon reactivation can give rise the new infectious viral particles[153,154].

Viral reservoirs have been defined as cell types or anatomical sites in which a replication-competent virus persists for much longer than it does in the main pool of productively infected cells[155]. This broad definition suggests that any infected cell with a half-life longer than the infected activated CD4+ T lymphocytes one (<2 days), could represent a viral reservoir for HIV-1. Temporal analysis of the rate of viremia decay following the initiation of HAART demonstrated a biphasic drop in HIV-1 plasma levels. The first phase of decay is rapid and sharp, occurring during the first two weeks of therapy. Viremia levels decrease by 99% of initial values due to the rapid decline of free virus in the bloodstream and the fast turnover in activated infected CD4+ T lymphocytes[31]. Plasma HIV RNA copies transiently settle below the 50 copies/ml limit of detection of most of the clinical assays. The second phase of decay proceeds slowly and it is thought to be driven by infected cells with longer half-lives such as macrophages (half-life 14 days[156]) and productively infected resting CD4+ T cells rendered susceptible to the virus by soluble cytokines[157]. Nevertheless, the nature of these cells remains elusive. After the second drop, viremia can still be detected by sensitive assays and usually 1 HIV RNA

copy/ml is recorded in many patients[158,159]. This so-called residual viremia possibly indicates ongoing viral replication in HAART patients and was one of the first clues of viral persistence.

Theoretically, residual viremia under HAART and viral rebound after HAART interruption could be sustained by two types of reservoirs that may both contribute to HIV-1 persistence: the stable reservoir and the latent reservoir (Figure 4). The stable reservoir has been defined as those cells that sustain ongoing viral replication even under HAART regimens. Few studies have demonstrated viral evolution in virally suppressed individuals suggesting that the therapy is not able to efficiently prevent the totality of replication events[160]. To support the existence of stable reservoirs and their role in supporting residual viremia, some evidence show that HIV-specific CD8+ specific T cells do not reach anatomical sites such as immune-privileged organs (testis, GALT, CNS[161]) and that HAART has sub-optimal distribution in lymphoid tissues. Although this latter scenario is possible, especially for individuals who receive less efficient antiretroviral drugs and never restore physiological immune functions[162], multiple studies have failed in identifying ongoing replication and viral evolution in patients under HAART therapy, shedding uncertainty on this hypothesis[163,164].

Even though the existence of a stable reservoir actively producing virus can be hypothesized, most persistently infected cells do not produce viral particles during antiretroviral treatment. This second reservoir is represented by latently infected cells that persist for decades, even under HAART(Figure 4)[22,154,165].

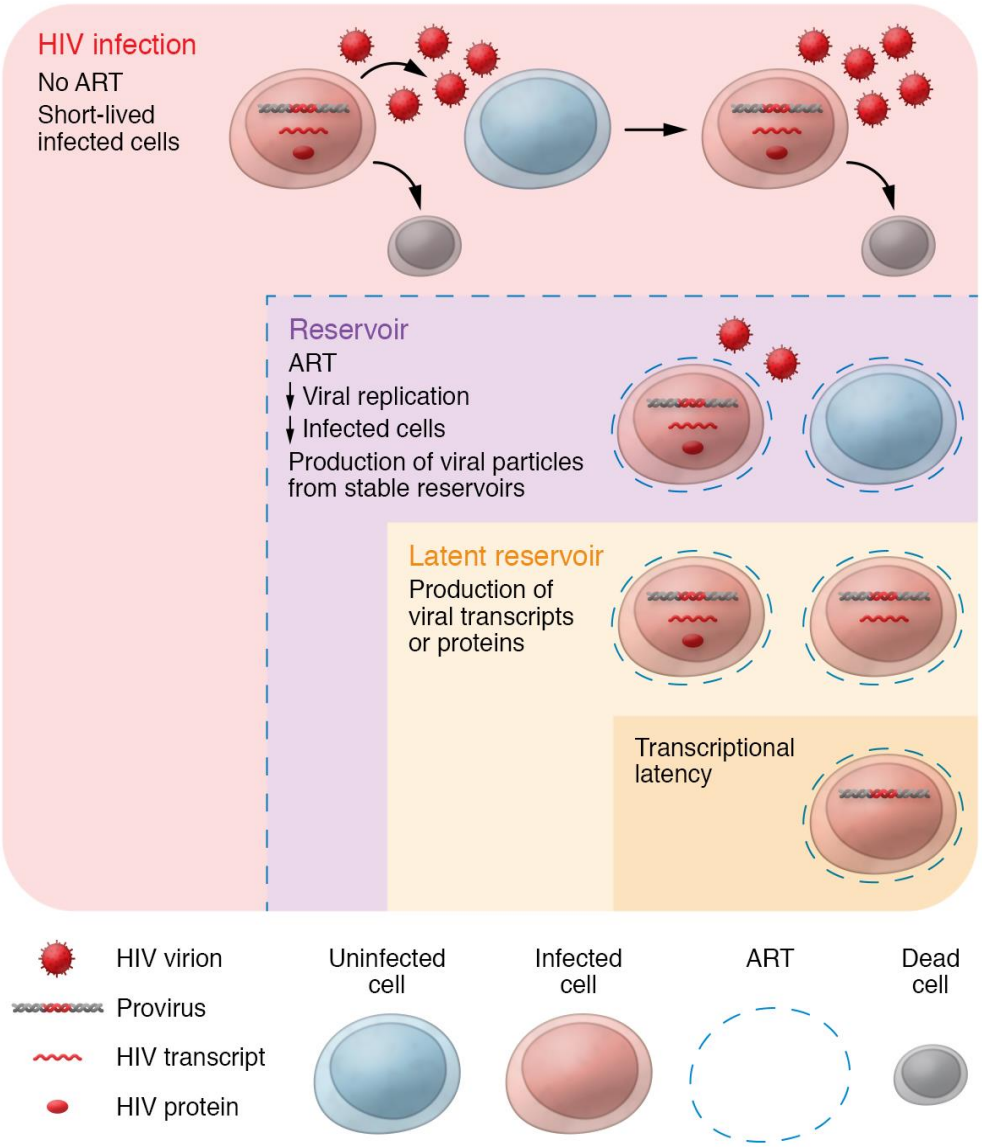

Figure 4 *HIV latent reservoir. During untreated HIV infection, most of the infected cells are short-lived and actively produce viral particles because of new rounds of infections. When HAART is initiated (blue dashed lines), viral replication decays sharply and uninfected cells are protected from being infected (blue cells with dashed borders). A persistent viremia in most patients is sustained by stable reservoirs represented by infected cells that harbor a productive infection and are insensible to antiretroviral therapies or by latently infected cells that revert from the latent state. Under HAART, most of the infected cells are latently infected and can express different degrees of latency, with molecular mechanisms blocking viral particle production at different steps such as transcription, post-transcription, and translation. Image from Dufour, Caroline, et al. "The multifaceted nature of HIV latency". The Journal of clinical investigation 130.7 (2021).*

Latency can be defined as a reversible non-productive state of infection of individual cells. Latently infected cells retain the capacity to produce infectious viral particles upon a stimulation, such as the recall antigen or various cytokines or when HAART is discontinued. These cells are majorly represented by memory CD4+ T lymphocytes that became infected as they were reverting to a quiescent state or directly during their resting state[166]. HIV-1 latent reservoir consistently differs from the classic latent infection established by other viruses, such as components of the *Herpesviridae* family. For herpesviruses, the expression of specific transcripts and proteins sustains a latent program that allows immune evasion. These episodes are interspersed between active periods of replication[167]. By contrast, no HIV-1 genome product is known to be associated with latency, which is then considered to be a consequence of the viral tropism for CD4+ T cells and specifically for some long-lived memory subsets. HIV-1 latency has been suggested to be an epiphenomenon that occurs at extremely low frequencies in infected cells, has a minor role in the natural course of the infection but is extremely important because is a barrier to a cure[168].

The latent reservoir was first described as relatively stable, and many attributed an apparently static feature retracing the characteristics of the long-lived and resting state of the non-dividing infected memory CD4+ T cells. Advancements in technology and renewed endeavors demonstrated that the latent reservoir is far more dynamic and that its persistence during HAART is driven by the clonal expansion of infected cells[169–171]. Even when HAART is initiated during the late-chronic stages of the infection, residual viremia is often dominated by identical sequences that tend to increase in proportion with time, consistently with clonal proliferation of infected cells[172]. Several mechanisms are thought to sustain the dynamics and the increasing clonality of the latent reservoir: integration within genes associated with cell growth, homeostatic proliferation and antigen-driven proliferation[173].

Proviral integration is not random and preferentially occurs in actively transcribing genes[107,108]. Many of these genes are involved in cell proliferation and their altered expression via the introduction of a viral promoter could drive the infected cell clonal expansion. Particularly, two studies have associated multiple and independent HIV-1 integration events in intronic regions of BACH2 and MKL2 genes, involved in the growth and development of T cells, with clonal expansion[110,172,174,175]. These data suggest that many of the infected cells within the latent reservoir have undergone clonal expansion and this could be a consequence of integration in specific genes that promote survival and expansion of the cell.

A second mechanism believed to drive the clonal expansion of the latent reservoir is homeostatic proliferation. T cell homeostasis relies on the survival of long-lived memory T cells maintained in response to many cytokines such as interleukin 7 (IL-7) and interleukin 15 (IL-15)[176]. This and other cytokines ensure a minimal proliferation level to sustain the survival of memory cells and these same factors are likely to contribute to the maintenance of the latent reservoir[171,177]. In addition, homeostatic proliferation occurs in the absence of proviral reactivation[178], allowing latently infected cells to remain invisible to both immunity and HAART.

The third mechanism involved in the maintenance and expansion of the reservoir is driven by antigenic stimulation. Latently infected cells with antigen-specific T receptors could expand in response to their cognate antigen stimulating the clonal expansion of the reservoir. Some studies reported HIV enrichment in HIV-specific CD4+ T cells, possibly because these cells are present and susceptible to infection at the sites of viral replication[179]. Other studies found HIV DNA enrichment in cytomegalovirus (CMV) and Epstein-Barr virus (EBV) specific CD4+ T cells[180], promoting the idea that recurrent exposure to antigens could sustain the clonal expansion of antigen-specific latently infected cells.

These three mechanisms likely coexist and precisely demonstrate the dynamics of the reservoir, which waxes and wanes by continuous reactivation of latently

infected cells to sustain residual viremia and balances cell death with clonal expansions)[181].

Establishment of the reservoir

When and how HIV-1 latency establishes is not fully understood. It is clear that a latent reservoir seeds rapidly in all HIV-infected individuals[182]. However, how rapid is controversial. Non-human primate models infected with SIV have been crucial to understand the duration of untreated infection required to establish a latent reservoir and produced in many cases discordant results. HAART initiation as early as 3 days post-infection with SIV prevented the detection of viremia in rhesus macaques but not the reservoir establishment. Indeed, after 24 weeks of continuous HAART, the virus rebounded in all animals considered[183]. Another similar study concluded that HAART initiation 4-5 days post-SIV infection and sustained for 2 years elicited viral control and possibly reservoir seeding in rhesus macaques[184]. In any case, both studies did not exclude the chance of a reservoir formation, even when starting the therapy before the detection of circulating viral particles. Studies on individuals that were infected despite receiving post-exposure prophylaxis (PEP) or initiating HAART at the earliest stage diagnosable (Fiebig I stage) as well as rare, documented cases of HIV-infected individuals receiving HAART 10 days post-infection showed that there is a drastic reduction in the reservoir sizes but not the absence of a reservoir formation[185–187]. In addition, a persistent latent reservoir establishment has been reported also in maternal-to-fetal transmission and/or birth, even when HAART was initiated within hours after the delivery[188]. Early HAART initiation has thus been proven to decrease the reservoir size, possibly accelerating a reservoir clearance, but did not block the establishment. Particularly, when the infection is clinically diagnosable, a rather small latent reservoir is unavoidably established.

Activated CD4+ T lymphocytes are highly susceptible to HIV, produce most of the viruses detected in plasma and for this reason display a short half-life when

infected. Contrary, resting memory CD4+ T cells are the main components of the latent reservoir[22,154,177]. The transition from an active to a resting memory state could offer a narrow window of permissiveness able to sustain the latency establishment[166]. Adaptive immunity relies on the formation of a long-lived immunological memory. Upon the re-exposure of an antigen, memory T and B cells are more efficient in clonally expanding into effector populations rather than T and B naïve cells, thus providing a better pathogen clearance. Nevertheless, there is still no consensus about the relationship between memory and effector cells and how memory cells arise after the antigen encounter[189]. Some recent reviews have strengthened the classical notion supporting that memory cells were once effector cells that survived the immune contraction phase and became memory-resting cells afterward. However, emerging data are more consistent in supporting the direct differentiation of naïve cells into memory populations, that will persist, and effector populations, that will die during the pathogen clearance[189].

Indeed, several lines of evidence, *in vivo* and *ex vivo*, now confirm that latency can also be directly established in resting naïve and memory CD4+ T cells[190,191], and perhaps other type of cells[192]. Even though numerous blocks render these cells refractory to HIV infection, some factors have been discovered to overcome them and thus increase the susceptibility to infection. CCL19 and CCL20, two chemokines involved in the homing of cells to mucosal tissues such as GALT and lymph nodes, are known to induce the cytoskeletal modification in target cells and by consequence increase the PIC nuclear import and integration of proviral DNA in resting CD4+ T cells[193]. Similarly, other soluble, both natural and synthetic, factors such as interleukin 15 (IL-15) gained much attention on their multiple roles in susceptibility to infection, latency establishment and perhaps proviral reactivation[194,195].

IL-15 is a widely expressed 14 to 15 kDa cytokine encoded by exons 5 to 8 of the IL-15 gene, structurally and functionally related to IL-2. Both cover pivotal and

pleiotropic roles in T-cell homeostasis, expansion and elimination of self-reactive lymphocytes and natural killer cells (NK)[196,197]. Specifically, IL-15 causes selective proliferation of T and NK cells[198] while promoting differentiation of naïve T cells in combination with interleukin 7 (IL-7)[199].

It is comprised, along with IL-2, IL-4, IL-7, IL-9 and IL-21, in the common cytokine-receptor γ-chain family of cytokines. All these cytokines share a subunit in their receptors, the γ one (also known as CD132), that explains the certain degree of redundancy in their functionalities. Furthermore, IL-15 shares also the β-chain (or CD122) with IL-2 in both their receptors (IL-2R and IL-15R). IL-2R and IL-15R are the only heterotrimers of the receptor family and composed by the γ -chain shared by all components of the receptor family, the IL-2/15R β chain shared by IL-2 and IL-15 and a unique third chain called IL-2Rα (also CD25) or IL-15Rα. The heterotrimeric form of the IL-2R and IL-15R receptor represents the high-affinity form, while receptors made only by the β and a γ chain are functional but present an intermediate affinity for their cytokine ligands.

The signal transduction cascade of IL-15 mediated by the activation of the IL-15R involves common JAK 1/2 (Janus kinase), STAT (single transducer and activator of transcription), PI3K and the mitogen-activated protein kinase 1/2 (MEK1/2) signaling molecules[200]. Specifically, it has been shown that IL-15 plasma levels strongly correlate with higher viremia and may be upregulated during the acute phase of the infection, when the latent reservoir is established[201,202]. Moreover, IL-15 regulates CD4+ T cell susceptibility to HIV-1[194]. In this latter case, IL-15 induces the phosphorylation of the restriction factor SAMHD1 in a JAK-dependent manner. SAMHD1 has been first identified as a restriction factor in the myeloid lineage and subsequently in resting CD4+ T cells[11,13,203,204]. It is believed that the antiviral activity of SAMHD1 is expressed by depleting the dNTP pool in the cytoplasm of resting CD4+ T cells and thus blocking the RT activity of HIV-1[205]. SAMHD1 fails to target the viral enzyme when phosphorylated at residue T592, generally in activated CD4+

T cells[206,207]. Thus, pathological plasma IL-15 abundance possibly induced by HIV-1 acute infection can be linked to the enhanced cytokine availability to relieve an early block in HIV-1 replication (phosphorylation of SAMHD1), broadening the cell population susceptible to infection.

The role of non-CD4 cells as latent reservoir has been theorized but it is still debated[192,208,209]. Especially when considering macrophages and microglia, which are susceptible to HIV, it is unclear if these cells can be latently infected and concur to the maintenance of the latent reservoir. Humanized-myeloid mouse models confirmed the presence of replication-competent virus in macrophages but the relatively short half-live of these cells did not support them as candidates as reservoirs[210]. To date, long-term persistence of replication-competent virus under optimal HAART regimens has been demonstrated only in resting CD4+ T cells. Surely these partial conclusions are influenced by sampling problems that reflect the difficulty to analyze latency in particular sites such as CNS, or mucosa tissues where other type of cells could retain infectious viruses. Less than 2% of total T lymphocytes are circulating in the blood and studies that aim at characterizing the geography of HIV infection must be aware of this unbalance. In a SIV-infected animal model under HAART, 98% of latently infected cells were found in the gut[211,212], while in another comprehensive human autopsy study HIV DNA was found in all 28 tissues analyzed[213]. Given the fact that a large portion of HIV genomes are defective, and that HIV DNA quantification could overestimate the real dimensions of the reservoir, the exact contribution of each anatomic region to the latent reservoir is largely undefined.

Latency in CD4+ T cell subsets

Memory T cells represent the most abundant lymphocytic population in the human body for most of its life[214]. Nonetheless, our understanding in the generation, maintenance, and organization of both CD4+ and CD8+ memory T cells is still fragmentary and mainly relies on studies on mouse models. It is well documented

that the acquisition of antigen experience is driven by the activation of CD4+ and CD8+ naïve cells upon the TCR or BCR engagement. Naïve cells undergo proliferative expansion and generate a plethora of subpopulations with effector or memory phenotypes (Figure 5). These latter persist *in vivo* to antigen clearance and retain the antigen memory indefinitely, sustained by homeostatic signals such as IL-7 and IL-15[176]. Upon antigen re-exposure, these subsets of memory populations coordinate an efficacious immune response.

The memory compartment once believed to be homogeneous, has been proven to be far more complex. Nearly 25 years ago, first studies from Sallusto and colleagues identified the heterogeneity of the memory compartment in human peripheral blood by analyzing the expression of a lymph-node homing receptor, CC-chemokine receptor 7 (CCR7)[215]. After 20 years of considerable advances, the naïve and memory T cell subsets picture is far more characterized and a maturational profile for both CD8+ and CD4+ T cells has been conceptualized based on biological functions, differentiation levels, and surface markers. Currently there are six generally accepted subsets, from the least to the most differentiated: naïve, stem cell like memory (T_{SCM}), central memory (T_{CM}), transitional memory (T_{TM}) effector memory (T_{EM}) and effector memory re-expressing RA (T_{EMRA})[216].

The first surface marker that is generally considered is the CD45 with its two isoforms, RA and RO[217,218]. Memory subsets are characterized by the expression of the CD45RO isoform and the lack of the CD45RA isoform (CD45RO+/CD45RA-). In addition, a more profound hierarchy in between CD45RO+ memory subsets is dictated by the presence or absence of the CCR7 receptor. This receptor is involved in the homing of T cells to secondary lymphoid organs such as the spleen and lymph nodes. CD45RO+/CCR7+ phenotype defines the T_{CM} subset, while CD45RO+/CCR7- defines the T_{EM}. T_{CM} traffic from the bloodstream to the lymph nodes while T_{EM} can migrate to inflamed peripheral tissues and display effector functions[219].

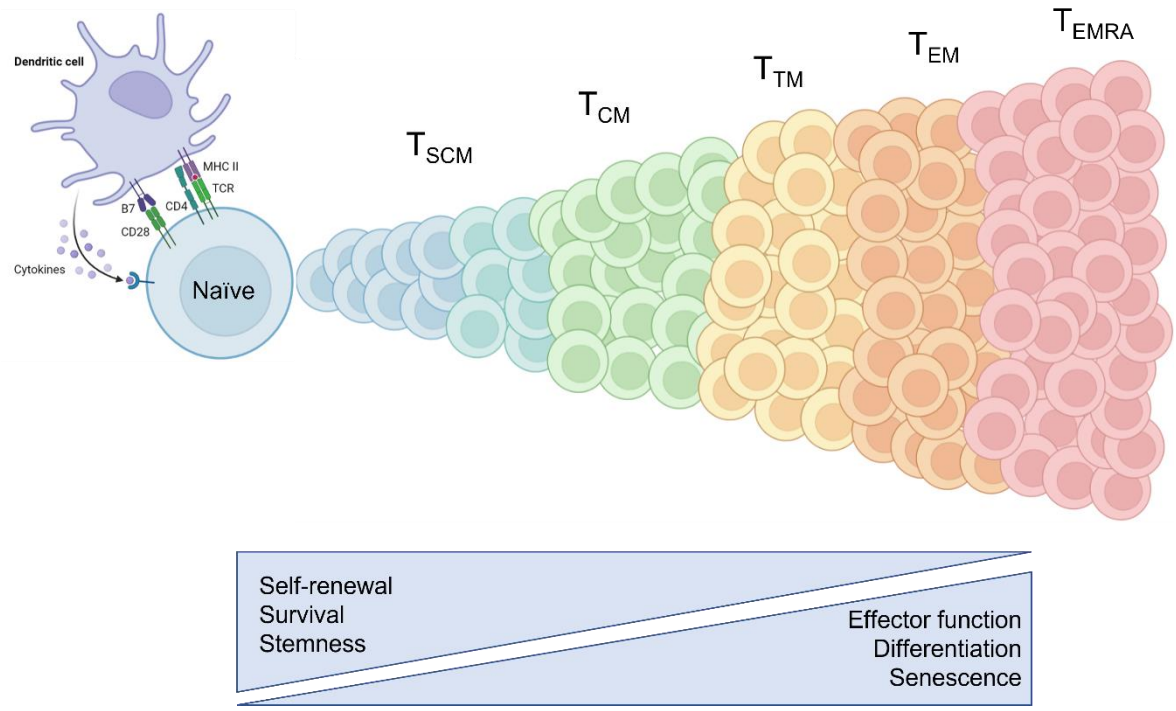

Figure 5 *CD4+ T cell population is heterogeneous and has been compartmentalized in at least six different subsets, which differ for the maturational state, stem or effector properties, and half-live: naïve, stem-cell memory (TSCM), central memory (TCM), transitional memory (TTM), effector memory (TEM) and effector memory re-expressing RA (TEMRA). The naïve compartment has not encountered its cognate antigen, while TSCM is the most long-lived memory subset. TCM retains homing receptors and settles into T cell areas of secondary lymphoid tissues, while TTM and TEM migrate to inflamed tissues and have immediate effector functions. TEMRA displays the most effector phenotype. Created with BioRender.*

Apart from the different expression of cell-surface markers, TCM and TEM were shown to secrete a different profile of cytokines, which was predominated by IL-2 for TCM and by effector cytokines such as TNF-α, IFN-γ and IL-4 for the TEM subset[220]. TCM were then proposed to cover an intermediate differentiation stage between naïve cells and TEM subset. Upon antigenic stimulation, TCM can differentiate in TEM, while TEM cannot revert to a TCM phenotype. The existence of these two subsets was also confirmed in a mouse model and TCM were shown to retain a higher proliferative capacity compared to TEM[221]. An intermediate phenotype that defines the TTM subset between TCM and TEM is recognized by the expression of another cell-surface marker, CD27[222]. Member of the TNFR family, CD27 is expressed by naïve CD4+ and CD8+ cells as much as most of memory T cells. The combination of CCR7 and CD27 markers defines the three memory subsets TCM (CCR7+/CD27+), TTM (CCR7-/CD27+) and TEM (CCR7-/CD27-). *In vitro* stimulation studies confirmed the intermediate phenotype of TTM, which were able to differentiate only towards the

T_{EM} subset. In addition, telomers lengths were shown to decrease following the stepwise differentiation pathway proposed (T_{CM} > T_{TM} > T_{EM})[223].

Recently another memory subset designated T_{SCM} was discovered in both animal models and humans[224–226]. By analyzing the expression patterns of the CD95 receptor (also FAS receptor), this discrete memory subset peculiarly expresses the RA isoform typical of naïve cells together with the CD95 marker, typical of memory subsets (CD45RA+/CD45RO-/CD95+). T_{SCM} have been recognized as the least differentiated CD4+ and CD8+ memory subset, capable of reconstituting the full diversity of memory and effector T lymphocytes[227]. This subset accounts for only 2-4% of total CD4+ and CD8+ cells in the blood, has superior survival potential, stem-cell properties such as self-renewal and multipotency[226]. T_{SCM} can evolve from naïve differentiation after antigen encounter through *in vitro* IL-7/IL-15 stimulation, the activation of the Wnt/β-catenin pathway or the modulation of mTOR signaling[199,226,228]. These T_{SCM} stem-like properties have catalyzed the attention of many fields and this subset is increasingly considered pivotal for the maintenance of long-term protective T cell immunity[229]. A concrete number of studies confirmed that CD8+ T_{SCM} are elicited by natural infections or vaccination such as the live-attenuated yellow fever virus (YFV) vaccine and multiple COVID-19 vaccines and that this subset mediates lifelong protection[230]. Particularly, multiple groups detected the generation of CD8+ T_{SCM} in COVID-19 convalescent or vaccinated individuals, significantly correlating the persistence of this subset with the durability of infection or vaccine-induced CD8+ T cell response[231–233]. Interestingly, CD4+ T_{SCM} are gradually appearing to cover a pivotal role in HIV-1 latency due to their intrinsic features: they are long-lived cells, with a high capacity of self-renewal and mature into more differentiated subsets[226].

It is estimated that the T_{SCM} half-life is double compared to the T_{CM} one, indicating a possible primary role in HIV-1 persistence during prolonged HAART. This subset is susceptible to HIV-1 and its relative contribution to HIV-1 maintenance increases over time[234]. Longitudinal analysis in HAART-treated patients revealed the stability

of HIV DNA values in T_{SCM} while observing at the same time decay in the other CD4+ memory subsets[235,236]. This disproportionate increase in latently infected T_{SCM} consistently matches with a role as a stable and durable reservoir.

The more differentiated and short-lived CD4+ T cell subsets are named T_{EMRA}. They have an effector function and are characterized by the re-expression of RA isoform and downmodulation of both CD27 and CCR7. This subset has been studied mostly in the CD8+ memory compartment and its molecular characteristics and functions are largely unknown[215]. T_{EMRA} express effector molecules such as granzyme B and perforin[237] and are a short-lived effector subset[238]. Given these hallmarks, it is still not clear whether T_{EMRA} represents an homogeneous[239] subset and its contribution to the latent reservoir might be minimal if not absent.

HIV-1 persists in all CD4+ memory T subsets (T_{SCM}, T_{CM}, T_{TM}, T_{EM}) and these cells harbor the bulk of HIV DNA, being the major component of the latent reservoir under HAART. The differentiated T_{TM} and T_{EM} subsets are the most susceptible to HIV-1 infection, while T_{SCM} and T_{CM} are thought to be more refractory to infection[240,241]. Naïve cells can also be infected and could play a role in HIV-1 persistence[242,243], although many doubts have been raised. The presence of active SAMHD1 and the extremely low levels of CCR5 displayed in these non-antigen-experienced cells are clear barriers to HIV-1[244]. In addition, there is a technical limit regarding the precise definition of the naïve subset when using only the classical CD45RA/CCR7/CD27 cell-surface markers. Indeed, the discovery of T_{SCM} has imposed the implementation of CD95 to distinguish the two populations, and recent studies have succeeded in isolating CD45RA+/CCR7+/CD27+ cells depleted by CD95-expressing cells, detecting replication-competent HIV-1 and thus sustaining the naïve susceptibility to HIV-1[244]. In the memory compartment, it is generally accepted that less differentiated subsets such as T_{SCM} and T_{CM} might be the most recalcitrant source of viral production under HAART. Particularly, a study that quantified replication-competent HIV-1 in the T_{CM} subset have demonstrated that this subset is the major contributor of the latent reservoir[245]. Upon antigen

stimulation, T_{CM} are also the source of most differentiated T_{EM}, which contribute less to HIV DNA persistence but have been demonstrated to account for most of the clonal expansion and possibly viral rebound when HAART is interrupted[246,247]. HIV DNA is known to be present at higher levels in T_{SCM} than in other memory compartments[234]. Even though T_{SCM} are rare and represent a minute fraction of the latent reservoir, their importance may result fundamental in HIV-1 latency because of their long-lived feature.

Such heterogeneity in the biology of CD4+ naïve and memory T cells reveals an equal complexity in the distribution of latently infected cells that is far to be understood. The mechanisms of latency establishment and maintenance of the latent reservoir has been analyzed mainly in total CD4+ T cells. However, the many distinct subsets that characterize the CD4+ population demands a deeper analysis.

Mechanisms of latency

The mechanisms by which HIV-1 latent infection is established and maintained in resting naïve and memory CD4+ T cells retrace the complexity and heterogeneity of susceptible cells. Unlike classical latent infections such as the one established by herpesviruses[167], HIV-1 latency cannot be intrinsically recapitulated to the expression of latent viral factors. Indeed, it has become increasingly clear that HIV-1 latency is likely a multifactorial process in which both viral and cellular factors interact to form a variety of non-productive infectious states. Challenging the classical association between the latent state with a transcriptionally silent HIV-1 provirus, an increasing number of studies indicate that several other blocks may contribute to the inability of persistently infected cells to yield viral progeny. Indeed, a complete silencing of the proviral LTR promoter has been proven a rare event[248], and possibly most latently infected cells may produce low levels of viral transcripts without producing viral particles[249]. These blocks could vary in each infected CD4+ subset and take place during the transcription initiation, transcription elongation, nuclear export as much as translation impairment[250]. In

addition, also the site of integration and chromatin modifications could deeply influence the infection output[251]. These pathways are of high interest and can be targeted *in vivo* by latency-reversing agents (LRAs) to revert latency to a productive infection and take advantage of the host immunity or HAART to clear the infected cell and theoretically decrease the viral reservoir dimensions. LRAs have been used within a strategy named "Shock and Kill", where the "Shock" phase consists of the LRA-induced proviral reactivation and the "Kill" phase that relies on the cytopathic effects or clearance of virus-producing cells by the immune system. These drugs, which will be further discussed, can be divided into many pharmacological classes, each of them targeting a molecular pathway involved in maintaining HIV-1 latency: histone deacetylase inhibitors (HDACis), protein kinase C (PKC) agonists, P-TEFb agonists, second mitochondrial-derived activators of caspase (SMAC) mimetics.

It is known that HIV-1 integration preferentially occurs into actively transcribed genes[107,108] and that nuclear topography is a major determinant during the integration process[112]. Many membraneless structures (known as nuclear bodies, NB) are known to be present inside the nucleus and have multiple implications for genome function and gene expression regulation. Specifically, promyelocytic leukemia (PML) nuclear bodies (NB) are dynamic nuclear regions enriched in more than 200 types of proteins, with PML itself[252], that are heavily modified by cellular stress, viral infections included[253]. In quiescent cells, genomes of DNA viruses such as Herpes Simplex Virus 1 (HSV-1) accumulate at the periphery of PML NBs. Indeed, it has been shown that PML NBs have a role in inducing the latent/quiescent state of HSV-1 genomes chromatinization[254,255]. Emerging data have also demonstrated that HIV-1 latently infected cells exhibit interactions between PML NBs and the silent proviral DNA, mediated by the methyltransferase enzyme G9a[256]. During reactivation, a physical rearrangement was observed, with the active provirus being repositioned away from PML NBs by nuclear cytoskeletal polymerizations. As a whole, nuclear topology covers a prominent role in HIV-1

latency, with PML NBs and their repressive nature demonstrating the importance of the localization of the proviral integrated DNA for the fate of an active or latent infection.

Transcriptional interference could also silence HIV-1 transcription through promoter occlusion or convergent transcription. In the first scenario, the proviral integration takes place downstream of a host gene following the same polarity. RNA pol II initiates the host gene transcription and reads through the HIV-1-LTR displacing the TFs necessary for viral transcription (Sp1, NF-κB, NFAT) avoiding proviral expression[257]. This phenotype is reversible *in vitro* by inhibiting the upstream gene transcription or activating the proviral initiation of transcription through viral Tat or TNF-α induced NF-κB activation[258]. If HIV DNA is integrated in opposite orientation relative to the host gene, convergent transcription may prevent the proviral transcription by collision of the RNA pol II complexes placed on the host and viral promoters. A competition between the two promoters could occur, from which the strongest of the two may be the only one to be transcribed[259]. Convergent transcription can also result in the transcription of both DNA strands, regardless of the obstruction, producing a dsRNA that might interfere with proviral transcription via RNA interference[260].

During latency, the HIV-1 promoter is tightly controlled by epigenetic factors, including DNA methylation, histone modifications and nucleosomal position. DNA methyltransferases enzymes catalyze DNA methylation, which typically occurs at C-phosphate-G (CpG) dinucleotides sites and acts to repress gene transcription. CpG methylation occurs at the 5' HIV-1 LTR and possibly avoids the binding of multiple important TFs[261]. A study performed by Kauder and colleagues reported the presence of two CpG islands flanking the transcriptional start site in the HIV-1 promoter, in both J-Lat cell lines and primary total CD4+ cells. The abrogation of methylation of these two sites promoted a sharp increase in viral gene expression[262]. However, opposite data have also been reported regarding CpG methylation and

one study found this signature in only 2.5% of viral promoters in infected individuals receiving HAART[263]. Methylation at the level of histones have also been investigated and correlated with proviral transcriptional activity. In the latent state, the 5′ LTR is predominantly characterized by dimethylation (H3K9me2)[256,264] or trimethylation of histone H3 lysine 9 (H3K9me3)[265] or trimethylation of histone H3 lysine 27 (H3K27me3)[266]. Such variability suggests a complex landscape that modulates the accessibility to the HIV-1 promoter. The extent of this plethora of modifications in silencing the viral DNA, plus the existing differences in naïve and CD4+ memory subsets, is still unclear.

Upon integration, proviral DNA is immediately chromatinized and two nucleosomes, nuc-0 and nuc-1, are positioned on the 5′ LTR flanking several transcription factors binding sites comprised in the DNase I hypersensitive sites II and III and thus modulating proviral activity[267]. These histone complexes are post-translationally modified to promote proviral transcription through acetylation by histone acetyltransferases (HAT) or silencing through deacetylation by histone deacetylases (HDAC)[268,269]. By transferring an acetyl group from acetyl-CoA to the lateral chain of lysine residues within N-terminal tail regions of histones, HATs loosen the interactions between histones and DNA causing easier access to the region to the transcriptional machinery[270]. HATs such as p300 and associated factors such as P/CAF (P300/CBP associated factor) display a well-documented role in proviral transcriptional activation and are recruited to the LTR promoter in a Tat-dependent manner (P/CAF) or following also other stimulation pathways such as NF-κB (P300)[271–274].

By contrast, HDACs are well known to promote and contribute to HIV-1 latency by enzymatically removing acetyl groups from lysine residues and compacting chromatin. HDAC1 is recruited by the p50 homodimer repressive form of NF-κB and bind to the LTR promoter, inducing histone deacetylation and the consequent repressive state that disfavors RNA pol II activity[275]. Given these characteristics,

HDAC inhibitors have been studied as potential LRAs[276]. Most of the clinical studies have concentrated on vorinostat (also known as SAHA), panobinostat and romidepsin, showing a transient increase in cell-associated HIV RNA in HAART-individuals without witnessing a decrease in the total HIV DNA[277–279]. At a subset level, HDAC inhibitors (vorinostat/SAHA, panobinostat, romidepsin) have been tested *ex vivo* aiming at reactivating latently infected cells[280]. The authors reached a modest reactivation of proviral DNA in all the CD4+ memory subsets (T_{CM}, T_{TM}, T_{EM}) considered and recorded different activities in distinct subsets, concluding that each subset is differentially responsive to LRA. Disappointingly, none of the mentioned studies demonstrated a decrease in the latent reservoir sizes.

Another crucial checkpoint for HIV-1 latency establishment and maintenance is at the level of transcription initiation. As already mentioned, the U3 region of the 5' LTR viral promoter contains multiple binding sites for cellular TFs, such as NF-κB, able to enhance proviral transcription. In resting CD4+ T cells, active NF-κB dimers are excluded from the nucleus supporting the silencing of the provirus[135]. The p50/RelA (also named p50/p65) heterodimer interacts with the IκB inhibitor protein (IKK) in the cytoplasm of these cells and the p50/p50 homodimers, lacking the transactivation domain, localize in the nucleus. NF-κB p50/50 inhibits proviral transcription by condensing the regional chromatin and recruiting the histone deacetylase HDAC1 at the LTR site[275]. This scenario drastically changes upon the CD4+ resting cell activation, which induces the p50/RelA heterodimer translocation to the nucleus and the subsequent p50/p50 dislocation. Transcriptional activation is then achieved by p50/RelA-mediated HAT recruitment[139]. Such studies have been mostly performed in total CD4+ T cells or analyzing the NF-κB role in the development of CD4+ and CD8+ effector population. It is still not clear whether NF-κB availability and translocation vary between CD4+ naïve and memory subsets.

The understanding of the NF-κB pathway in HIV-1 latency has helped to identify LRAs also targeting the initiation of viral transcription such as PKC agonists and

SMAC mimetics. Bryostatin, ingenol and prostratin PKC agonists induce HIV-1 expression both *in vitro* and *in vivo* by activating NF-κB and binding RelA to the latent HIV-1 promoter[281]. Particularly, prostratin was shown to efficiently reactivate HIV-1 in a mouse model but displayed a variable activity when tested on a single CD4+ memory subset[280,282]. The same study reported that a combination of one PKC agonist (ingenol) plus two HDACs (panobinostat and romidepsin) showed the highest levels of p24+ cells, with the T_{TM} and T_{EM} subsets being the most reactivated subsets[280]. Similarly, SMAC mimetics have been shown to induce HIV-1 transcription by activating the ncNF-κB pathway. SMAC mimetics are small molecules peptidomimetics developed from conserved binding motifs of SMAC, cellular proteins that inhibit the IAP protein family. IAPs are components of the ncNF-κB pathway, and they constitutively degrade the NIK kinase, avoiding the p100 to p52 processing of NF-κB2 and accumulating inactive p100 in the cytosol.

A study by Pache and colleagues identified in 2015 a negative regulator of HIV-1 transcription of the IAP family, named BIRC2/cIPA1, that could be targeted to reverse HIV-1 latency[283]. BIRC2 depletion induced by the SMAC mimetics SBI-0637142 efficiently activated the NF-κB signal and HIV-1 proviral transcription *in vitro*. Combining SBI-0637142 with the HDAC panobinostat resulted in synergistic reactivation of the reservoir *ex vivo*. These promising results were confirmed by the same group in an HIV-1-infected humanized mouse model using a bivalent next-generation version of SBI-0637142 named Ciapavir[284], and in rhesus macaques infected with SIV with a structurally unrelated SMAC mimetics named AZD5582[285]. In both cases, SMAC mimetics induced HIV-1 and SIV RNA production in resting CD4+ cells but no reduction in the total HIV/SIV replication-competent reservoir was observed. Furthermore, none of these studies addressed the proviral reactivation at the subset level.

Another mechanism that modulates latency acts at the level of elongation of transcription. Efficient HIV-1 proviral transcription depends upon the viral protein

Tat and the interaction with the TAR RNA viral element and the cellular factor P-TEFb, composed by Cyclin T1 (CycT1) and the Cyclin-dependent kinase 9 (CDK9). CDK9 subunit, by phosphorylating the RNA pol II CTD, promotes elongation from the viral promoter. This Tat-mediated RNA pol II phosphorylation increases by 99% the elongation activity at the TAR binding site, promoting much higher levels of full-length proviral transcripts[126]. In resting cells, P-TEFb is sequestered in the cytoplasm and this phenotype has been associated with latency in primary CD4+ T cells[286]. Similarly, the absence of viral Tat can induce the permanent inactivation of viral transcription, as demonstrated using Tat dependent transcription inhibitors such as didehydro-cortistatin A (dCA) in primary latently infected CD4+ T cells[287]. P-TEFb agonists such as JQ-1 and I-BET have also been tested as LRAs to revert proviral latency. These drugs display high affinity for bromodomains of the BET protein family (Brd2/Brd3/Brd4), which in turn bind to P-TEFb complex. Specifically, Brd4 interacts with both P-TEFb subunits (CycT1 and CDK9), possibly competing with Tat. By preventing the binding between P-TEFb and Brd4, JQ-1 could promote binding of Tat to P-TEFb and so proviral reactivation, as shown in multiple cell lines[288].

As already mentioned, soluble factors such as cytokines are also known to play a role in HIV-1 latency establishment and maintenance. IL-7 is crucial for T cell homeostasis and drives CD4+ memory T cell persistence through homeostatic proliferation without reactivating the silent provirus[178]. IL-15 increases the susceptibility of resting CD4+ T cells to HIV-1 infection by inducing the phosphorylation of the restriction factor SAMHD1 in a JAK dependent manner[194]. For this many implications, IL-15 has been suggested to have a role also as reactivating directly or indirectly silent proviral DNA. Heterodimeric IL-15, the stable native complex composed by the soluble IL-15 and the IL-15Rα, reduced viral RNA in lymph nodes and plasma of SHIV-infected macaques[289]. Taking advantage from these promising results, an IL-15 superagonist has been developed and tested

for its LRA activity *in vivo*. The so-called N-803 is an engineered structure composed by a N72D mutant IL-15 molecule attached to its IL-15Rα and a human IgG1 fragment. The result molecule is at least 25 times more biologically potent than its natural counterpart[290]. N-803 displayed robust and persistent proviral reactivation in two animal models when administered after a CD8+ depletion[195], while showed a small but significant decrease in inducible PBMC hosting a replication-competent HIV-1 provirus in HAART-suppressed individuals[291]. This phase I clinical trial had an explorative objective of assessing the N-803 impact on the circulating latent reservoir. As much as for most of the other LRAs considered, it is unknown if these drugs potentially can decrease the latent reservoir dimension and if the efficacy displayed is similar for the CD4+ naïve and memory subsets. Different states of latency sustained by multiple mechanisms here described could render viral reactivation challenging in less differentiated CD4+ subsets such as naïve and T_{SCM}. Some evidence suggest that triggering differentiation of less differentiated subsets prior to LRA treatment may increase the inducibility of the latently infected cell and could be the best option to decrease the sizes of an otherwise non-inducible latent reservoir[292,293].

Another determinant for HIV-1 latency establishment is the metabolic state of the infected cells. Naïve lymphocytes have low levels of metabolic activity, and they rely almost exclusively on oxidative phosphorylation (OXPHOS). Upon antigen stimulation, a drastic metabolic reprogramming is needed to sustain clonal expansion and biomass production. An upregulation in glycolysis, tricarboxylic acid (TCA) cycle and OXPHOS is needed to cope with the production of effector cells and their rapid proliferation. On the other hand, memory subsets' maintenance relies majorly on glycolysis and anaerobic respiration[294]. These marked differences have been object of study and two recent works have correlated the metabolic status of CD4+ cells with their susceptibility to HIV-1[295,296]. Specifically, Valle-Casuso and colleagues demonstrated that HIV-1 selectively infects cells with enhanced

glycolysis and OXPHOS signatures. Interestingly, this metabolic activity enhancement was recorded mostly in differentiated CD4+ memory subsets such as T_{CM} and T_{EM}, correlating with the higher susceptibility to infection displayed by these subsets. On the other hand, Shytaj and colleagues focused on latently infected cells suggesting that this status is characterized by a glycolysis downregulation. Such signature could be exploited for a better targeting in the context of eradication strategies[296].

Latently infected cells are rare in HIV+ individuals, with approximately a frequency of one in a million infected CD4+ T cells, and no specific latency marker is known[149,151]. Indeed, current technologies do not allow the identification and separation of latently infected cells from uninfected cells in HIV+ patients. These technical challenges have motivated the development of multiple *in vitro* and *in vivo* models to facilitate the investigation of HIV-1 latency over the years. *In vitro* models include clones of transformed cells with integrated proviral DNA, reporter cell lines and reporter viruses, while preclinical animal models include the infection of rhesus macaques with SIV or immunodeficient mice engrafted with human immune cells and infected with HIV-1. In recent years, dual-reporter viruses have emerged as practical and rapid tools to study latency establishment, persistence and reversal [297–300]. These reporter viruses can discriminate between LTR-transcriptionally silent infected cells and LTR-transcriptionally active cells, combining the expression of multiple cell-surface markers or florescent proteins. Most of the dual reporter viruses are developed to express one reporter under the control of an LTR-independent promoter (for example PGK, EF1α, CMV), that allows the identification of cells containing an integrated silent provirus and another reporter under the control of the viral LTR that will allow the identification of cells containing an integrated provirus that is actively transcribing viral genes. One of the first developed reporter virus was produced by Calvanese and colleagues and named DuoFluo[298]. The virus was engineered as a single-round virus that carried

two fluorescent reporters (eGFP and mCherry) in the same ORF. The study was one of the first to report the heterogeneity of the latent reservoir and to demonstrate the robustness of this type of investigation. However, the system also demonstrated limits regarding the detection of latently infected cells and the suspected recombination between homologous regions within the N and C-termini of the adjacent reporter genes could have caused such spurious events[301]. Regardless the viral input, the percentage of latently infected cells (eGFP-/mCherry+) never increased proportionally nor exceeded 1% of totally infected cells. A second generation of the reporter was then generated by the same group and named HIV-GKO (Figure 1A, results)[302]. Silent point mutations were engineered in the GFP sequence to produce a codon switch GFP (csGFP) and the mCherry reporter was replaced with the unrelated mKO2 fluorescent protein to avoid homology recombination between the two new fluorophores carried by HIV-GKO. The study reported a more accurate quantification of latently infected cells that were increasing proportionally with the viral input, plus a higher percentage of double positive cells (GFP+/mKO2+) in HIV-GKO infected cells. Such improvements allowed a more accurate latency quantification and thus the feasibility of exploiting the tool for high-throughput screenings. In addition, HIV-GKO latently infected cells were treated with a panel of different LRAs to provoke proviral reactivation and only a small fraction of these cells were inducible to produce viral particles, closely mimicking what is observed in other studies[280,292,303].

Other strategies have been pursued to differently engineer the fluorescent proteins in the viral genome. One study, for example, developed a dual-reporter virus called Red-Green-HIV (RGH) bearing eGFP and mCherry in different ORFs. When tested in Jurkat cell line and in primary CD4+ T cells, the group observed that the majority of integrated RGH provirus was LTR-silent 4-5 dpi, deviating from other results obtained with different reporter viruses[297]. More recently, Kim and colleagues improved another dual reporter virus called pMorpheus-V5 that carried the latent

reporter and the productive reporter in two different open reading frames undergoing separate splicing events (Figure 6)[300,304]. Additionally, this reporter used PGK as a strong and constitutively promoter to control latency protein tags and included the gene for the Nef accessory protein. This tool was used to identify latently infected primary CD4+ T cells to assess the heterogeneity of the reservoir. pMorpheus infected cells were majorly LTR-silent in every subset considered, with T_{EM} and T_{REG} displaying the highest levels of latently infected cells.

Regardless the intrinsic limitations of such *in vitro* studies, developing a specific and reliable tool to detect latently infected cells using dual-reporter viruses is of high interest for many applications such as latency establishment, LRA assessments and host gene expression profiles following latency.

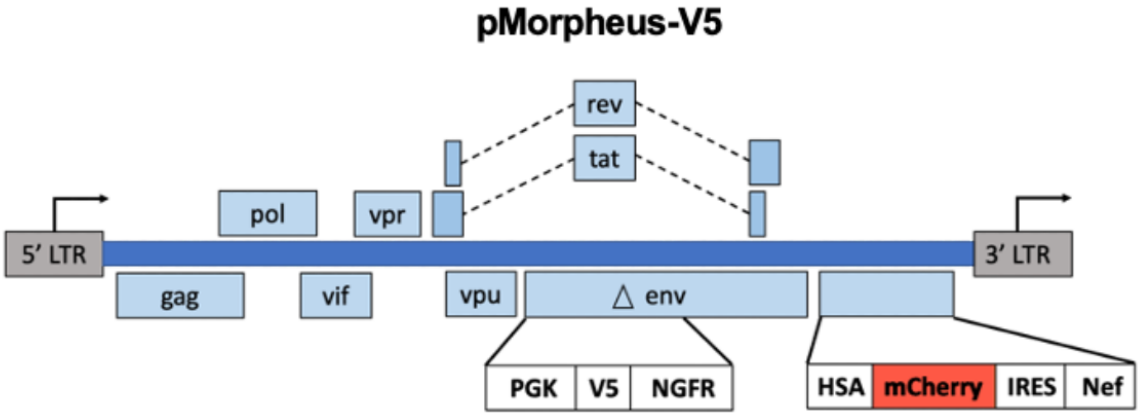

Figure 6 *Schematic representation of pMorpheus V5 viral vector. The genome bears a defective env gene and encodes for multiple reporters: NGFR, plus a V5 tag, under the cellular PGK promoter and mCherry, plus the HAS tag, under the LTR viral promoter. Image from Kim, Eun Hye, et al. "Development of an HIV reporter virus that identifies latently infected CD4+ T cells." Cell reports methods 2.6 (2022): 100238.*

AIMS of the work

This thesis explores HIV-1 latency establishment in *ex vivo* CD4+ naïve and memory T cell subsets stimulated with IL-15. The major contributors to the HIV-1 latent reservoir are resting CD4+ T cells that are generally refractory to the infection. However, these cells are rendered susceptible through various pathophysiological perturbations, including an up-regulation of IL-15 in the early phases of acute infection. The abundance of IL-15 in plasma of acutely infected individuals is correlated with higher viremia, increased viral set point and accelerated disease progression, while its signaling cascade leads to the relief of an early block in HIV-1 life cycle. The heterogeneity underling CD4+ susceptible subsets has been revealed to be a major issue for strategies that aim to revert latency. Even though the administration of multiple LRAs has successfully reactivated a percentage of latently infected cells, this fraction is negligible and varies from subset to subset. A better characterization of each subsets' role in the latent reservoir and the propensity of each of them to harbor a latent infection or a productive infection has become crucial to tailor a more effective reactivation strategy. To address this gap, this study has the objective to analyze at the single-cell level the establishment of latent or productive infection using a dual reporter virus named HIV-GKO able to discriminate between LTR-silent and LTR-actively infected cells[298,302]. The pathophysiological role of IL-15 during the reservoir establishment is still not well defined and by stimulating the infected cells with IL-15, the study aims to discover new molecular mechanisms that modify cell susceptibility to the infection.

Chapter 2 – Materials and methods

CD4+ lymphocytes isolation and culture

Buffy coats sacks were obtained from Centro Trasfusionale, Ospedale Maggiore Policlinico di Milano, where anonymous healthy donors were drawn their blood. Human peripheral mononuclear cells (PBMCs) were purified through density gradient centrifugation (Ficoll-Paque plus, GE Healthcare) and subsequently CD4+ T cells were enriched through immunomagnetic negative selection (CD4+ T cell isolation kit, Miltenyi biotech) according to manufacturer's instruction. Isolated CD4+ were cultured in culture in RPMI 1640 (Gibco) supplemented with 10% (vol/vol) heat-inactivated fetal bovine serum (FBS, Gibco), 100 U/ml penicillin (Euroclone), 0.1 mg/ml streptomycin (Euroclone), 1X minimal essential medium (MEM) non-essential amino acids (Gibco), 2mM L-glutamine (Euroclone), 10mM HEPES buffer solution (Gibco) and1mM Sodium pyruvate (Gibco). When needed, purified CD4+ T lymphocytes were stimulated with 20ng/ml IL-15 (R&D Systems) or 20 UI/ml IL-2 (Miltenyi biotech). Cells were maintained at 37°C, 5% CO_2 humidified incubator.

HEK 293 TN culture

Human embryonic kidney cells (HEK 293 TN) cell line (System Bioscience, catalog number LV900A-1) were cultured in Dulbecco's modified Eagle medium (DMEM, Gibco) supplemented with 10% (vol/vol) heat-inactivated FBS (Gibco), 100 U/ml penicillin (Euroclone), 0.1 mg/ml streptomycin (Euroclone), 1X minimal essential medium (MEM) non-essential amino acids (Gibco), 2mM L-glutamine (Euroclone) and1mM Sodium pyruvate (Gibco). Cells were maintained at 37°C, 5% CO_2 humidified incubator. Cell line was tested for mycoplasma on a monthly base (MycoAlert detection Kit, Lonza).

Plasmids

The following plasmids were obtained through the NIH-AIDS Reagent Program, Division of AIDS, NIAID, NIH: HIV-1 92HT593.1 gp160 expression vector (pSIVIII-92HT593.1) from Beatice Hahn (catalog number 3077)[305] and pSyngp140JR-FL. HIV-1 Duo-Fluo II GKO LTR Wild-Type (WT) plasmid was a kind gift from Eric Verdin (University of California San Francisco, Buck Institute for Research on Aging)[302]. pMorpheus-NWS and pMorpheus dual-color plasmids were a kind gift from Simon lab: we thank Viviana A. Simon, Lubbertus C. Mulder and Eun Hye Kim (Icahn School of Medicine at Mount Sinai).

Viral stock production

Dual-reporter HIV-GKO stocks were produced by calcium phosphate transfection of HEK 293 TN cells. Briefly, 10 µg of HIV-GKO genome encoding plasmid and 5 µg of the R5/X4 or R5 envelope encoding plasmid were co-transfected on 5x106 HEK 293 TN cells in a 145mm2 petri dish. Transfection media was replaced overnight, and supernatants were collected after 24- and 48-hours post-transfection. Viral supernatants were clarified through a polyether sulfone (PES) 0.45 µm membrane filter and ultracentrifuged for 2 hours at 4°C (Beckman, swinging-rotor bucket SW 32-Ti, 80 000 x g)[299]. Viral pellets were resuspended in 1:100 of initial volume in PBS, aliquoted and stored at -80°C. Concentrated viruses were titrated through HIV combo antigen-antibody enzyme-linked immunosorbent assay (ELISA, Dia.pro BioProbes).

Viral infections

Mock, IL-2 (20 UI/ml) or IL-15 (20ng/ml) stimulated primary CD4+ T cells and plated in a U-bottom 96well plate were spinoculated with 300ng of p24 of R5/X4 or R5 HIV-GKO per million cells, in the presence of 2 µg/ml of polybrene (Sigma). After 2 hours of spin-infection at 32°C, cells were placed in the incubator at 37°C for

one hours and media was subsequently replaced with fresh RPMI with or without stimulation.

Flow cytometry and cell sorting

Uninfected and infected primary CD4+ T cells were stained and analyzed on Symphony fluorescence-activated cell sorter (FACS) machine (BD Bioscience) or Cytek Aurora machine. Live and dead cells were discriminated through the fixable viability stain 780 (FV 780, BD Biosciences). To discriminate between CD4+ naïve and memory subsets, the following antibodies were used: APC-R700 anti-CD27 (BD Biosciences), BV421 anti-CD95 (BioLegend), BV711 anti-CCR7 (BD Biosciences), APC anti-CD45RA (BioLegend), BUV605 or 805 anti-CD45RO (BD Biosciences), BUV395 anti-CD4 (BD Biosciences). For staining, cells were washed with PBS and incubated for 10 minutes with 1:1000 FV780 in PBS, at room temperature (RT) in dark conditions. Cells were then washed in PBS and stained with the antibody panel for 20 minutes at 37°C. After a wash in MACS buffer (Miltenyi Biotech), cells were fixed in PFA 1% in PBS and acquired at Symphony or Aurora machines. Data was analyzed using FlowJo software (FlowJo, LLC).

To sort HIV-GKO latently and productively infected CD4+ cells, at least $20x10^6$ CD4+ T infected cells were filtered through 50 μm filters (Filcons, Syntec International) and then sorted at cell sorted BD FACSAria III (BD Biosciences). Sorted cells were left at 37°C in an incubator for one hour and then stained with the above-described panel of antibodies and acquired at Symphony machine. To sort CD4+ T cells from healthy donors' blood, at least $20x10^6$ cells were stained as follow: APC-R700 anti-CD27 (BD Biosciences), BV421 anti-CD95 (BioLegend), PE anti-CD45RO (BioLegend), BV711 anti-CCR7 (BD Biosciences), APC anti-CD45RA (BioLegend), APC-Fire 750 anti-CD4 (BioLegend). Cultured cells were washed once with PBS and incubated with the antibody panel for 20 minutes at 37°C. After a MACS wash, cells were filtered and sorted on BD FACSAria III. Protein expression an mRNA analyses were then performed. Cell sorting was performed by INGM

cytometry facility. Mariacristina Crosti, Marilena Mancino and Maria Lucia Sarnicola.

Immunoblotting

Stimulated and unstimulated CD4+ T total and subset cells were lysed in radioimmunoprecipitation assay (RIPA) buffer (150mM NaCl, 1% NP-40, 0,1% SDS, 50 mM TRIS HCl pH = 8) supplemented with protease inhibitors (Roche), sodium fluoride (10mM) and sodium orthovanadate (1mM) (both Sigma). Cell lysates were then mixed with 10X Sample Reducing Agent and 4X LDS Sample Buffer (both ThermoFisher). Prepared samples were then loaded on a pre-cast 4-12% SDS-PAGE gels (Blot Bis-Tris precast gel, ThermoFisher) and run at a constant 200 V voltage for 45 minutes. Protein transfer from the SDS-PAGE to the 0.2 μm nitrocellulose membrane (Amersham Protran Western Blotting membrane, GE Healthcare) was performed at a constant 90V voltage at 4°C for 1 hour. Nitrocellulose membrane was then blocked with 5% milk in 1X Tris buffered saline with 0.1% Tween 20 (TBS-T) for 1h while gently rocking. Three washes in 1x TBS-T were performed and primary antibody was diluted 1:1000 in 5% bovine serum albumin (BSA) in TBS-T and membranes were incubated with the solution at 4°C overnight. TBS-T washed membranes were then incubated with appropriate secondary antibody (1:5000 in 5% milk in TBS-T) for 1h at RT, with gentle rocking. Three TBS-T washes were performed before developing the membranes with ECL reagents (Amersham, GE Healthcare), fully covering the membranes. Images were capture at IBright FL 1500 machine (ThermoFisher). The following primary antibodies were used: anti-SAMHD1 (Cell Signaling Technology, catalog no. 12361), anti-CDK9 (2316), anti-phospho-SAMHD1 (89930), anti-phospho-CDK9 (2549), anti-CyclinT1 (81464), anti-GAPDH (2118).

RNA extraction and reverse transcription qPCR (RT-qPCR)

Cellular RNA from CD4+ T cells was extracted using PureLink RNA minikit (Invitrogen), following manufacturer's instructions. Extracted RNA was treated with PureLink DNase (Invitrogen) and cDNA was generated using the SuperScript Vilo cDNA synthesis kit (ThermoFisher). Gene expression was quantified by quantitative real-time PCR using SensiFAST SYBR lo-ROX kit (Bioline) following manufacturer's instructions on a QuantStudio 5 real-time PCR machine (Applied Biosystems). To normalize data, RSP11 housekeeping gene expression was used. The following primers were used for the reactions: RSP11 forward, GCCGAGACTATCTGCACTAC; RSP11 reverse, ATGTCCAGCCTCAGAACTTC; CDK9 forward, CAAGTTCACGCTGTCTGAGA; CDK9 reverse, TAGCAGCCTTCATGTCCCTA; CyclinT1 forward, AACCTT CGCCGCTGCCTTC; and CyclinT1 reverse, ACCGTTTGTTGTTGTTCTTCCTCTC.

Immunofluorescence

Primary CD4+ T cells were sorted on FACSAria III machine (BD Bioscience) using the following antibody panel: BV421 anti-CD27 (BD Bioscience), PE anti-CD95 (BioLegend), PeCy7 anti-CCR7 (BD Bioscience), APC ani-CD45RA (BioLegend), BV605 anti-CD45RO (BD Bioscience), APC/Fire 750 anti-CD4 (BioLegend) and fixable staining LD FV780 (ThermoFisher). Sorted cells (naïve, T_{SCM}, T_{CM}, T_{TM} and T_{EM}) were plated in a U-bottom 96 well plate and cultured in 20ng/ml IL-15 for 8 days. 80x104 CD4+ T cells were seeded in duplicate, for each subset, on a 96well imaging plate (Eppendorf cell imaging plate) previously coated with 0.5 mg/ml poly-L-lysine at 4°C overnight. After a PBS wash, cells were left to attach to the plate bottom for 30 minutes, at 37°C in the incubator. Subsequently, cells were fixed with 4% PFA on ice at 4°C for 15 minutes and then washed 3 times with PBS. A permeabilization step was performed using 0.3% Triton X-100 for 15 minutes and then cells were blocked for 1 hour in a filtered PBS solution with 5% fetal calf serum (FCS), 3% BSA, 2% goat serum, 0.3% Triton X-100. After a wash in PBS, cells were

stained with anti-NF-κB p65 antibody (Abcam, clone E379, catalog no. 32536, 1:100) overnight at 4°C. The day after, 5 washes with PBS were performed and cells were incubated with the appropriate secondary antibody (goat anti-rabbit Alexa-Fluor 647, ThermoFisher) for 2 hours at RT. After 5 PBS washes, DAPI dye was used to stain nuclei (1:500 in PBS). A control with isotype was performed using goat IgG (ThermoFisher) using the same concentration used for the primary antibody. After PBS washes, cells were kept in a PBS solution with 10% glycerol until analysis. Fluorescent images were acquired with Leica SP5 confocal microscope (Leica microsystems) and using Las-AF v5 software.

Confocal microscopy and digital images analysis

IL-15 stimulated CD4+ T cell subsets populations from three different donors were seeded in duplicate and immunolabeled for NF-κB p65 and DAPI on 96well optical plates (Eppendorf cell imaging plates). The plates were semiautomatically acquired using a motorized stage mounter on an inverted true confocal laser scanning microscope (SP; Leica Microsystems) with 4 photomultiplier tube (PMT) detectors and 8 laser lines. Both Alexa-Fluor-647 NF-κB and DAPI staining were acquired simultaneously over two separate spectral detectors, using 405 nm and 633 nm laser lines, through a 1-arbitrary unit (AU) pinhole aperture. A 63x oil objective (numerical aperture, 1.43) was used together with a 3x zoom magnification. To achieve the best focal plan, an auto-focus system was used, and the best Z plan was acquired for each field of view (FOV). A minimum of n = 15 FOV were acquired for each well, with a minimum of n = 8 cells centered in each FOV over at least n = 4 independent biological replicates for each CD4+ T cell subset for each of the n = 3 donors. After the image acquisition through the LAS-AF software, ImageJ was used to convert files and NIS-Element v.5.30 software (Nikon-Lim instruments) was used to process and analyze the results. Semi-automatic image processing and quantification were achieved through ad-hoc pipelines of commands. The Richardson-Lucy deconvolution algorithm was applied to reach better image

details. Quantifications were performed via thresholding, binarization and object segmentation on the GA3 module of NIS-Element v.5.30. A global threshold algorithm was used to design both binary masks for DAPI signal and NF-κB-Alexa-Fluor-647 signal via pixel classification and morphological size restriction factors. Boolean operations were developed to generate combined masks for whole-cell segmentation and growing algorithm from DAPI-derived nuclei objects to water shedding of 640 signal. Binary subtraction was calculated for secondary objects segmentation (cytoplasmic and nuclear NF-κB enriched compartments). NF-κB compartmentalization in the nuclei and the cytoplasm, and over the whole cell, was calculated for each single identified cell object, both as mean fluorescent intensity (MFI) and number of compartmentalized NF-κB objects, and signal or object ratios. Data from single-cell objects was also elaborated via Excel and Graph Pad Prism software. Normalization was calculated by $X' = (X - X_{min}) / (X_{max} - X_{min})$ formula. Data acquisition and analysis was performed by Chiara Cordiglieri (INGM microscopy Facility manager).

Construction of pMorpheus dual-color and pMorpheus 15N tagged

The backbone of the pMorpheus-NWS dual-color viral vector (PGK-HA-NWS-HSA-mCherry-IRES-Nef) is based on a published version[304] that encodes for the full-length HIV-1 strain LAI[306]. The HA-NWS-T2A-eGFP fragment was built by overlapping PCR (CloneAmp HiFi PCR premix, Takara) using primers with nucleotide extensions homologous to the PmeI and SmaI restriction sequences, while the vector was digested with PmeI and SmaI enzymes (FastDigest restriction enzymes, ThermoFisher). The PCR amplified insert, encompassing the new latent reporter was cloned into the Env region of the vector using PmeI and SmaI restriction sites located 3' of the PGK promoter (In-fusion enzyme mix, Takara). Ligations were then transformed into competent cells (Stellar competent bacteria, Takara) following the manufacturer's instructions. The inserted fragment was

verified by sequencing. The substitution between the mCherry fluorophore with mKate2 fluorophore in the productive cassette was performed by using the HSA-mKate2-IRES-Nef or HSA-T2A-mKate2-IRES-Nef reporters obtained by overlapping PCR (CloneAmp HiFi PCR premix, Takara) using primers bearing extensions for the SanDI and Xho restriction sequences. These PCR products were separately cloned in the SanDI/Xho digested vector and transformed as described above.

Two versions of pMorpheus 15N tagged were constructed from the pMorpheus original backbone (PGK-HA-NWS-HSA-mCherry-IRES-Nef), following a similar procedure to the one used for the pMorpheus dual-color cloning. A pool of primers was designed encoding a 15-nucleotides random sequence and PmeI and SmaI restriction sequences that were then used to amplify the HA-NWS-15N or eGFP-15N inserts. The resulting PCR product was cloned into PmeI/SmaI digested vectors (FastDigest, ThermoFisher and In-fusion enzyme mix, Takara) and then transformed into competent cells (Stellar, Takara). To produce a plasmid library retaining a broad diversity at the 15N site, the totality of bacterial colonies produced by multiple transformation was collected and combined. The presence of the random 15N UMIs (unique molecular identifiers) was confirmed by Sanger sequencing (Figure 13, results).

<u>List of primers used for pMorpheus dual-color cloning:</u>

- PGK PmeI NWS 5': AGCTTACCgtttaaacATGGGGGCAGGTGCCACCGGC
- NWS T2A 3': ctccacgtcaccgcatgttagaagacttcctctgccctcGAGGATACCCCTGTTCCAC
- eGFP T2A 5': ctaacatgcggtgacgtggaggagaatcccggccctGTGAGCAAGGGCGAGGAGCTG
- eGFP SmaI 3': ATATCTCCTCCTcccgggTTACTTGTACAGCTCGTCCATGC

<u>List of primers used for pMorpheus HA-NWS-15N:</u>

- PGK PmeI NWS 5': AGCTTACCgtttaaacATGGGGGCAGGTGCCACCGGC
- NWS SmaI 3': TATCTCCTCCTcccgggNNNNNNNNNNNNNNNCTAGAGGATACCCCTGTTCC

<u>List of primers used for pMorpheus eGFP-15N:</u>

- PGK PmeI eGFP 5': AGCTTACCgtttaaacATGGTGAGCAAGGGCGAGGAGCT

- eGFP-15N SmaI 3': TATCTCCTCCTcccgggNNNNNNNNNNNNNNNTTACTTGTACAGCTCGTCCATGCC

List of primers used for pMorpheus mKate with or without T2A:

With T2A:

- LAI 5' SanDI: CAACCCCGAGGGGACCCGACAGGC
- HSA T2A 3': ctccacgtcaccgcatgttagaagacttcctctgccctcACAGTAGAGATGTAGAAGAGA
- T2A mKate 5': ctaacatgcggtgacgtggaggagaatcccggccctATGgtgtctgagctgattaagg
- mKate IRES 3': AATTGGCCGCCCTAGATGTCAtctgtgccccagtttgcta
- IRES 5' seq: catctagggcggccaattcgcc
- NEF 3' Fus XhoI: TTTTCCAGGTCTCGAGATGCTGCTCCC
- eGFP-15N SmaI 3': TATCTCCTCCTcccgggNNNNNNNNNNNNNNNTTACTTGTACAGCTCGTCCATGCC

Without T2A:

- LAI 5' SanDI: CAACCCCGAGGGGACCCGACAGGC
- HSA Kozak 3': GGTGGCGGCCTAACAGTAGAGATGTAGA
- HSA Kozak mKate 5': TCTACTGTTAGGCCGCCACCATGgtgtctgagctgattaag
- IRES 5' seq: catctagggcggccaattcgcc
- NEF 3' Fus XhoI: TTTTCCAGGTCTCGAGATGCTGCTCCC
- eGFP-15N SmaI 3': TATCTCCTCCTcccgggNNNNNNNNNNNNNNNTTACTTGTACAGCTCGTCCATGCC

Chapter 3 – Results

HIV-GKO dual reporter virus in *ex vivo* primary CD4+ T cells

Dual reporter viruses have been shown to be a potent tool to study HIV-1 latency *in vitro* and *ex vivo*[297,298,302,307]. We used a dual reporter second-generation virus named HIV-GKO that carries a codon-switched green fluorescent protein (csGFP) under the 5' LTR promoter and Kusabira Orange (mKO2) under the constitutively active cellular EF1α promoter[298,302]. The genome lacks the *env* and the *nef* gene (Δenv Δnef) and does not support spreading infection. The two reporters are positioned in place of *nef* and EF1α promoter is placed in between. Primary CD4+ T lymphocytes support the infection with HIV-GKO and the discrimination between latently infected cells, which are LTR-silent, and productively infected cells, which are LTR-active, is achieved by the expression analysis of the two fluorophores controlled by the two promoters (Figure 1). Latently infected cells express only mKO2 (mKO2+/GFP-) while productively infected cells express both mKO2 and csGFP (mKO2+/csGFP+). HIV-GKO lacks a functional *env* gene in its genome, for this reason we generated viral stocks by pseudotyping HIV-GKO with a dual-tropic (R5/X4) HIV-1 subtype B envelope or a CCR5-tropic envelope (R5).

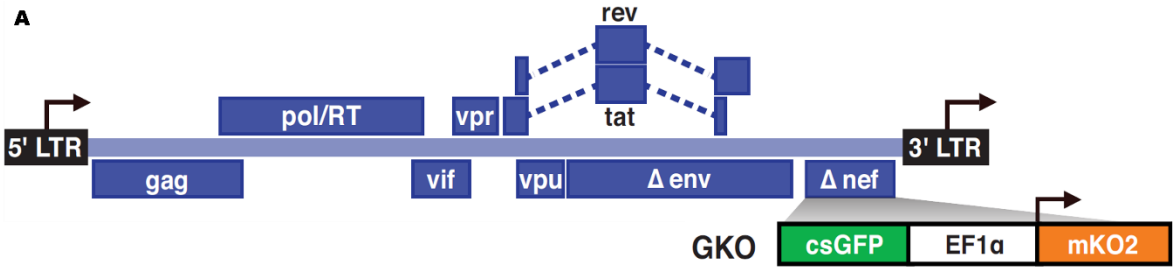

Figure 1 *Second generation dual-reporter virus HIV-GKO. Schematic representation of the genome organization lacking a functional env gene and bearing csGFP and mKO2 reporters instead of the nef gene. Infected CD4+ T cells with HIV-GKO express mKO2 reporter (if latently infected) or both mKO2 and csGFP (if productively infected). Image from Battivelli, Emilie, et al. "Distinct chromatin functional states correlate with HIV latency reactivation in infected primary CD4+ T cells." Elife 7 (2018): e34655.*

To determine our experimental set up for all experiments we started by performing a time course analysis of infection with two different viral amounts.

Primary CD4+ T cells were stimulated with IL-2 or IL-15 at equimolar concentrations for 3 days and infected with R5/X4 HIV-GKO. Total infection (mKO2+/csGFP-, mKO2-/csGFP+ and mKO2+/csGFP+) was monitored every day over a period of 7 days. A high dose of 500 ng of p24 (Figure 2 left) and a low dose of 50 ng p24 (Figure 2 right) per million cells was used. IL-15 stimulation increased overall infection compared to IL-2 in both high and low dose infections. The peak of infection was observed at day 5-6 regardless the viral input and the stimulation (Figure 2 left and right). To avoid infection saturation or low percentages of infected cells, we then decided to perform the rest of infection experiments with an intermediate p24 concentration equal to 300 ng/million cells.

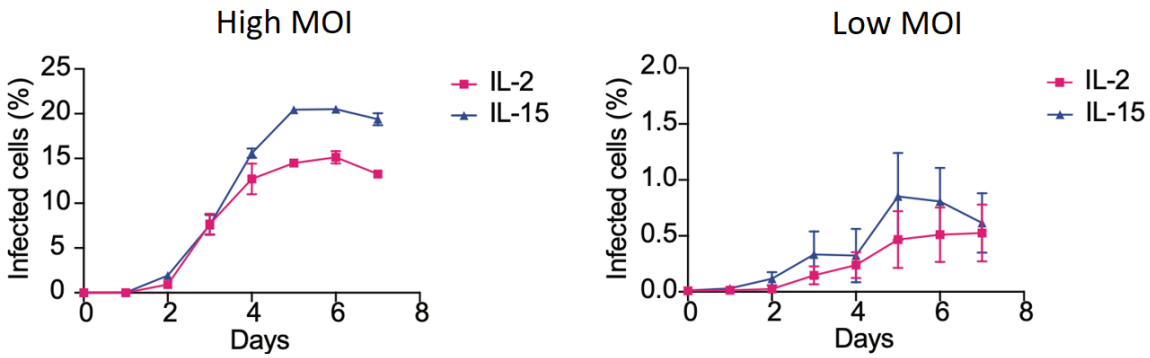

Figure 2 *R5/X4 HIV-GKO infection time-course at high multiplicity of infection (MOI, 300ng of p24 per million CD4, left) and low MOI (50 ng of p24 per million CD4, right). Primary CD4+ T cells were stimulated with equimolar levels of IL-2 and IL-15, and infection output was analyzed at flow cytometry measuring GFP and mKO2 signals. The percentage of total infected cells was calculated summing cells positive for GFP, mKO2 and both (n=3, data shown as ±SD of the mean).*

IL-15 increases the susceptibility to HIV-1 infection and transcription

IL-15 covers an important role in increasing the susceptibility of CD4+ T lymphocytes to HIV-1 but its role in the establishment of HIV-1 latency is still poorly characterized[194,308]. To investigate IL-15 role in HIV-1 latency establishment we stimulated CD4+ T lymphocytes with equimolar concentrations of IL-2 and IL-15, infected with 300 ng p24 of R5/X4 HIV-GKO and analyzed by flow cytometry 5 to 6 days post-infection (dpi) the expression of mKO2 and csGFP. Expression of csGFP

and mKO2 was used to discriminate latently infected (mKO2+/csGFP-) from productively (mKO2-/csGFP+ and mKO2+/csGFP+) infected cells, as previously reported (Figure 3 upper panel)[302].

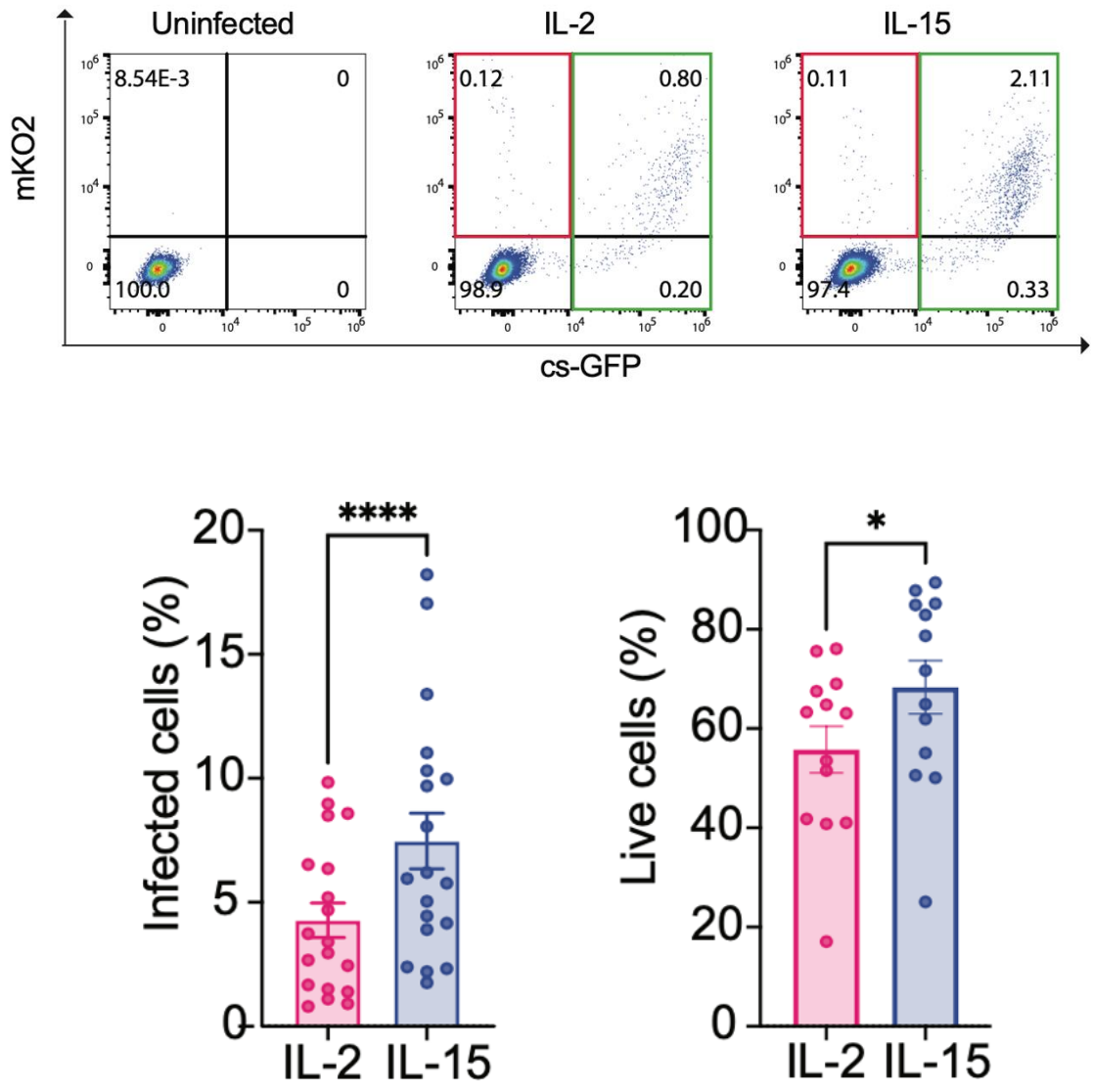

Figure 3 (Upper panel) *Representative FACS plot of R5/X4 HIV-GKO infection. csGFP and mKO2 were used to discriminate between latently infected cells (mKO2+/csGFP-) and productively infected cells (mKO2+/csGFP+ and mKO2-/csGFP+).* ***(lower panel)*** *Bar graph representing the percentage of total infected cells after IL-2 or IL-15 stimulation (left) and cell viability in the two conditions (right). Significance was determined by Wilcoxon matched-pairs rank test. *, P ≤ 0.05; **, P ≤ 0.01; ***, P ≤ 0.001; ****, P ≤ 0.0001.*

IL-15 stimulation increased both percentage of infected cells and cell viability, compared to IL-2 stimulated cells (Figure 3 lower panel). Subsequently, we specifically analyzed both productively and latently infected cells stimulated with IL-2 and IL-15 within total CD4+ cells. IL-15 stimulation increased the percentage of

productively infected cells but not the latently infected cells, compared to IL-2 stimulated cells (Figure 4A and B). Next, we calculated the proportion of latently and productively infected cell within the total infected CD4+ cells by quantifying the reported gene expression and calculating the percentage of positive cells. Most cells were productively infected by HIV-GKO under both stimuli (IL-2 and IL-15), while only a minority was latently infected. Specifically, IL-15 stimulation increased the percentage of productively infected cells compared to the IL-2 stimulation and decreased the percentage of latently infected cells compared to IL-2 stimulation (Figure 4C and D).

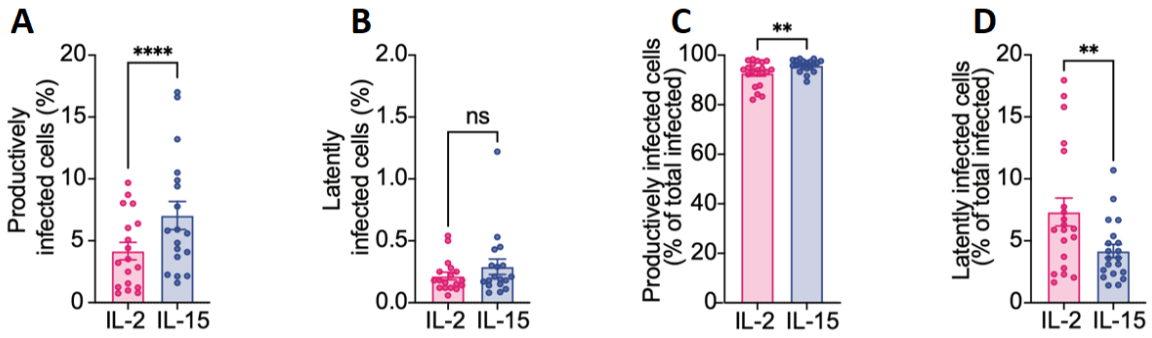

Figure 4 ***(A)*** *Bar graph showing the percentage of productively infected cells and* ***(B)*** *latently infected cells in the two experimental conditions over the total primary CD4+ T cells. Percentage of* ***(C)*** *productively infected cells within the total infected cells and* ***(D)*** *latently infected cells. Significance was determined by Wilcoxon matched-pairs rank test. *, P ≤ 0.05; **, P ≤ 0.01; ***, P ≤ 0.001; ****, P ≤ 0.0001.*

It has been shown that IL-15 induces SAMHD1 phosphorylation thus relieving an early block in reverse transcription and increasing overall infection compared to IL-2 treated CD4+ T cells. We analyzed also in our experimental settings the protein levels of the phosphorylated SAMHD1 on threonine 592 position (T592) in both IL-2 and IL-15 stimulated CD4+ T lymphocytes. In three different donors, IL-15 treatment increased almost 10-fold the phosphorylation of SAMHD1 (Figure 5A and B)[194,206,207]. However, when we analyzed the levels of csGFP and mKO2 expression by the mean fluorescence intensity (MFI) of the two fluorophores we observed that IL-15 stimulation increased almost by 2-fold the LTR-driven csGFP MFI when compared to IL-2 condition, while the mKO2 MFI remained stable under

both stimulations (Figure 5C), suggesting the involvement of IL-15 also during HIV-1 transcription.

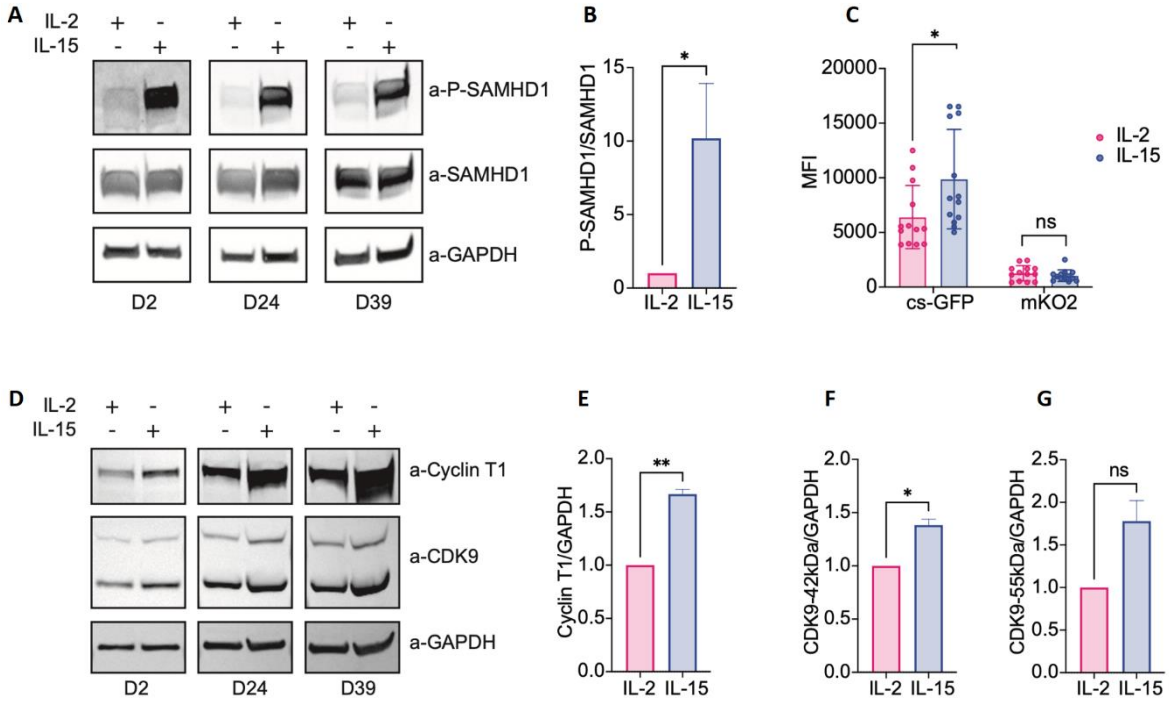

Figure 5 *(**A**) Primary CD4+ T cell lysates from three different donors (D2, D24, D39) were analyzed by immunoblotting for protein levels of SAMHD1, P-SAMHD1 and GAPDH, in IL-2 and IL-15 after 3 days of equimolar stimulation of IL-2 or IL-15. **(B)** Densitometric analysis of P-SAMHD1 levels normalized on total SAMHD1 level, in the two experimental conditions. **(C)** Mean Fluorescence Intensity (MFI) of both csGFP and mKO2 in primary CD4+ T cells infected with R5/X4 HIV-GKO after IL-2 or IL-15 stimulation. **(D)** Primary CD4+ T cell lysates from three different donors (D2, D24, D39) were analyzed by immunoblotting for protein levels of Cyclin T1, CDK9 and GAPDH after 3 days of stimulation with equimolar levels of IL-2 or IL-15. **(E)** Densitometric analysis of Cyclin T1 expression levels normalized on housekeeping protein GAPDH levels, in both conditions. **(F)** CDK9 42 kDa isoform expression level normalized over GAPDH levels, in both conditions. **(G)** CDK9 55 kDa isoform expression levels normalized over GAPDH. Significance was determined by Wilcoxon matched-pairs rank test. *, P ≤ 0.05; **, P ≤ 0.01; ***, P ≤ 0.001; ****, P ≤ 0.0001.*

We next sought whether IL-15 also modulated the protein expression of different subunits of P-TEFb, a pivotal cellular complex recruited by the viral Tat protein to increase proviral transcription elongation[125,309]. In three different donors, both the expression of Cyclin T1 and CDK9 subunits was upregulated after 8 days of IL-15 stimulation compared to IL-2 (Figure 5D). An average 50% increase was observed for both Cyclin T1 and the 42 kDa isoform of CDK9 under IL-15 condition (Figure 5E and F), while the 55 kDa CDK9 isoform increased without reaching statistical significance (Figure 5G).

Overall, we demonstrated that IL-15 increases CD4+ T lymphocytes susceptibility to HIV-1 not only by abrogating SAMHD1 activity, but also increasing the viral transcriptional activity by upregulating both P-TEFb subunits CyclinT1 and CDK9.

R5/X4 HIV-GKO infection does not alter CD4+ T cell subset distribution

Both IL-2 and IL-15 are members of the γ-chain cytokine family and play a role in T cell homeostasis and differentiation[310]. Upon stimulation with these family of cytokines, resting CD4+ T cells can undergo homeostatic proliferative events or differentiate into more effector phenotypes[177,199]. Therefore, we analyzed the effect of the experimental conditions, both IL-2/IL-15 stimulation and R5/X4 HIV-GKO infection, on the CD4+ subsets (naïve, T_{SCM}, T_{CM}, T_{TM}, T_{EM}, T_{EMRA}) immunophenotype and distribution. The six CD4+ naïve and memory T subsets were classified based

on the expression of the following cell-surface markers: CD45RA, CD45RO, CD27, CCR7, CD95 (Figure 6A)[216,311].

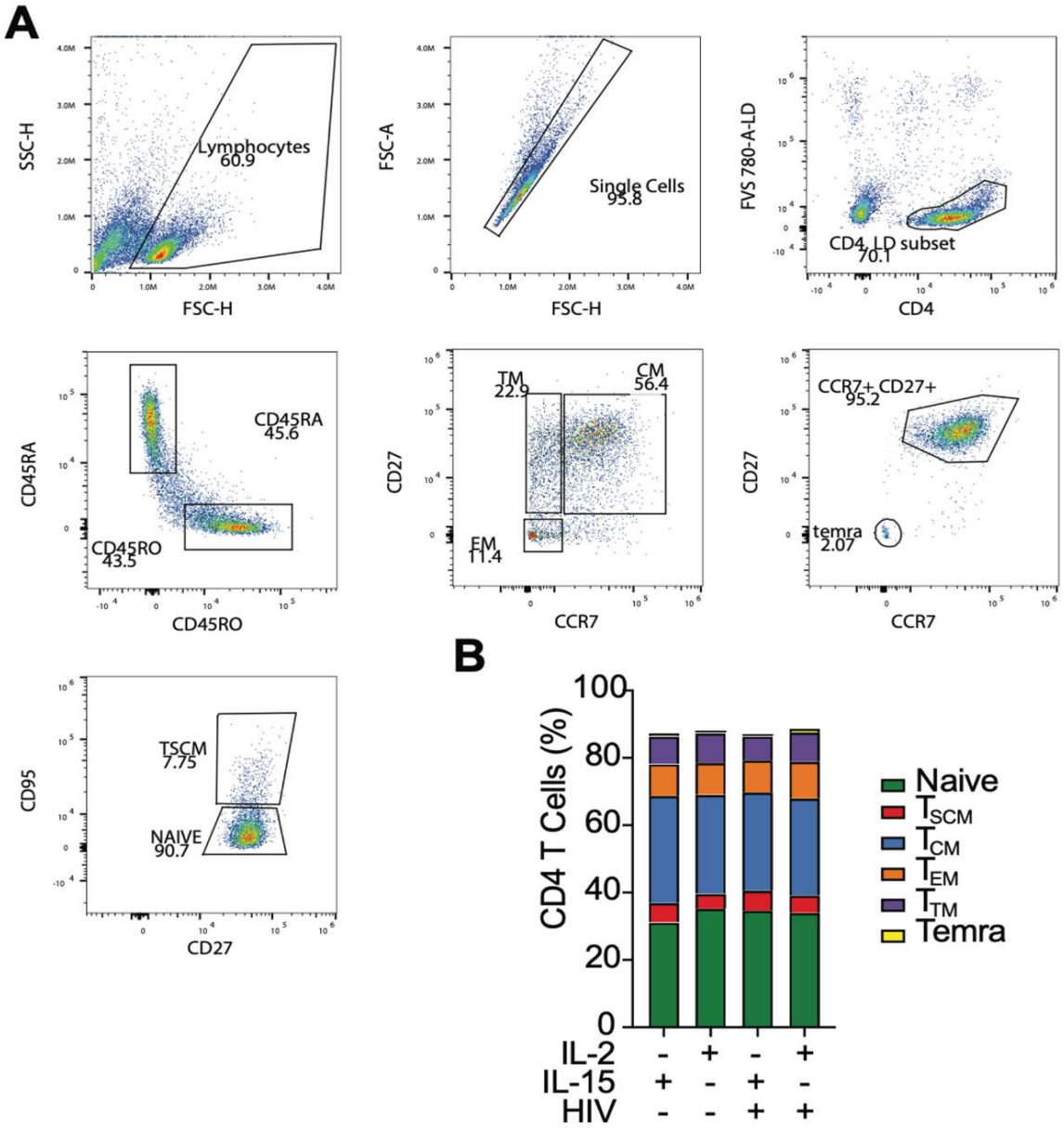

Figure 6 (A) *Flow cytometry gating strategy of primary CD4+ T cells. Representative gates are shown: naïve cells were identified as CD45RO+/CD45RA+/CD27+/CCR7+/CD95+,* T_{SCM} *cells were defined as CD45RO+/CD45RA+/CD27+/CCR7+/CD95+, Temra cells were defined as CD45RO+/CD45RA+/CD27+/CCR7+,* T_{CM} *cells were defined as CD45RO+/CD45RA+/CD27+/CCR7+,* T_{TM} *cells were defined as CD45RO+/CD45RA+/CD27+/CCR7+, and* T_{EM} *cells were defined as CD45RO+/CD45RA+/CD27+/CCR7+.* ***(B)*** *Stacked bar chart representing the relative percentage of each CD4+ subset to the total CD4+ population, in the indicated experimental conditions (equimolar levels of IL-2 or IL-15, R5/X4 HIV-GKO infection or not).*

A slight, but significant decrease in the T_{EMRA} subset was observed in IL-15 condition after infection, and an increase in the T_{SCM} proportion of IL-15 stimulated CD4+ lymphocytes was observed in both infected and uninfected condition (Figure 6B

and 7). Based on these results, we concluded that the overall distribution of the different CD4+ subsets was comparable among all conditions.

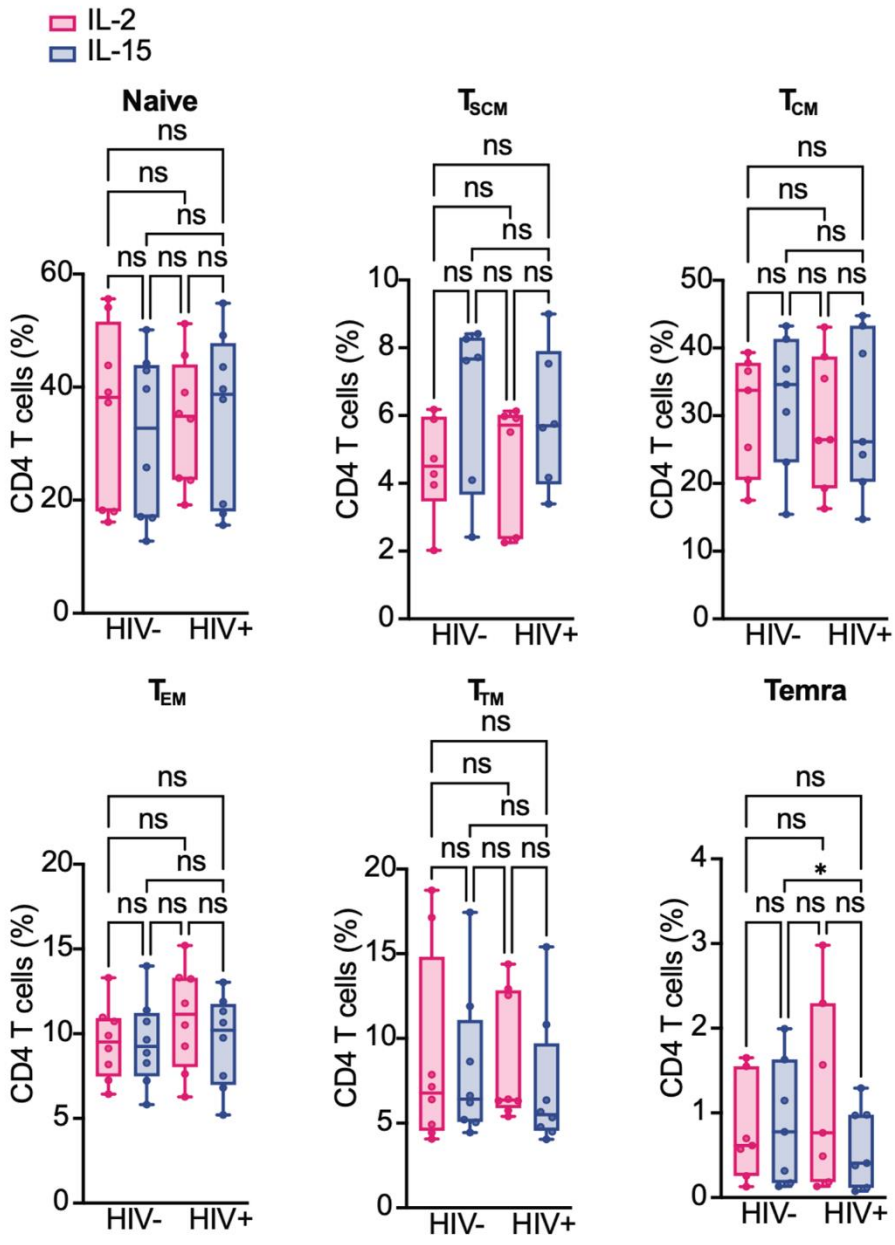

Figure 7 *Boxplots representing the frequency (%) of each CD4+ T cell subset in the experimental conditions: infected or non-infected cells and IL-2 or IL-15 stimulated cells. Significance was determined by Friedman test. ns, P> 0.05; *, P ≤ 0.05.*

R5/X4 HIV-GKO productive infection is more frequent in TCM, TTM, TEM

Each CD4+ T subset display different susceptibility to HIV-1 infection and proviral reactivation[292,303]. However, the proclivity of these subsets to establish a latent infection is still poorly understood. We then analyzed latency establishment in CD4+ naïve and memory subsets, for a total of five subpopulations (naïve, TSCM, TCM, TTM, TEM). TEMRA were excluded from this analysis due to poor availability and high variability among donors. Primary CD4+ T lymphocytes were stimulated with equimolar concentrations of IL-2 or IL-15 for 72 hours and subsequently infected with R5/X4 HIV-GKO. 5 dpi, cells were stained with the previously described panel of antibody against cell-surface markers to detect both latently infected and productively infected cells among the five CD4+ subsets. The high-dimensional data were visualized through the employment of t-distributed stochastic neighbor embedding (t-SNE) plots. The resulting two-dimensional maps allow to cluster phenotypically similar cells close to each other while separating them from phenotypically diverse cells, preserving at the same moment their local and global geometry[312].

Infected primary CD4+ T lymphocytes stimulated with IL-2 or IL-15 are shown in Figure 8A (upper left and bottom left), overlayed with latently infected cells in red and productively infected cells in green. We observed that productively infected cells were clustering in specific regions, while latently infected cells (red) followed a scattered motif without a pronounced clustering. To visualize the infection at the subset level, we next included the cell-surface markers in the t-SNE analysis (Figure 8B left panels) and overlayed the map with productively infected cells (Figure 8B middle panels) and latently infected cells (Figure 8B right panels). Most of the productively infected cells were clustering on top of the TCM (light blue cluster), TTM (purple cluster) and TEM (orange cluster), while occupying few spots in the right peninsula of the map were less differentiated subsets such as naïve and TSCM cluster

(Figure 8B, upper and bottom center). The distribution of latently infected cells was heterogeneous and evenly present throughout all the maps. If a qualitative, stronger presence of both latently and productively infected cell dark cloud was evident in t-SNE representing IL-15 compared to IL-2 treated cells, no differences could be appreciated in the distribution of latently or productively infected cells in the t-SNE of IL-2 treated (Figure 8A and B, upper panel) or IL-15 treated cells (Figure 8A and B, lower panel) regarding single subsets.

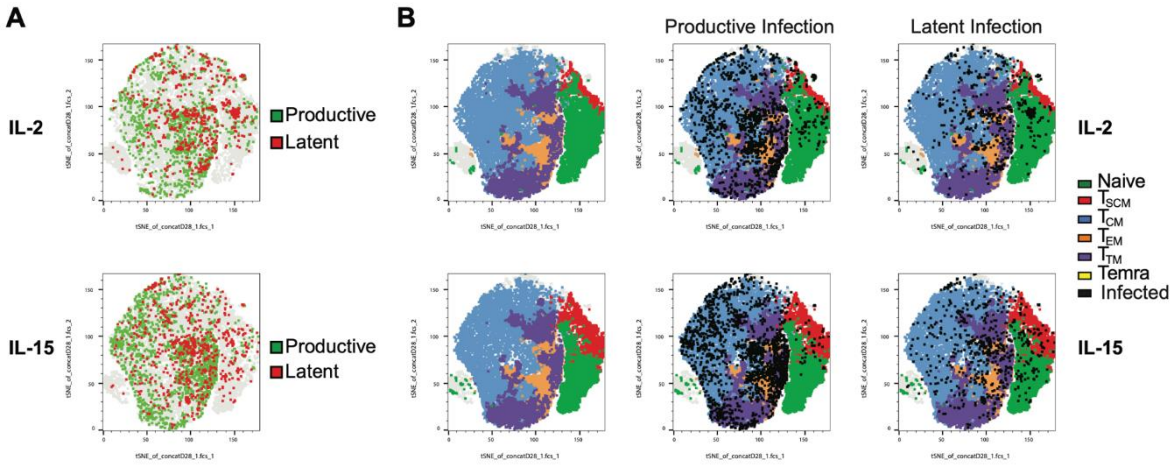

Figure 8 (A) *Representative t-SNE plots of R5/X4 HIV-GKO infections highlighting latently (red) and productively infected cells (green) overlayed on total CD4+ T cells, after IL-2 (top) or IL-15 (bottom) conditions.* ***(B)*** *Representative t-SNE plots of uninfected (left), productively infected (middle) and latently infected cells (right, black dots) overlayed on CD4+ naïve and memory subsets phenotypes (TSCM, TCM, TTM, TEM, Temra), in IL-2 (top) and IL-15 (bottom) conditions.*

The infection outcome was then analyzed more quantitatively, for both IL-2 and IL-15 experimental conditions. Figure 9 shows percentages of total infected, productively infected and latently infected cells (Figure 9A from left to right, respectively) over the total of IL-2 stimulated CD4+ T cells. Naïve subset was the most resistant to infection, with an average of 0.8% of infected cells (Figure 9A, upper left). TEM displayed infectious rates 10 times higher, with an average of 8% in the total infection (Figure 9A, upper left). Productively infected cells followed the same pattern, with naïve being the most refractory and TEM being the most permissive subset (Figure 9A, upper center), while latently infected cells showed similar percentages across all memory subsets with a significant exception between naïve and TEM (Figure 9A, upper right). To understand the latency enrichment in

each subset, we then calculated the proportion of latently infected cells within all the infected cells for each subset (Figure 9B). IL-2 treated naïve and T_{SCM} subset showed a slight propensity to harbor an LTR-silent provirus compared to the most differentiated subsets (T_{CM}, T_{TM}, T_{EM}) but these differences did not reach statistical significance.

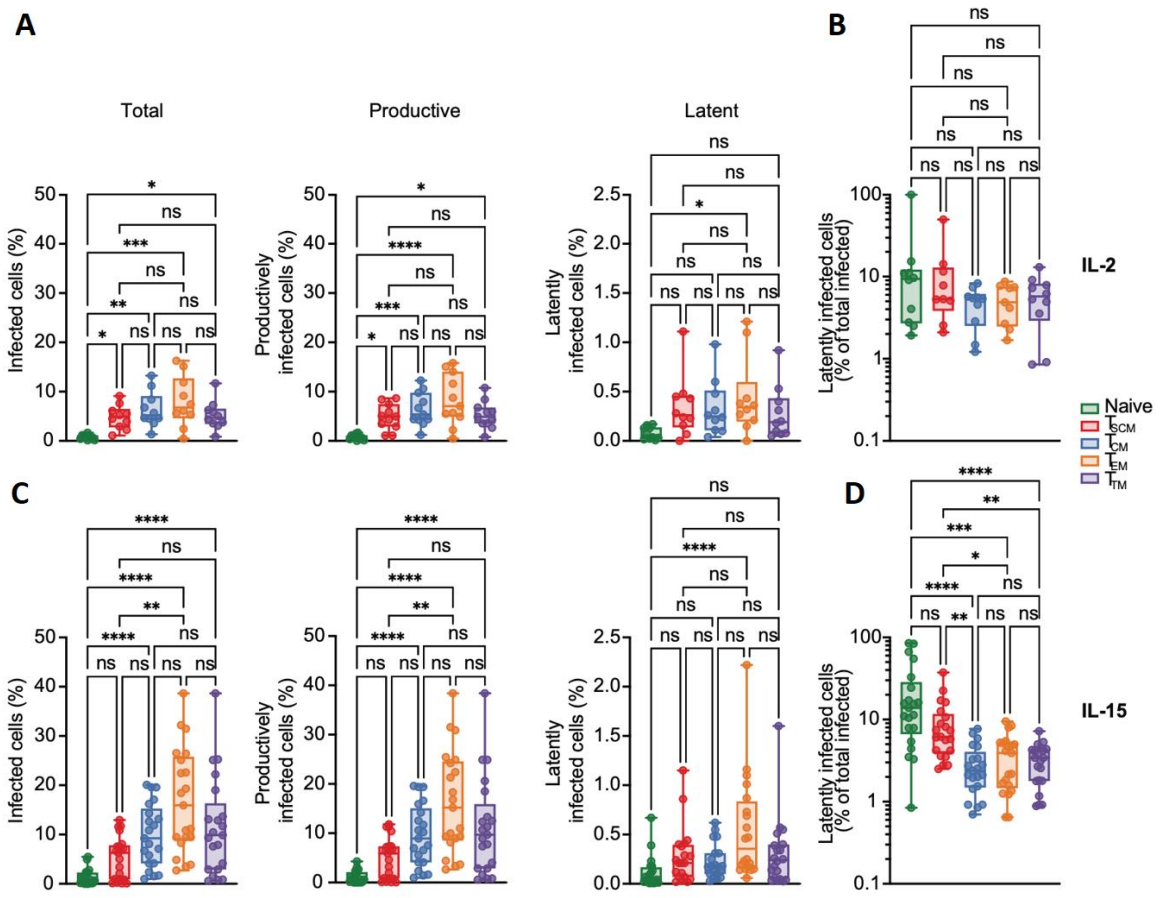

Figure 9 ***(A)*** *Boxplots of R5/X4 HIV-GKO infection in CD4+ T cells showing percentage of total, productive, latent infection (from left to right) in IL-2 condition in CD4+ naïve and memory subsets (T_{SCM}, T_{CM}, T_{TM}, T_{EM}).* ***(B)*** *Boxplot showing the percentage of latently infected cells over the total infected cells, in IL-2 condition.* ***(C)*** *Boxplot showing the percentages of total, productive and latently infected cells (from left to right) in CD4+ naïve and memory subsets in the IL-15 condition.* ***(D)*** *Boxplot representing the percentage of latently infected cells over the total infected cells, in IL-15 condition. Significance was determined by Kruskal-Wallis test. *, P ≤ 0.05; **, P ≤ 0.01; ***, P ≤ 0.001; ****, P ≤ 0.0001; ns, not significant.*

When we quantitatively analyzed IL-15 treated CD4+ cells, naïve was confirmed as the most resistant subset to infection, with an average 1.2% of infected cells over total CD4+, and T_{EM} remained the most permissive subset with an average infection of 16.8% (Figure 9C left). 9.8% of T_{CM} and 11.5% of T_{TM} were on average infected

after IL-15 stimulation, while the most resistant CD4+ memory subset was T_{SCM} with an average of 5.2%. Subsequently, we also analyzed the productively infected cells and latently infected cells after the IL-15 stimulation. Similarly to IL-2 condition, the percentage of productively infected cells resembled the total infection (Figure 3E, middle) and latently infected cells displayed less differences. T_{EM} was the subset harboring the highest percentage of LTR-silent latently infected cells (0.5% on average), followed by T_{TM} (0.3%), T_{SCM} (0.27%), T_{CM} (0.22%) and naïve (0.12%). For IL-15 treated cells, we performed the same analysis to quantify latency enrichment in each subset. By dividing the percentage of latently infected cell to total infected cells within each subset, we observed that naïve and T_{SCM} compartments displayed significantly higher values compared to the three most differentiated subsets. On average, 23.4% of infected naïve were LTR-silent, T_{SCM} were 9.3%, 2.9% for T_{CM}, 3.7% for T_{EM}, 3.2% for T_{TM} (Figure 9D). Overall, we concluded that naïve and T_{SCM} subsets are highly resistant to HIV-1 infection but when infected they are more likely to harbor a transcriptionally silent integrated provirus compared to the more differentiated CD4+ T subsets.

IL-15 increases R5/X4 HIV-GKO infection in all memory subsets

T-SNE plots in Figure 8 qualitatively represented the increased susceptibility of CD4+ T cells to infection after IL-15 stimulation, without presenting informative data regarding the effects compared to IL-2 at a subset level. We then compared the total and latent infection in each subset in both IL-2 and IL-15 condition (Figure 10A and B respectively). IL-15 stimulation significantly increased percentages of total infected cells in all CD4+ memory T cell subsets compared to IL-2 treated cells (Figure 10A). Naïve levels of infection did not differ in IL-2 or IL-15 treated cells, which could possibly be attributed to a lower expression of specific subunits in the IL-15R[313]. On the other hand, IL-15 decreased the percentage of cells harboring LTR-

silent provirus without reaching statistical significance in T_{SCM}, T_{CM} and T_{TM} (Figure 10B).

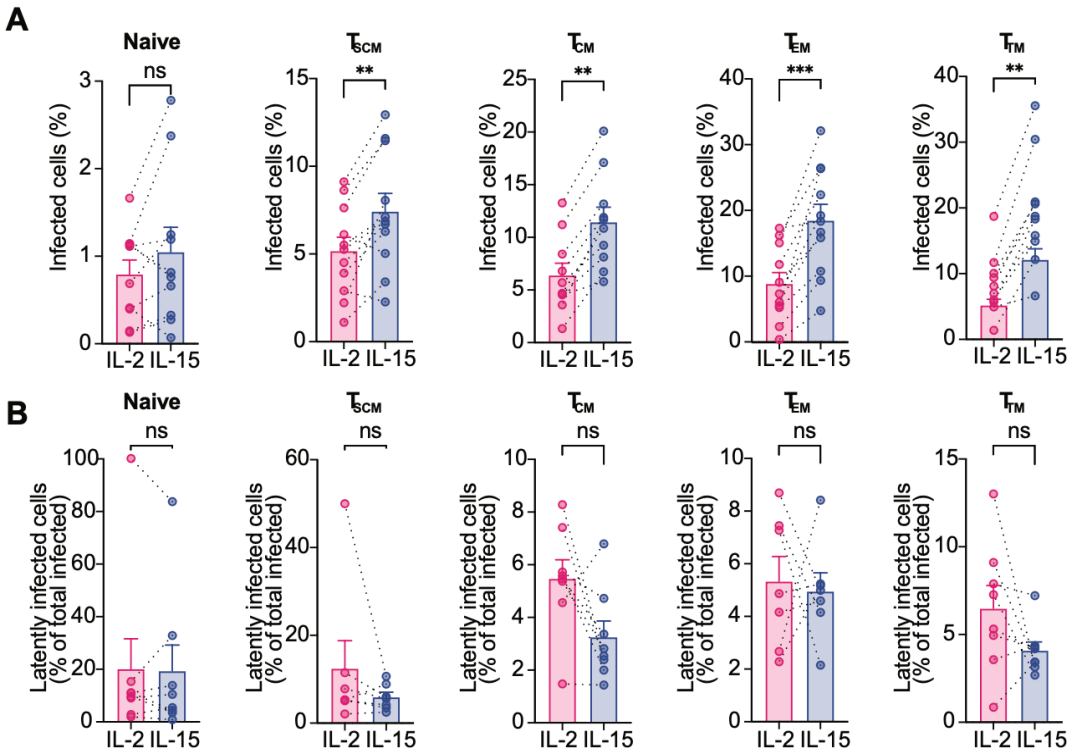

Figure 10 ***(A)*** *Bar graphs representing the percentages of totally infected cells for each CD4+ subset (naïve, T_{SCM}, T_{CM}, T_{TM}, T_{EM}), in the two conditions (IL-2 and IL-15 stimulated CD4+ cells).* ***(B)*** *Bar graphs showing the percentages of latently infected cells within total infected cells, in all CD4+ subsets analyzed and in the two experimental conditions. Significance was determined by Wilcoxon signed-rank test. *, P ≤ 0.05; **, P ≤ 0.01; ***, P ≤ 0.001.*

CCR5 HIV-GKO infection is enhanced after IL-15 stimulation

Latency establishment occurs during the acute phase of the infection and T/F viruses are mainly CCR5 tropic and are associated with the first stages of infection[183,314,315] We thus investigated the role of IL-15 in infection and latency establishment of HIV-GKO bearing a CCR5-tropic only envelope (R5 HIV-GKO, Figure 11), analyzing the expression of mKO2 and csGFP fluorescent reporters to discriminate between LTR-silent and LTR-active infected cells (Figure 11A).

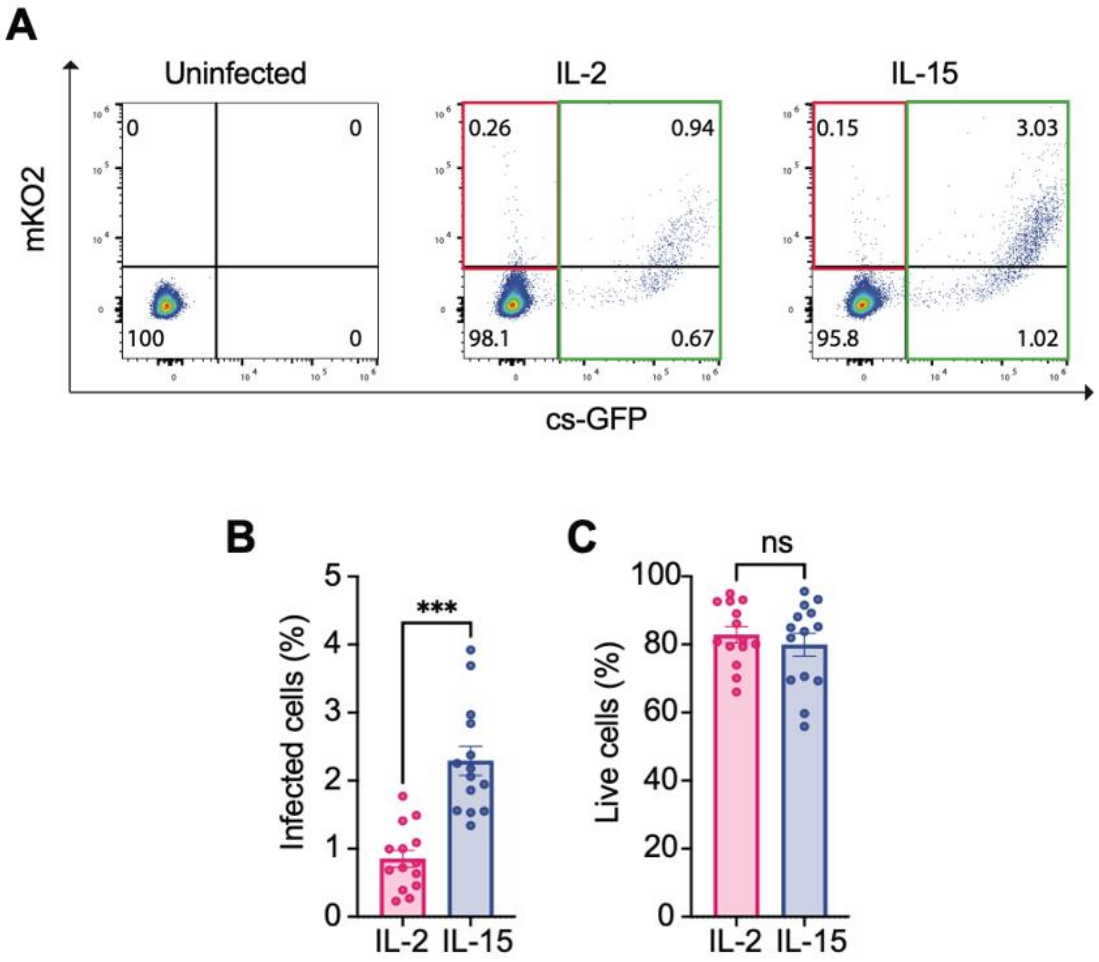

Figure 11 (A) *Representative FACS plots of primary CD4+ T cells mock (left) and infected with R5 HIV-GKO in IL-2 (middle) and IL-15 (right) conditions. Plots show the gating strategy to discriminate between latently infected cells (mKO2+/csGFP-) and productively infected cells (mKO2+/csGFP+ and mKO2-/csGFP+).* ***(B)*** *Bar graph representing percentage of total infected CD4+ cells in IL-2 compared with IL-15 condition.* ***(C)*** *Percentages of viability of CD4+ cells stimulated with equimolar levels of IL-2 and IL-15. Significance was determined by Wilcoxon signed- rank test. *, P ≤ 0.05; **, P ≤ 0.01; ***, P ≤ 0.001.*

IL-15 significantly increased total infection of CD4+ T lymphocytes compared to IL-2 (Figure 11B), without affecting cell viability (Figure 11C). Similarly to the observations collected in CD4+ T lymphocytes infected with R5/X4 HIV-GKO, IL-15 significantly increased the percentage of productively infected cells (Figure 12A) with no impact on latently infected cells, compared to IL-2 (Figure 12B) in total CD4+ cells. When we focused only on the portion of productively infected cells within total infected cells, IL-15 treatment increased the percentage compared to IL-2 (Figure 12C) while decreased the percentage of latently infected cells (Figure 12D).

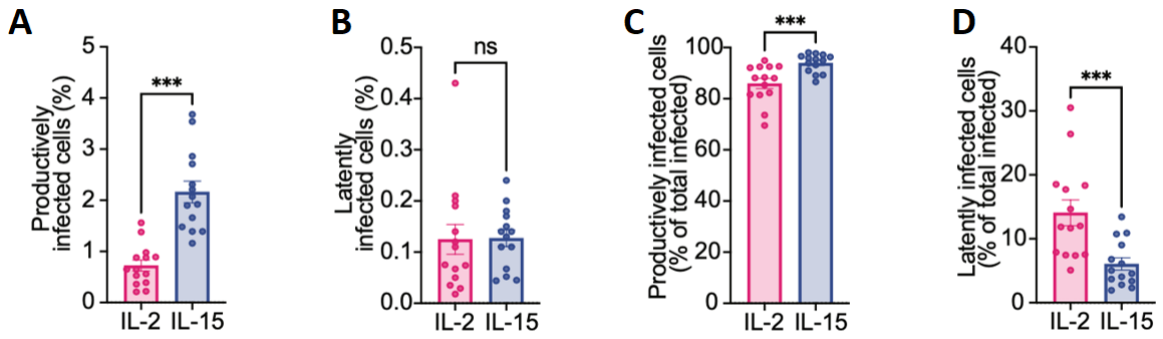

Figure 12 ***(A)*** *Percentage of R5 HIV-GKO productively infected cells and* ***(B)*** *latently infected cells within total CD4+ cells stimulated with IL-2 or IL-15.* ***(C)*** *Percentage of productively infected cells and* ***(D)*** *latently infected cells within infected cells stimulated with either IL-2 or IL-15. Significance was determined by Wilcoxon signed- rank test. *, P ≤ 0.05; **, P ≤ 0.01; ***, P ≤ 0.001.*

We hypothesized that IL-15 could upregulate the CCR5 co-receptor, partially explaining the sharper increase in the total infection of R5-tropic virus compared to the R5/X4 tropic one (Figure 3 lower panel and 11B). By analyzing the expression of CCR5 in total CD4+ T lymphocytes at flow cytometry, we observed an increase in the CCR5 expression and in the MFI in cells stimulated with IL-15 compared to IL-2 (Figure 13A, B and C). These observations suggest that IL-15 may impact on R5-tropic HIV-1 infection by upregulating CCR5.

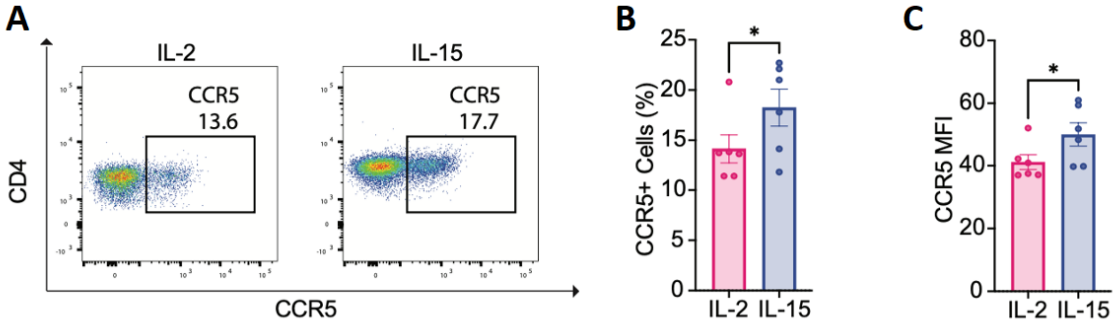

Figure 13 ***(A)*** *Representative FACS plots showing the percentages of CD4+ T cells expressing CCR5 on the cell-surface, after 3 days of either IL-2 or IL-15 stimulation.* ***(B)*** *Bar graph displaying the percentage of CCR5+ cells in both IL-2 and IL-15 conditions.* ***(C)*** *Mean Fluorescence Intensity (MFI) values for CCR5 in CD4+ cells stimulated with IL-2 or IL-15. Significance was determined by Wilcoxon signed- rank test. *, P ≤ 0.05; **, P ≤ 0.01; ***, P ≤ 0.001.*

T_{SCM} and T_{CM} subsets express higher levels of CCR5 after IL-15 stimulation

We then investigated the role of IL-15 stimulation at the subsets level on CCR5 expression. In both IL-2 and IL-15 stimulated cells, the percentage of CCR5+ cells were higher in the more differentiated subsets. Specifically, T_{EM} displayed the highest percentage of CCR5 expressing cells while in naïve compartment CCR5 co-receptor was virtually absent (Figure 14A, left and right).

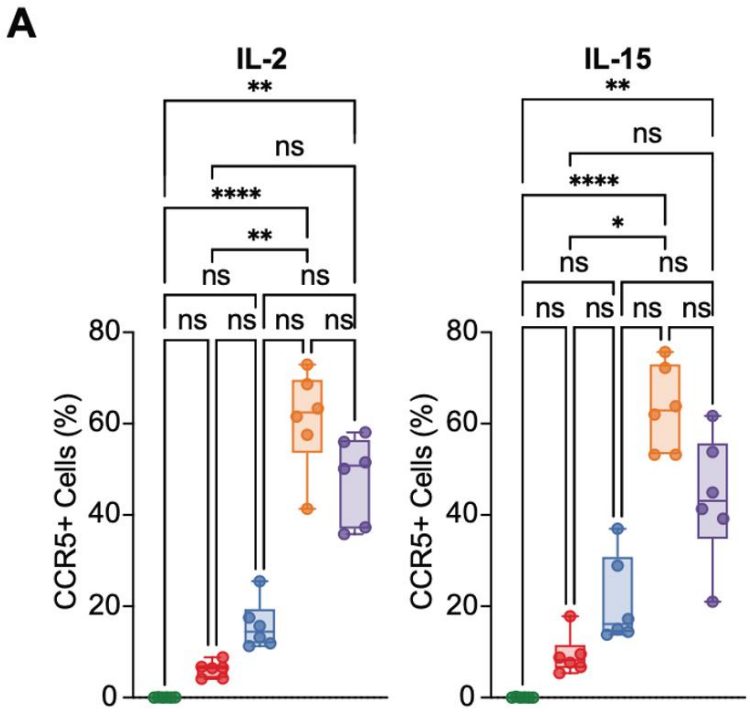

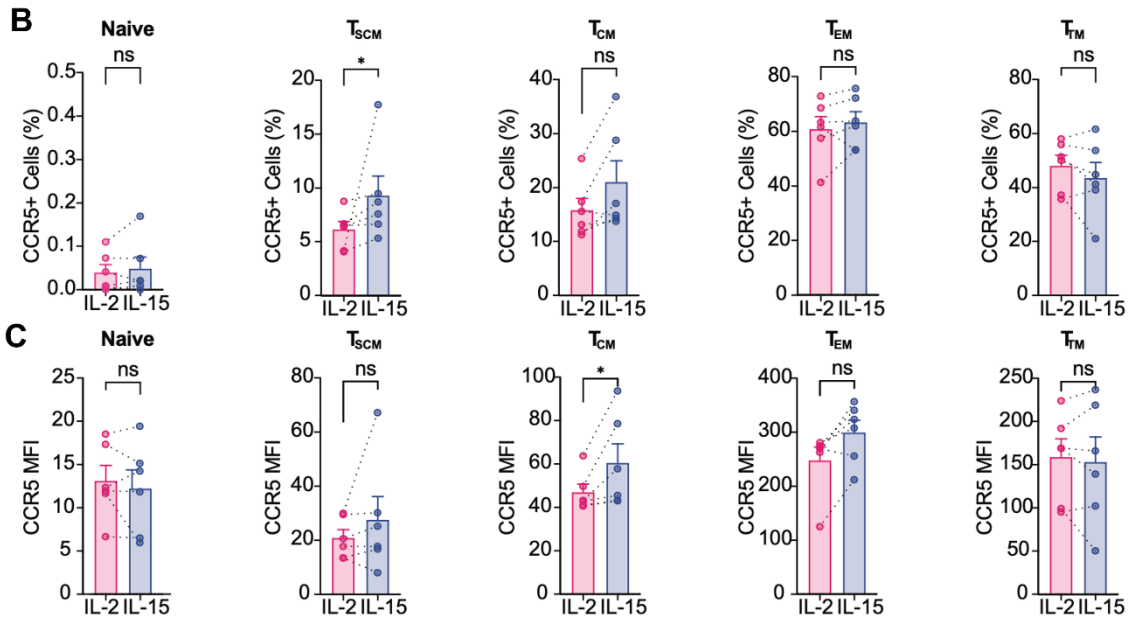

Figure 14 (A) *Percentages of cells expressing CCR5 divided by CD4+ naïve and memory subsets (Tscm, Tcm, Ttm, Tem), in IL-2 stimulated (left) and IL-15 stimulated (right) cells.* ***(B)*** *Bar graphs displaying the percentages of CCR5+ cells for each CD4+ subsets studied (naïve, Tscm, Tcm, Ttm, Tem), in samples treated with IL-2 or IL-15.* ***(C)*** *CCR5 Mean Fluorescence Intensity (MFI) values for each CD4+ subset and for both experimental conditions (equimolar levels of IL-2 and IL-15). Significance was determined by Wilcoxon signed- rank test. *, P ≤ 0.05; **, P ≤ 0.01; ***, P ≤ 0.001.*

When we analyzed IL-2 and IL-15 stimulation pairwise in each subset (Figure 14B and C), we observed that IL-15 increased the percentage of Tscm expressing CCR5 and increased the overall levels of CCR5 expression in Tcm compared to IL-2 treatment. IL-15 treatment did not alter the expression of CCR5 in the other subsets, suggesting that the overall increase in CCR5 expression observed in total CD4+ T cells was mainly traceable to an increase in CCR5+ cells within Tscm and Tcm subsets.

Latency establishment levels in CCR5 HIV-GKO infected CD4+ T cells are comparable in Tcm, Ttm, Tem

We then performed an analysis of latency establishment in each of the considered CD4+ T cell subset in the context of R5-tropic HIV-GKO. Primary CD4+ T lymphocytes were stimulated with IL-2 or IL-15 for 3 days, infected with R5-tropic HIV-GKO and both immunophenotype and the infection outcome were analyzed 5 dpi at flow cytometry (Figure 15). Tem was the most susceptible subset to infection and displayed the highest percentages for total infected cells in both ILs conditions

(Figure 7A, left). Naïve and T_{SCM} subsets were virtually resistant to R5 infection. These values were in line with what we observed for R5/X4 HIV-GKO infection, but the differences between levels of infection in each subset were more prominent and followed the expression of CCR5 (Figure 15A and C, left). Consistently, productively and latently infected cells in both ILs stimulations resembled data regarding the total infection (Figure 15A and C, middle and right). When we focused on latency enrichment by dividing latently infected cells from the total infected percentages, no differences were observed in the three most differentiated subsets (T_{CM}, T_{TM}, T_{EM}, Figure 15B and D) in both experimental conditions. We were not able to draw any conclusions regarding naïve and T_{SCM} percentage of latency over total infected cells due to their intrinsic refractory to R5 infection associated with low expression of CCR5 (Figure 15B and D).

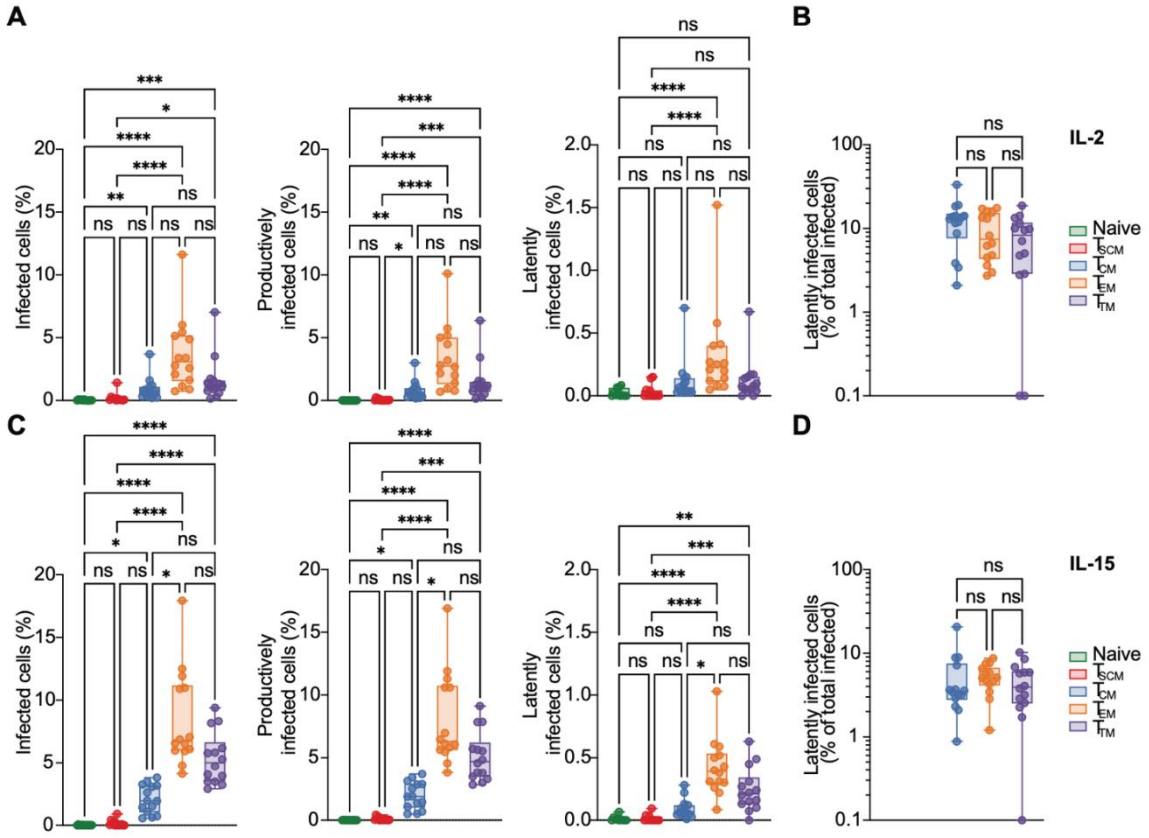

Figure 15 ***(A)*** *Boxplot representing the percentages of total (left), productively (middle) and latently infected cell (right) with R5 HIV-GKO after IL-2 stimulation. Each of the 5 CD4+ subset is displayed (naïve, T_{SCM}, T_{CM}, T_{TM}, T_{EM}).* ***(B)*** *Percentage of latently infected cells within total infected CD4+ cells in each subset analyzed after IL-2 stimulation.* ***(C)*** *Boxplot showing the percentages of total (left), productively (middle) and latently (right) infected cells with R5 HIV-GKO after IL-15 stimulation.* ***(D)*** *Percentage of latently infected cells over total infected cells, in CD4+ subsets after IL-15*

*stimulation. Significance was determined by Kruskal-Wallis test. ns, P > 0.05; *, P ≤ 0.05; **, P ≤ 0.01; ***, P ≤ 0.001; ****, P ≤ 0.0001.*

The analysis of pairwise levels of total infected cells in IL-2 and IL-15 conditions at the subset level was in line with what was observed with the R5/X4 infection. IL-15 significantly increased the percentage of R5 HIV-GKO infected cells in the three most differentiated CD4+ memory subsets (TCM, TTM, TEM, Figure 16A). TSCM levels of infection slightly increased without reaching statistical significance, while naïve R5 HIV-GKO+ cells were almost undetectable in both experimental conditions. Conversely, IL-15 decreased the percentage of latently infected cells over the total infected cells in all the subsets analyzed (TCM, TEM, TTM, Figure 16B), reaching significance in TCM and TEM.

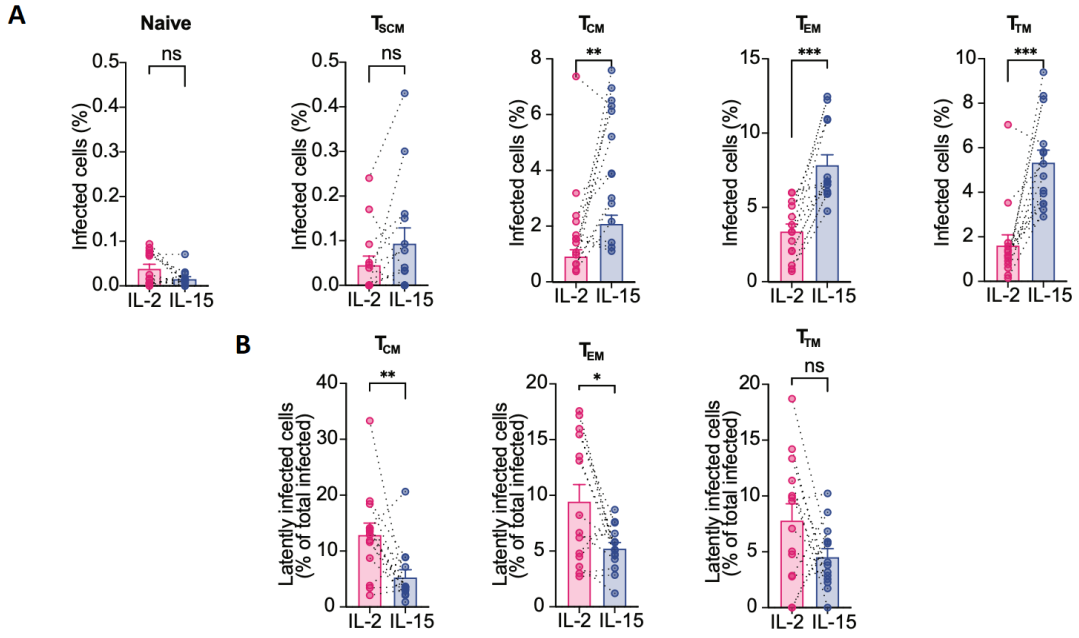

Figure 16 *(**A**) Bar graphs displaying the percentages of total infected cells for each CD4+ subset (naïve, TSCM, TCM, TTM, TEM) in cells stimulated with IL-2 or IL-15. **(B)** Bar graph showing the percentages of latently infected cells over total infection, in both experimental conditions. Significance was determined by Kruskal-Wallis test. ns, P > 0.05; *, P ≤ 0.05; **, P ≤ 0.01; ***, P ≤ 0.001; ****, P ≤ 0.0001.*

The susceptibility of CD4+ subsets to R5-topic virus resulted comparable to the R5/X4 infection and IL-15 increased levels of infection in all CD4+ memory subsets (TSCM, TCM, TTM, TEM). As an exception, naïve resulted highly resistant to R5 infection and IL-15 condition did not increase this low susceptibility.

Productively infected cells are enriched in more differentiated CD4+ memory T cells

Our data demonstrated that productive and latent infection occur differentially in each CD4+ naïve and memory subset. To better understand the composition of uninfected, productively infected and latently infected populations, we decided to sort the three pools based on the expression of mKO2 and csGFP reporters. We sorted uninfected (mKO2-/csGFP-), productively infected (mKO2+/csGFP+ and mKO2-/csGFP+) and latently infected (mKO2+/csGFP-) cells from six donors stimulated with IL-15 and infected with the dual tropic R5/X4 HIV-GKO (Figure 17A). In addition to the two viral reporter expression, CD4+ T cells were stained with anti-CD4, anti-CD45RA, anti-CD45RO, anti-CD27, anti-CCR7 and anti-CD95 fluorescent antibodies. T-SNE plots were considered to qualitatively visualize subsets clustering in each of the three sorted populations. T_{EM} (orange) and T_{CM}

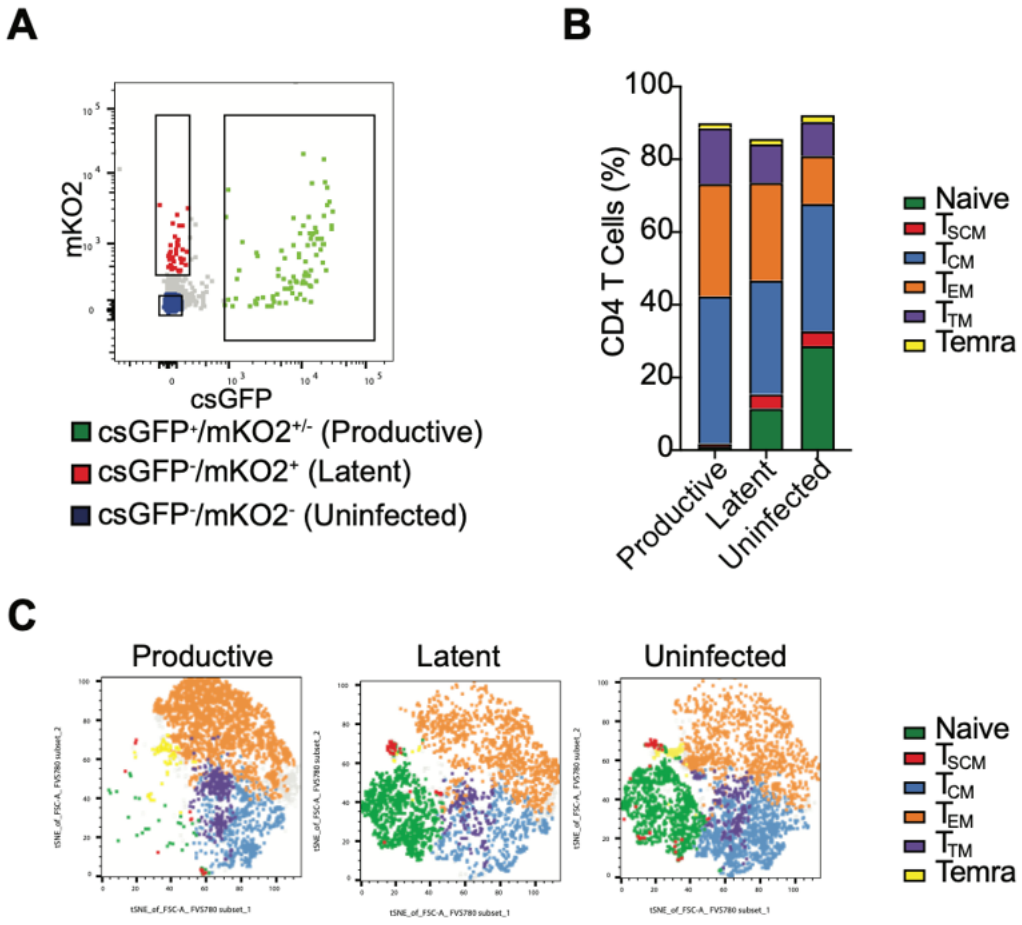

Figure 17 (A) *Representative FACS plot showing the gating strategy for the sorting of uninfected CD4+ cells (mKO2-/csGFP-), latently infected cells (mKO2+/csGFP-) and productively infected cells (mKO2+/csGFP+ and mKO2-/csGFP+) using R5/X4 HIV-GKO.* ***(B)*** *Stacked bar chart showing the relative percentages of each CD4+ subset (naïve, TSCM, TCM, TTM, TEM, Temra) for each condition (productively infected cells, latently infected cells and uninfected, n=6).* ***(C)*** *Representative t-SNE plots showing the global distribution of the five CD4+ subsets in sorted productive, latent or uninfected cells stained with cell-surface markers to discriminate between subset phenotypes.*

(blue) are the most extended clouds in all the conditions, while naïve (green) can be clearly visualized in latent and productive cells, with only few dots in productive cells (Figure 17C). Naïve and TSCM compartments were significantly depleted in the productive sorted cells (Figure 17B and 18) compared to uninfected population.

Donor variation was observed in naïve latent cells and no significant difference was displayed between latent an uninfected TSCM. A 25% increase in productive TCM was observed compared to latent and uninfected, while a 2-fold increase in the TEM compartment was observed in the infected populations (both productive and latent) compared to uninfected. TTM tend to be more represented in percentage in productive infected population, while TEMRA showed similar values in all three populations (Figure 17A and 18). Taken together, the less differentiated naïve and TSCM subset were underrepresented in infected cells, with this phenomenon being marked in productive infected naïve and less pronounced in latent naïve. Observed TSCM general decrease was minimal in productive and latent population compared to uninfected TSCM. In opposition, TCM were more represented in productive cells, suggesting a major role of this subset in the productive infection of CD4+ memory T cells.

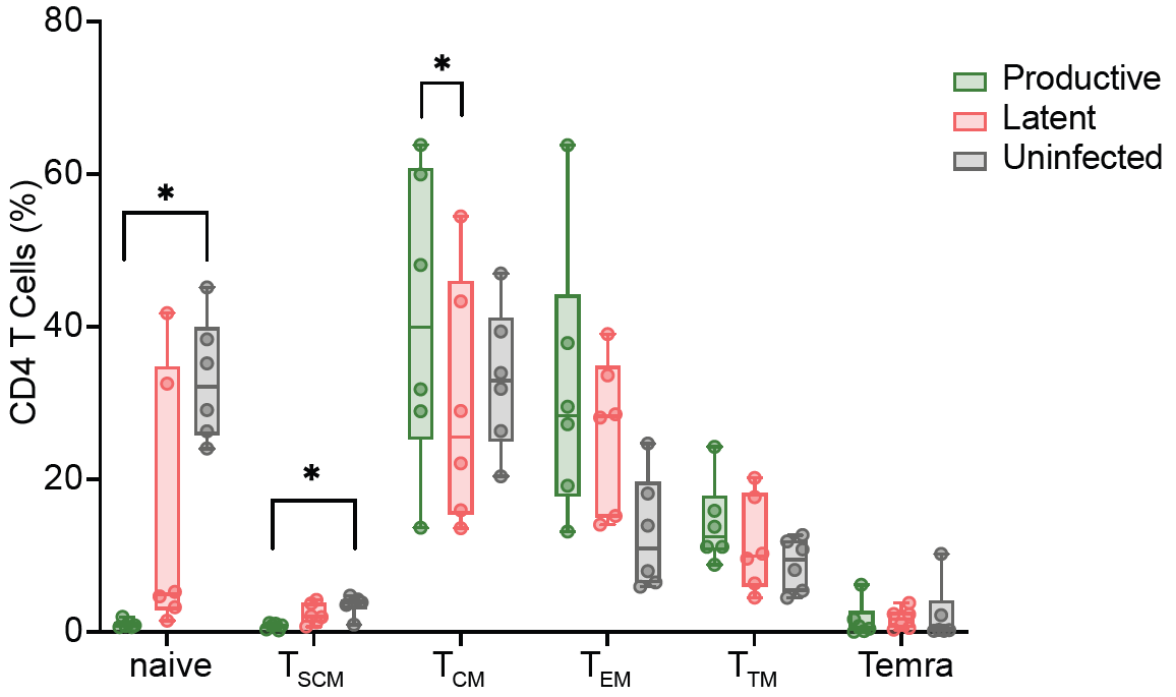

Figure 18 *Boxplot showing the relative abundance of each CD4+ subset (naïve, TSCM, TCM, TTM, TEM) in three different sorted CD4+ populations: productively infected R5/X4 HIV-GKO (green bars), latently infected R5/X4 HIV-GKO (red bars) and uninfected CD4+ cells (grey bars, n=6). Significance was determined by Friedman test. ns, P > 0.05; *, P ≤ 0.05.*

CDK9 and CycT1 expression is equal in naïve and CD4+ memory subsets

We previously showed that IL-15-driven increased HIV-1 susceptibility of CD4+ T cells is associated with higher levels of the P-TEFb complex, compared to IL-2 treatment (Figure 5D, E, F and G). We also showed that naïve and TSCM subsets are more prone to latency than the other differentiated CD4+ memory subsets. We then hypothesized that naïve T cells and TSCM could be more prone to latency because of lower levels of P-TEFb complex. The expression of P-TEFb subunits is tightly regulated in resting/activated CD4+ T lymphocytes and macrophages. However, differences of expression and activity of these subunits in different CD4+ T cells are still unknown[316–319].

First, we analyzed the mRNA expression of both CDK9 and CyclinT1 in CD4+ naïve and memory subsets after 8 to 9 days of IL-15 stimulation, a period of stimulation similar to all our previous analysis of HIV-1 infection. After the stimulation period,

total CD4+ T cells were sorted in naïve, T_{SCM}, T_{CM}, T_{TM}, T_{EM}. The levels of CDK9 and CyclinT1 mRNA in each subset was comparable, with no recorded significant differences (Figure 19A, left and right respectively). Protein expression levels of CDK9, P-CDK9 and CyclinT1 were also assessed, given the fact that CDK9 phosphorylation at residue threonine 186 is known to play a role in P-TEFb activity[319,320]. IL-15 stimulated total CD4+ T cells were sorted in naïve, T_{SCM}, T_{CM}, T_{TM}, T_{EM} and analyzed by immunoblotting for their P/CDK9 and CyclinT1 protein expression levels (Figure 19B). The number of sorted naïve and T_{SCM} cells in D27 and D72 was limiting for the immunoblotting experiments, given also that these two subsets are characterized by the smallest amount of cytoplasm throughout memory CD4 subsets. A lower concentration of cell lysate was used for these subsets (Figure 19B, naïve and T_{SCM} GAPDH bands for D27 and D72) and data could be compared to the other subsets through GAPDH normalization.

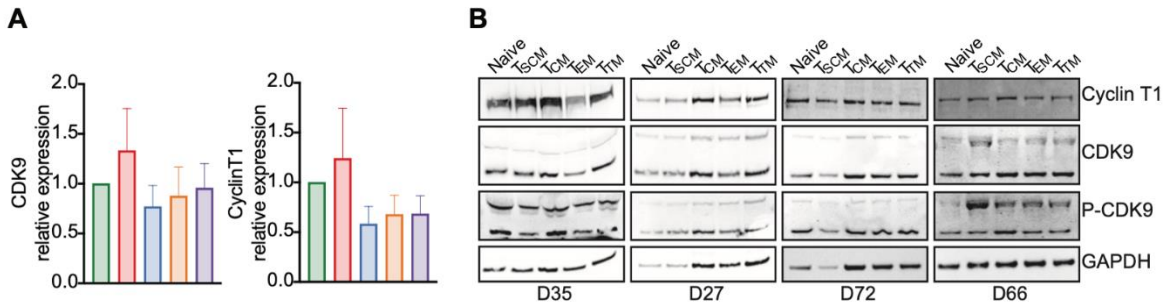

Figure 19 (A) *Bar graphs showing CDK9 (left) and Cyclin T1 (right) mRNA expression in 5 different sorted CD4+ T cell subsets (naïve, T_{SCM}, T_{CM}, T_{TM}, T_{EM}). Expression in naïve cells was set as 1 (n=2).* ***(B)*** *Protein expression of Cyclin T1, CDK9, P-CDK9 and GAPDH was assessed by immunoblotting in sorted CD4+ T cell subsets (naïve, T_{SCM}, T_{CM}, T_{TM}, T_{EM}), in four different donors (D35, D27, D72, D66). Significance was determined by Kruskal-Wallis test. ns, $P > 0.05$; *, $P \leq 0.05$; **, $P \leq 0.01$; ***, $P \leq 0.001$; ****, $P < 0.0001$.*

Densitometric analysis for each of the protein assessed showed no differences in expression levels compared to GAPDH, for every subset considered (Figure 20A, B, C, D and E). Even CDK9 phosphorylated at threonine 186 displayed similar protein levels in each subset (Figure 20D and E). Hence, we concluded that neither P-TEFb expression nor phosphorylation of CDK9 at residue threonine 186 were associated to latency modulation observed in the different CD4+ naïve and memory subsets.

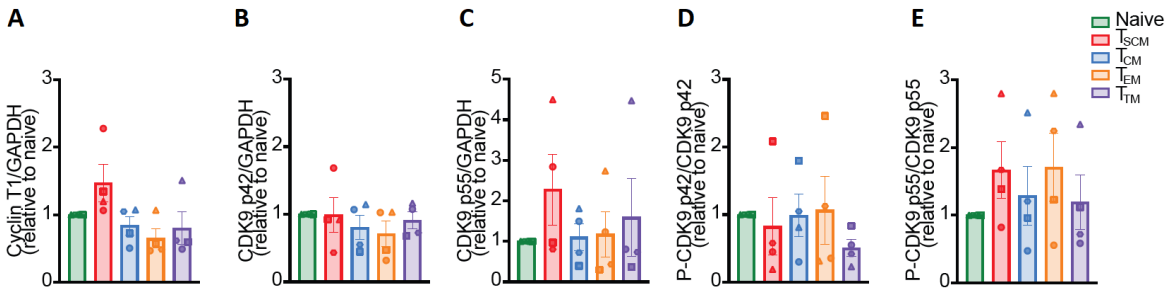

Figure 20 *Densitometric analyses of Cyclin T1* ***(A)****, CDK9 42 kDa isoform* ***(B)****, CDK9 55 kDa isoform* ***(C)****, P-CDK9 42 kDa isoform* ***(D)*** *and P-CDK9 55 kDa isoform* ***(E)*** *normalized over GAPDH levels in CD4+ subsets (naïve, TSCM, TCM, TTM, TEM). Significance was determined by Kruskal-Wallis test. ns, P > 0.05; *, P ≤ 0.05; **, P ≤ 0.01; ***, P ≤ 0.001; ****, P < 0.0001.*

NF-κB nuclear translocation differs in naïve and CD4+ memory subsets

Since we did not observed differences in a pivotal transcriptional factor for HIV-1 such as P-TEFb, we hypothesized that the availability of NF-κB, another cellular factor involved in HIV-1 transcription and latency maintenance, could be modulated throughout CD4+ subsets. The 5' proviral LTR has two adjacent binding sites for NF-κB and NFAT TFs and their recruitment is associated with HIV-1 transcription and active replication[130,131]. Furthermore, one of the several blocks that has been shown to inhibit proviral transcription is the unavailability of NF-κB in the nucleus of resting CD4+ T cells[135]. Our aim was to study the cellular distribution of NF-κB in the different CD4+ T subsets to address the inefficient proviral transcription observed in naïve and TSCM compartments. To do so, we sorted naïve, TSCM, TCM, TTM and TEM from total CD4+ cells stimulated for 8 to 9 days with IL-15 from three different donors (D44, D45 and D66), and we analyzed the NF-κB localization in both cytoplasm and nuclear compartments by confocal microscopy (Figure 21 with merged channels and Figure 22 with separate channels in grayscale).

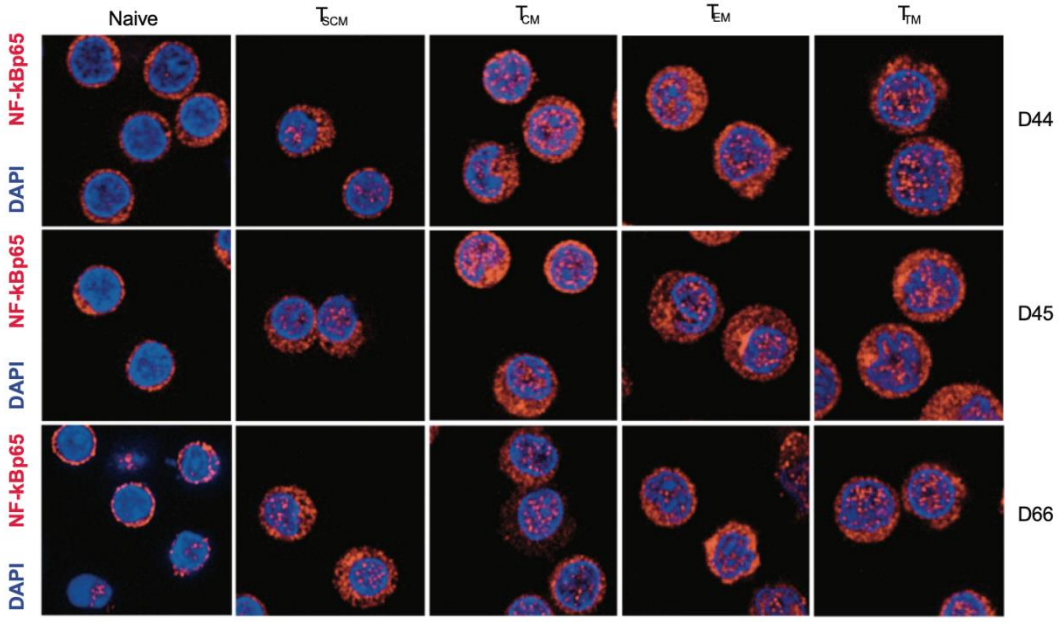

Figure 21 *Representative confocal microscopy images of the different CD4+ T cell subsets (naïve, TSCM, TCM, TTM, TEM) sorted from three different healthy donors and cultured for 8 to 9 days in the presence of IL-15. CD4+ cells were stained with anti-NF-κB p65 antibody, a secondary antibody Alexa 647-conjugated (red) and DAPI to visualize the nuclei (blue bars, 10 mm).*

The most abundant form of active NF-κB is a heterodimer of p50 and p65 (or RelA). We chose to detect NF-κB p65 monomer because it contains the transactivation domain (TAD) able to enhance HIV-1 proviral transcription. We observed that naïve subset displayed lower levels of nuclear mean fluorescence intensity (MFI) of NF-κB, calculated for each single identified cell object (mean, n = 427 analyzed cells per T cell subset, and mean, n = 1820 cells for each donor), compared to all the other CD4+ memory subsets. This was true for all three donors, with different extent (Figure 23A, B and C). All CD4+ memory subsets displayed similar levels of nuclear NF-κB MFI. Of note, TCM levels of nuclear NF-κB MFI were higher compared to TEM and TTM in two donors out of three, regardless similar levels of observed latency establishment (Figure 23B, C and 9D). To optimally compare data collected from the three donors, we firstly normalized the unclear NF-κB MFI and then calculated the median nuclear NF-κB MFI for each of the CD4+ subset. Nuclear NF-κB MFI was preferred to cytoplasmic MFI (Figure 23 A to C) because this compartment dimension is less variable among memory CD4+ T subsets and represents a more

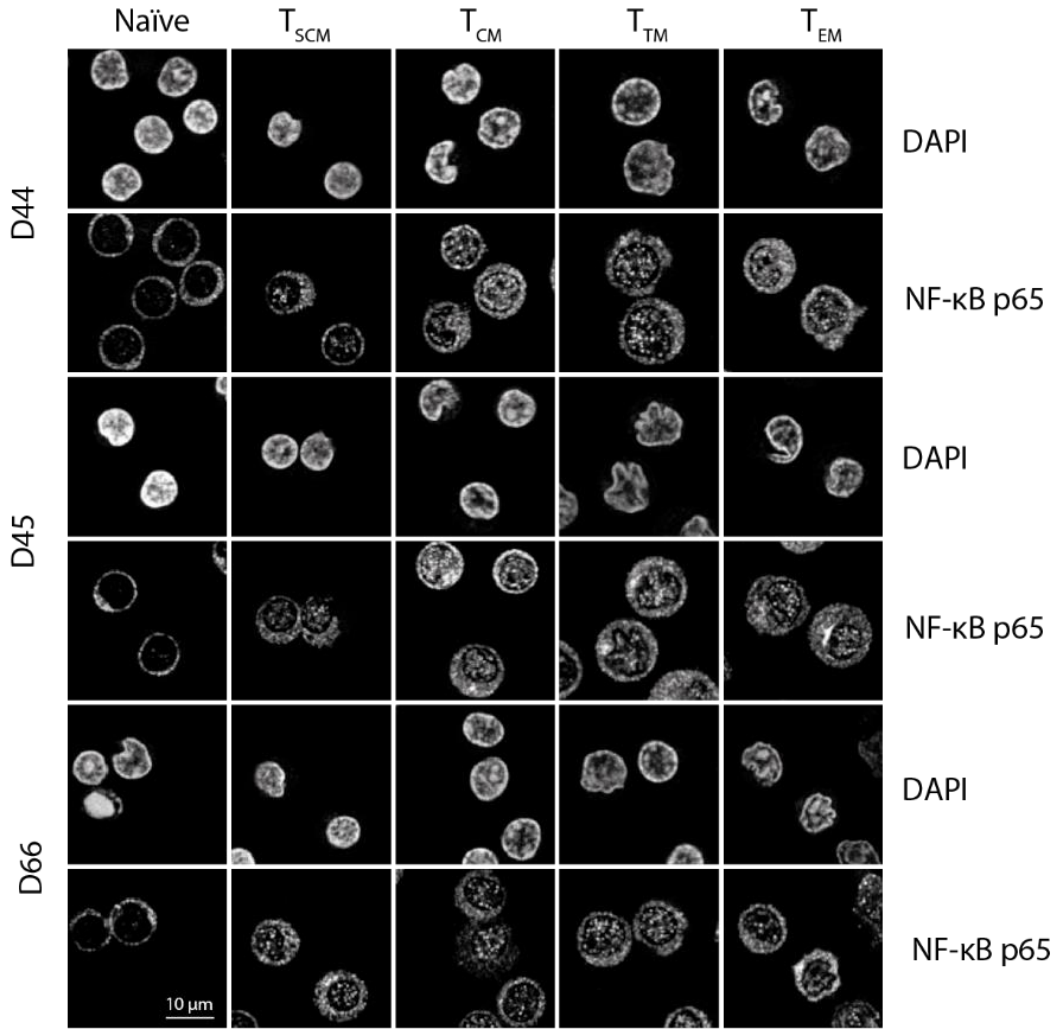

Figure 22 *Representative confocal microscopy images of the different CD4+ T cell subsets (naïve, TSCM, TCM, TTM, TEM) sorted from three different healthy donors and cultured for 8 to 9 days in the presence of IL-15. CD4+ cells were stained with anti-NF-κB p65 antibody, a secondary antibody Alexa 647-conjugated (red) and DAPI to visualize the nuclei (blue bars, 10 µm). Color channels are displayed as separate in grayscale.*

informative data about the transcriptional activity in each subset driven by NF-κB, as its biological activity is fulfilled only inside the nucleus. The result was an observed decrease in the median MFI for the naïve subset compared with all the other CD4+ memory subsets, with the difference that was significant when comparing naïve median MFI with TCM median MFI (Figure 23D). On the other hand, TSCM subset displayed levels of nuclear NF-κB that were comparable with the other memory subsets and not with the naïve compartment.

Hence, IL-15 stimulated CD4+ memory subsets showed higher levels of nuclear NF-κB compared to the naïve subsets, suggesting that the poor availability of NF-κB in the nucleus of naïve cell could concur to the latency propensity in this compartment.

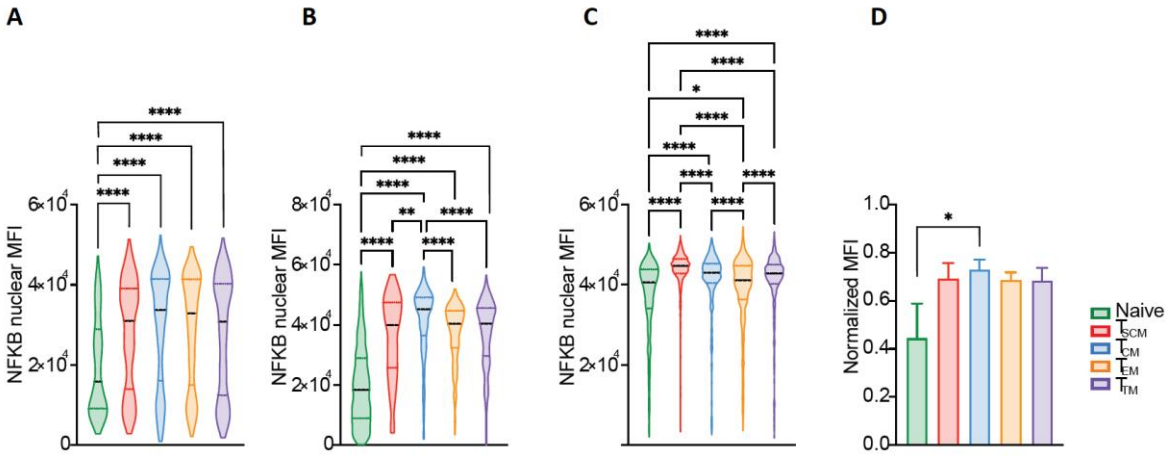

Figure 23 *Mean Fluorescence intensity (MFI) of nuclear NF-κB-p65-Alexa-Fluor-647 quantified for each CD4+ subset (naïve, TSCM, TCM, TTM, TEM). MFI was calculated on a total of 1286 cells for D44* ***(A)****, 2122 cells for D45* ***(B)*** *and 2998 cells for D66* ***(C)****.* ***(D)*** *Bar graph showing the data normalization and median calculation for the three donors regarding MFI of nuclear NF-κB-p65-Alexa-Fluor-647. Significance was determined by Kruskal-Wallis test. ns, P > 0.05; *, P ≤ 0.05; **, P ≤ 0.01; ***, P ≤ 0.001; ****, P < 0.0001.*

Improvement of pMorpheus dual reporter virus

HIV-1 dual-reporter viruses have greatly improved the efficacy of studies aiming at understanding the biology of HIV-1 latency and the molecular mechanisms involved in the establishment and maintenance of latently infected cells. Some dual-reporter viruses described in the literature detect a higher percentage of latently infected CD4+ T cells when compared with HIV-GKO[297,300]. We set out to further optimize a version of pMorpheus-V5 described by Kim[300]. This version of the reporter bears a latent cassette in the *env* ORF controlled by the PGK promoter and composed by the HA-NWS, plus a productive cassette in the *nef* ORF controlled by the 5' LTR and composed by HSA-mCherry-IRES-Nef. Of note, while the productive cassette features both the expression of a cell-surface marker such as the heat-stable antigen (HSA) and the mCherry fluorophore, the latent region expresses only a tagged (HA) and wild-type short version (NWS) of the nerve growth factor receptor (NGFR), which localizes at the cell surface of infected cells. In collaboration with Viviana Simon's group, we engineered the latent cassette by adding eGFP fluorophore and a T2A sequence in between the fluorophore sequence and the upstream NWS, thus allowing the expression of both proteins. The resulting

pMorpheus dual-color improved the versatility of the system, adding a detection choice in the latent cassette without the necessity of antibody staining (Figure 24).

Transfected HEK 293T cells with pMorpheus dual-color plasmid expressed both eGFP and mCherry proteins, confirming the cloned phenotype.

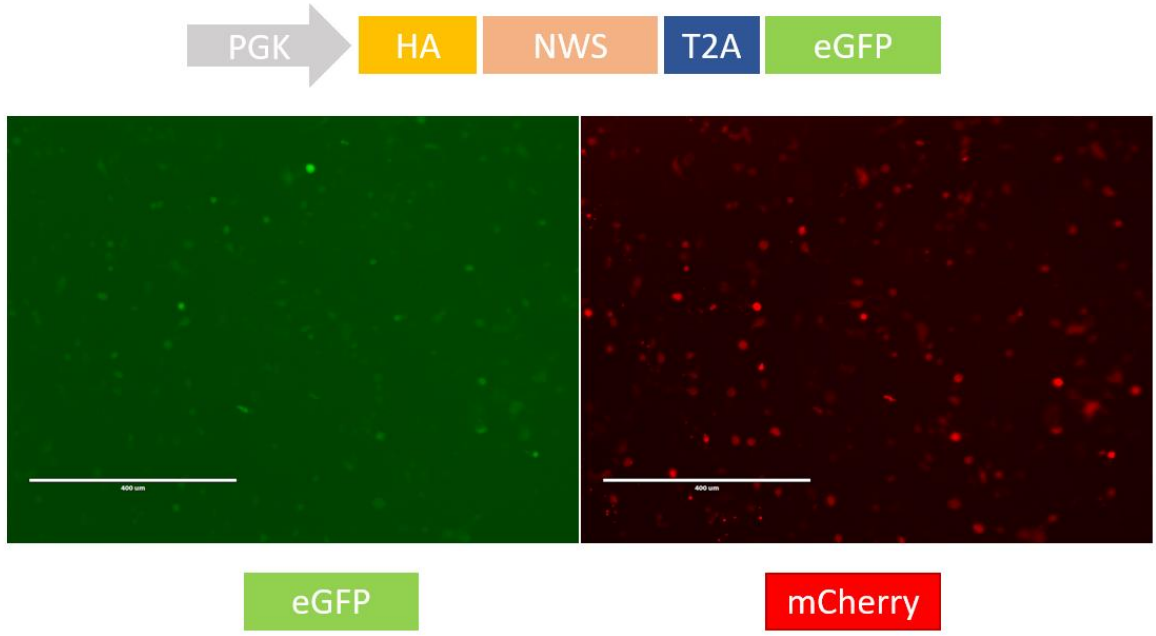

Figure 24 *Schematic representation (top) of the cloned latent cassette in the pMorpheus dual-color viral vector. Cloned pMorpheus dual-color in transfected HEK 293 T cells (microscope images, bottom). eGFP expression on the left and mCherry expression on the right. Images acquired 48 hours post-transfection.*

A second modification was performed on the productive cassette of the original pMorpheus (PGK-HA-NWS-HSA-mCherry-IRES-Nef) to substitute mCherry fluorophore with another red fluorescent protein called mKate2. Both fluorophores are excited at the same wavelength (588nm), but their emission spectra are slightly different, with peak emission at 610nm for mCherry and 633nm for mKate2. We thus engineered the original productive cassette HSA-mCherry-IRES-Nef by substituting the mCherry gene with mKate2 gene, with or without a T2A sequence

(Figure 25). When we transfected HEK 293T cells with the two cloned plasmids, only the construct without T2A expressed mKate2 protein (data not shown).

Both HIV-GKO and pMorpheus reporter systems are optimized to discriminate between latently and productively infected cells. However, both tools are inadequate to assess the clonality of the latent reservoir *in vitro*. It is hypothesized that HIV-1 reservoir under HAART is maintained by clonal expansion of single infected cells that divide without reactivation of the integrated provirus[170,178]. The

Figure 25 *Schematic representation of mCherry-mKate2 switch in the productive cassette of cloned pMorpheus. Two different constructs were generated, with or without T2A between the HSA gene and the mKate2 gene.*

extent and magnitude of this phenomenon still needs to be investigated, especially in the different CD4+ subsets. For this reason, pMorpheus (PGK-HA-NWS-HAS-mCherry-IRES-Nef) was engineered to harbor a UMIs (unique molecular identifiers) consisting of 15 random nucleotides (15N). Two versions of pMorpheus-15N were generated, one bearing eGFP upstream the UMI sequence and one bearing HA-NWS upstream the UMI sequence. The 15N UMI was inserted in the latent cassette and its presence confirmed by Sanger sequencing (Figure 26). The pMorpheus-15N plasmid library could generate a maximum of 10^9 unique molecular identifiers and produce viral libraries in which virions carrying a unique 15N tag are ideal to investigate the clonality level of HIV-1 reservoir establishment.

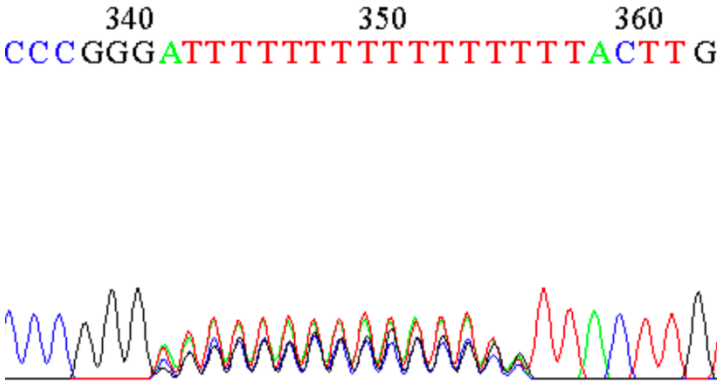

Figure 26 *Sanger sequencing of the cloned pMorpheus 15N-eGFP confirming the presence of the 15 nucleotide UMI.*

CD4+ T cells will be infected at a low multiplicity of infection (MOI) to avoid infecting a cell with more than one barcoded virus, and longitudinal analyses will be performed to track the expansion or contraction of clones of latently infected cells. Combined with our established panel of antibodies to discriminate between CD4+ naïve and memory subsets, our future aim will be to assess whether a specific subset sustains the clonality of the latent reservoir.

Chapter 4 – Discussion

The major obstacle to HIV cure is the presence of a latent reservoir composed mainly by CD4+ naïve and memory T lymphocytes bearing integrated and replication-competent proviruses[21,22,150,151,153,154,165]. Even under HAART treatment, this small pool of cells persists through various mechanisms. The complexity of the reservoir retraces the heterogeneity of the susceptible CD4+ subsets and such rich structure could explain the inefficient LRA reactivation strategies pursued so far[280,292,321].

To address this complexity, we investigated HIV-1 latency establishment in different primary human CD4+ T lymphocytes subsets in the presence of IL-15. This cytokine covers a pathophysiological role during the acute phase of the infection, a time when the latent reservoir is seeded[182–184]. A transient increase of IL-15 plasma levels was specifically observed between 7 and 14 post infection with HIV-1 but not with other viruses such as HBV (Hepatitis B virus) and HCV (Hepatitis C virus)[202]. In addition, a strong correlation between IL-15 levels and high viremia has been recorded in a large cohort of HIV-1 infected individuals[201]. A the molecular level, IL-15 increases CD4+ T cell susceptibility to HIV-1 by inducing the phosphorylation of the restriction factor SAMHD1, causing the abrogation of its antiviral activity[194].

Taking advantage of a dual-reporter virus (HIV-GKO), we investigated how latency is established in different CD4+ naïve and memory subsets, adding IL-15 as a stimulus to better recapitulate the pathophysiological condition in which HIV-1 seeds the latent reservoir during acute infection. The discrimination between LTR-silent (latent infection) and LTR-active (productive infection) infected cells in each subset was achieved by combining HIV-GKO infection with immunostaining of cell-surface markers specific for each CD4+ T cell subset and allowed us to conduct a comprehensive analysis of both productive and latent infection at the subset level.

In line with previous studies, we observed that CD4+ T cells stimulated with IL-15 were more susceptible to dual-tropic R5/X4 HIV-1 infection (Figure 2 and 3)

compared to cells stimulated with IL-2. These higher levels of infection were driven by a significant increase in the percentage of productively infected cells, measured by the cells positive to the LTR-dependent expression of the csGFP reporter (Figure 4A). When we addressed the molecular mechanisms that could explain such increase, we sought for host factors known to play a role in HIV-1 susceptibility and transcription and thus modulate latency. As previously reported, we observed that IL-15, but not IL-2, strongly induces phosphorylation of SAMHD1 on T592 causing the abrogation of its antiviral activity (Figure 5A and B)[194,207,322]. In addition, we observed higher levels of P-TEFb core components Cyclin T1 and CDK9 protein expression in cells stimulated with IL-15 compared to IL-2 (Figure 5D), suggesting an increase in HIV-1 transcription driven by the availability of P-TEFb components that can be recruited by the viral protein Tat[123–125].

Taken together these data suggest a dual role of IL-15: first, it induces inactivation of the restriction factor SAMHD1, thus increasing reverse transcription rates in CD4+ T cells, and second, it increases the levels of Cyclin T1 and CDK9 in resting CD4+ T cells thus increasing HIV-1 gene expression. This model fits with our data showing that after IL-15 we observed both an increase in the percentage of infected cells as well as an increase in the expression of csGFP that is under the control of HIV-1 LTR promoter (Figure 5C).

By sharing two receptor subunits (β and γ) and retaining one unique α-chain, IL-2 and IL-15 display both overlapping and specific roles in adaptive immune responses[196,323,324]. Indeed, both cytokines stimulate the proliferation of CD8+ and CD4+ T cells and are pivotal for the homeostasis of these compartments. CD4+ subset relative abundance did not change when we stimulated total CD4+ T cells with IL-2 or IL-15 and analyzed the immunophenotype (Figure 6B and 7). We recorded an increase in the T_{SCM} compartment after IL-15 treatment that did not reach statistical significance (Figure 7, upper middle). However, it has been previously reported that IL-15 induces proliferation of T_{SCM}[194,199,224]. Interestingly, an

expansion of T_{SCM} has been observed in the RV217 (ECHO) cohort[240] and it was correlated with higher viral loads. It is tempting to speculate that during acute infection, when the reservoir is seeded, a peak of IL-15 could increase the susceptibility of T_{SCM} as well as their proliferation, thus furtherly amplifying the proviral activity of IL-15 and supporting the emerging importance of T_{SCM} in latency establishment and persistence. The stem-properties and long half-life displayed by this compartment could overcome their low abundance in the CD4+ population and render them a privileged niche for HIV-1 to persist. It is already known that T_{SCM} contribution to the latent reservoir increases during long-term treatments[234], and the multiple roles of IL-15 on T_{SCM} in the acute phase could thus have a long-term impact.

Our most prominent observations emerged from the analysis of HIV-1 susceptibility and latency establishment at the subset level. While some studies already reported differences in susceptibility to HIV-1 in various CD4+ naïve and memory subset, it is still poorly understood if HIV-1 latency establishment preferentially occurs in a particular subset, especially in the presence of IL-15. By immunophenotyping HIV-GKO infected primary CD4+ T cells we were able to assess both the state of infection (LTR-silent or active) and the immune identity at the single cell level (naïve, T_{SCM}, T_{CM}, T_{TM}, T_{EM}). We demonstrated that, regarding HIV-1 susceptibility, naïve and T_{SCM} revealed to be the most refractory to infection (Figure 9A), even in the presence of IL-15 (Figure 9C). The most differentiated subsets (T_{CM}, T_{TM}, T_{EM}) were more susceptible to HIV-1 infection and displayed higher levels of LTR-active infected cells. This last observation agrees with reactivation studies showing that more differentiated memory subsets displayed higher responsiveness to latency reversal and proviral transcriptional levels[241,280,292,325]. Nonetheless, the scenario is still not well defined and more than one study reports opposite results. Particularly, Kwon and colleagues challenged the

correlation between differentiated phenotypes and easiest proviral inducibility reporting similar low inducibility among many CD4+ memory subsets[303].

Nevertheless, the analysis of HIV-GKO infection provided multiple evidence on the proportion of latency within each CD4+ subset (Figure 9B and D), which essentially can be interpreted as the probability of a subset to harbor a latent infection rather than an active one. Naïve and T_{SCM} subsets displayed higher tendency to harbor an LTR-silent provirus, given by the significantly higher proportion of latent cells over the total infected cells compared to the three most differentiated subsets (T_{CM}, T_{TM}, T_{EM}, Figure 9B and D). This latency enrichment difference was pronounced after IL-15 stimulation and may be explained by molecular mechanisms acting differently in each subset.

Latency is established in the early phase of acute infection when usually only R5-tropic viruses are present. To further confirm the adherence of our findings to the *in vivo* infection, we also investigated latency establishment in the CD4+ naïve and memory subsets infected with HIV-GKO bearing a CCR5-tropic envelope (Figure 11A). T_{CM}, T_{TM} and T_{EM} showed comparable levels of latently infected cells and higher levels of infection compared to naïve and T_{SCM}, confirming what we observed with the dual-tropic HIV-GKO. The particularly low levels of R5 HIV-GKO infected cells within naïve and T_{SCM} were insufficient to draw conclusions on latency establishment in these subsets (Figure 15B and D). Their intrinsic resistance to R5-tropic viruses mirrored the low levels of expression of the CCR5 protein on the cell-surface (Figure 14A), which increases along with the degree of differentiation of the CD4+ subsets. Nonetheless, many lines of evidence support the presence of proviral DNA in naïve and T_{SCM} subsets in animal models and in HIV+ individuals under HAART, suggesting that these two subsets sustain HIV-1 infection to a certain degree and have a role both in latency establishment and HIV-1 persistence[234,240,244,303,326]. Most of these studies report lower frequencies in the infection of naïve and T_{SCM}[244,303], with naïve cells containing 10-fold fewer HIV-1

proviral copies. Still, inducibility of viral gene expression in latently infected cells has been demonstrated for both subsets, confirming the existence of replication-competent provirus able to produce new rounds of infection. Of note, studies on infant macaques have demonstrated the pivotal role of naïve cells in reservoir formation in the context of infection early in life, where naïve cell frequency in total T cell population largely overwhelms the ones of other subsets[327,328]. On the other hand, T_{SCM} expansion and degree of infection has been correlated positively with rapid disease progression during the acute phase[240], and negatively in rare asymptomatic individuals that do not progress to AIDS, even if untreated[329]. It is then important to also investigate latency establishment in naïve and T_{SCM}, regardless their intrinsic lower susceptibility to infection when compared to more differentiated CD4+ T cell subsets.

To explain the tendency displayed by naïve and T_{SCM} to be enriched in LTR-silent provirus, we investigated the involvement of molecular mechanisms that could explain such differences. In total CD4+ cell stimulated with IL-15 we observed an increased in the protein levels of Cyclin T1 and CDK9, core components of the host transcription factor P-TEFb. The expression of both subunits is believed to increase following immune activation or differentiation rather than being dependent on the cell cycle as much as conventional cyclins[309,330]. In total CD4+ T cells, antigen recall dramatically increases Cyclin T1 production and post-translational modification of CDK9, such as phosphorylation at threonine 186. Whether a homeostatic stimulation such as IL-15 would produce the same rearrangements is less characterized, especially in CD4+ subsets. We thus hypothesized that naïve and T_{SCM} compartments express lower levels of P-TEFb components. However, both mRNA and protein levels of Cyclin T1 and CDK9 were comparable among all CD4+ naïve and memory subsets (Figure 19 and 20). Also, protein levels of phosphorylated CDK9 at threonine 186 did not change in any subset stimulated with IL-15. The kinase activity of CDK9 is heavily influenced by this post-translational

modification, as phosphorylation of the threonine residues conformationally renders the catalytic pocket available to the ATP substrate. Our data show that P-TEFb expression levels is not correlated to discrepancy in the latency enrichment observed in less differentiated subsets, and that IL-15 driven increase in P-TEFb components observed in total CD4+ T cell is not sustained by an equal increase in a specific subset. In addition to phosphorylation at threonine 186, other post-translational modifications are known to modulate CDK9 activity, and their presence should be considered in the future in the context of latency establishment at a subset level. Phosphorylation on Serine 175 (pS175) is used as a surrogate of P-TEFb activation and low levels have been found in naïve subset while higher expression was recorded in T_{TM} compartment[280]. At the same time, acetylation at different CDK9 lysines affect the ability of P-TEFb to hyperphosphorylated the CTD of RNA pol II. In particular, acetylation in conserved position 44 and 48 catalyzed by histone acetyltransferases (HAT) members causes CDK9 transcription impairment and association with transcriptionally silent HIV-1 proviruses[331,332].

To address the different levels of latency establishment observed in the CD4+ naïve and memory subsets, we also investigated the localization of NF-κB p65 (Figure 21 and 22). The role of this cellular transcription factor has been widely analyzed, in both HIV-1 infection and other human pathologies. In resting CD4+ cells, NF-κB is predominantly in its inactive homodimeric p50 form that is retained in the cytosol. T-cell activation results in the switch from p50/p50 to the heterodimeric p50/p65 (RelA) monomer, which comprises the transactivator domain (TAD) able to bind to NF-κB DNA binding sites and promote transcription and its translocation into the nucleus[333]. However, there is still no evidence regarding differences in localization or availability of these factors in different CD4+ T subsets. Using confocal microscopy, we then quantified the levels of total and nuclear NF-κB p65 in sorted naïve, T_{SCM}, T_{CM}, T_{TM}, T_{EM} after IL-15 stimulation (Figure 21 and 22). Differences among CD4+ memory subsets were modest, while naïve cells displayed consistent

lower levels of nuclear NF-κB p65. The choice of focusing on the nuclear levels of NF-κB p65 instead of the cytosolic ones was due to the higher homogeneity of this compartment throughout the different subsets (Figure 23A, B and C).

This poor availability of the active transcription factor could explain the proclivity of naïve T cells to latency that we have reported. Unavailability of nuclear NF-κB p65 could explain the lower susceptibility to HIV-1 transcription that we observed in naïve cells[135]. In addition, naïve compartment displayed the lowest responsiveness to IL-15 and the differences in nuclear NF-κB p65 levels could reflect the intrinsic failure of these cells in responding to this γ-cytokine[313]. This type of analysis also provided insights regarding the T_{SCM} compartment. Nuclear subcellular localization of NF-κB p65 in this subset was more comparable to the distribution recorded in the other CD4+ memory subsets (T_{CM}, T_{TM}, T_{EM}) rather than naïve one, showing that the tendency to harbor a latent infection compared to the most differentiated subsets may be driven by other types of mechanisms. The highest nuclear NF-κB p65 values were displayed by the T_{CM} subset, and these reached significance in two donors out of three when comparing with T_{TM} and T_{EM} values (Figure 23B and C). We previously showed that these three differentiated subsets share comparable levels of latently infected cells, however this higher availability of active NF-κB in the nuclear compartment of T_{CM} is in line with values reported for phosphorylated NF-κB in the same subset[280]. This discrepancy could be driven by kinetics in the NF-κB negative loop, where T_{TM} and T_{EM} could be more rapid in activating the feedback than T_{CM}[334].

Inducing the nuclear translocation of NF-κB family members has been proven promising especially during the last years, when *in vitro* studies focusing on second mitochondria-derived activator of caspases (SMAC) mimetics have moved to the testing in animal models with the aim of confirming the reactivation potential of integrated latent provirus. Of note, the potential of AZD5582 to induces the activation of the non-canonical NF-κB pathway has been proven efficacious in

reactivating latently infected cells in both humanized mice and in non-human primates[283–285]. This SMAC mimetics compound could enter clinical trials soon to assess its efficacy in humans. However, if AZD5582 increased HIV RNA levels by inducing proviral transcription, there have been no observations regarding a decrease in the reservoir dimensions, neither in AZD5582 studies nor other LRAs. Investigating whether different CD4+ T cell subsets display similar sensitivity to SMAC mimetics would provide many insights on latency reversal and details at the subset level.

Our findings on different availability of NF-κB in the nucleus of CD4+ T cells, especially low in naïve subset, reveals to be pivotal in this context. A comprehensive analysis of reactivation SMAC-mimetic-driven in all CD4+ subsets would shed light on those subsets which display latency enrichment. As already many groups have concluded, an effective reactivation strategy must consider the diversity of the susceptible populations and achieve levels of reactivation that are substantial even in those subsets were the provirus could be in a deep latency mode.

Although NF-κB is one of the few indispensable transcription factors for HIV transcription (TFs), other TFs such as NFAT are able to enhance transcription by various mechanisms[335]. It is known that naïve cells display low levels of this protein complex, but less is known about NFAT availability and localization in T_{SCM}[336]. A better characterization of the abundance of this TF in the different subset would surely disclose details about the latency establishment and maintenance.

As mentioned, another mechanism of latency establishment is the epigenetic silencing characterizing the landscape surrounding the proviral integration site[106,274,337,338]. Epigenetic modifications are crucial for a physiological modulation of T cell development and activity, which is characterized by long periods of quiescence interspersed by parenthesis of dramatic proliferative activity. Chromatin condensations, rather than DNA methylation or global histone modification, have been demonstrated to prevent cytokine driven proliferation in

cells which have still not encountered their cognate antigen (naïve). In a specific study, the nuclei of naïve T cells appeared to be rich of condensed chromatin, and this structure could be dispersed only in response to TCR engagement and not after a cytokine stimulus such as IL-2[339] or other gamma-chain cytokines such as IL-15 also used in our study. T_{SCM} have already encountered their cognate antigen but retain stem properties such as high proliferative capacity and the ability to differentiate into other memory phenotypes. Studies in CD8+ naïve and memory cells generated genome-wide histone H3 lysine 4 (H3K4me3, associated with gene expression) and histone H3 lysine 27 (H3K27me3, associated with gene repression) trimethylation maps in different subsets to understand how histone architecture remodels during T cell differentiation[340]. Results showed a strong segregation of naïve and T_{SCM} from T_{CM} and T_{EM} subsets, demonstrated by the acquisition of permissive H3K4me3 coupled with loss of repressive H3K27me3 histone modifications in differentiated subsets. These observations could correlate with the latency tendency we showed in naïve and T_{SCM} compartments and the low productive infectious rates.

The study described in my thesis has several limitations. The dual-reporter virus HIV-GKO is a powerful tool that provides a method to detect latently infected cells both *in vitro* and *ex vivo*. However, the latency reporter gene mKO2 is under the EF1α cellular promoter, which has been observed to be poorly expressed in resting CD4+ T cells[307]. Therefore, mKO2 expression may not be always detected in latently infected cells and HIV-GKO could thus underestimate the frequency of latently infected cells. Exploitation of pMorpheus-V5, which has a stronger cellular promoter (PGK) could overcome this issue, as higher percentages of latently infected cells were reported[300]. For this reason, we developed in collaboration with the Simon Lab the reporter virus pMorpheus dual-color engineering the pMorpheus-V5 version. By adding eGFP to the latent cassette (Figure 24), pMorpheus dual-color allows the discrimination of productive from latently

infected cells and could bring new evidence on the latency enrichment of each subset. Secondly, our findings are based specifically on CD4+ T cells present in the peripheral blood of healthy donors. It is known that other CD4+ T cell subsets, such as follicular T helper cells and Th17 cells, are susceptible to HIV-1 infection and play a pivotal role in the pathogenesis[341–344]. Furthermore, most of the recognized latent reservoir is found in mucosa tissues and lymphoid organs rather that in the blood[212,345]. Dendritic cells and monocytes are known to have a role in HIV infection and interact with T cells modulating infectivity and thus latency establishment[346]. A comprehensive study that resembles the human dynamics of HIV infection must consider these elements. Lastly, we focused on the expression of specific cellular factors (CDK9, Cyclin T1 and NF-κB) at a time-point equal to the outcome of the infection. A role of these same factors at different time-points could be even more relevant of what we observed. In the future we will take advantage of the cloned pMorpheus-15N-eGFP to broaden our study and track the dynamics of the latent reservoir and the role of clonal expansion in HIV persistence. As it has been reported, latently infected cells in HAART-treated individuals often have proviruses integrated in genes associated with the cell-cycle and underwent episodes of clonal expansion[169–172]. A barcoded virus such as pMorpheus-15N-eGFP could mimic in *in vitro* or *ex vivo* these dynamics by tracking clones of infected cells and characterize key mechanisms for HIV maintenance.

Chapter 5 – Concluding remarks

This thesis brings findings observed in an infection model based on a dual reporter virus named HIV-GKO in primary CD4+ T lymphocytes. By analyzing latency establishment in different CD4+ T cell subsets and subcellular distribution of P-TEFb and NF-κB complexes in the presence of IL-15 stimulation, we brought evidence of a different tendency to harbor a latent infection in CD4+ subsets. Specifically, naïve and T_{SCM} compartments were more refractory to HIV infection but harbored higher frequencies of LTR-silent proviruses, while more differentiated memory subsets such as T_{CM}, T_{TM}, and T_{EM} were enriched in LTR-active provirus. Interestingly, T_{SCM} displayed similarities with the naïve compartments regarding latency enrichment but segregated with memory subsets when we analyzed the nuclear localization of NF-κB, suggesting that other mechanisms are responsible of the tendency of this subset to harbor LTR-silent provirus. This small but long-lived subset covers a pivotal role in HIV latency establishment and persistence in the human body. For these facts, other studies are needed to fully uncover T_{SCM} role, especially in the first phases of the infection.

Chapter 6 – Ringraziamenti

La scrittura di una tesi porta con sé alcuni obblighi, formali o meno, ed i ringraziamenti sono uno di questi. In questo caso poco formali e molto goliardici, dovranno per forza passare in rassegna agli attori principali di questa commedia.

In laboratorio ci sono entrato grazie a Raffaele e Lara, in un periodo in cui non pensavo seriamente di perseguire una strada accademica. Raffale è per me un mentore a cui ispirarsi e grazie a lui ho in gran parte cambiato idea su questo tipo di carriera. Reputo la libertà di espressione e di movimento fondamentali per poter crescere al meglio, e il clima stimolante da te promosso costantemente non ha fatto altro che alimentare la crescita di tutti, mia compresa.

Di Lara posso dire che è il capo che tutti vorrebbero avere. Mentre io muovevo i primi passi da laureato, tu eri in rampa di lancio per avviare un tuo laboratorio. Io wannabe dottorato, tu wannabe PI, dopo qualche anno direi che ce l'abbiamo fatta: infatti non ci scambiano più per fidanzati ma per sposati. In questi anni ho provato a seguire le tue orme, da una parte e dall'altra dell'oceano, traendo ispirazione da te come ricercatrice e come persona. Ovunque andassi, trovavo persone a cui avevi lasciato qualcosa che il tempo non era riuscito a sbiadire, me compreso. In laboratorio sono cresciuto con i tuoi insegnamenti, tanti, e le tue arrabbiature, pochissime. Normalmente queste ultime erano accompagnate da locuzioni trivenete, ma rimanevano a me incomprensibili. Anche se non ci hai mai creduto, sono ancora convinto di essere finito nel laboratorio giusto. Grazie di tutto.

Se gli opposti si attraggono, ne abbiamo la prova proprio nell'ufficio al terzo piano. Oltre a Lara, la controparte Lorena. Dotata di energia infinita, mi hai insegnato più di quello che ho potuto ricambiare. Forse non lo sai, ma sei una grande motivatrice. Oltre ai molti insegnamenti pratici di laboratorio, grazie a te so come ricevere due tavoli in vetro al prezzo di uno e come scoprire a quale pianta assomiglio.

Arriviamo quindi agli abitanti della stanza 314C. Più che un laboratorio, uno spogliatoio o un centro sociale. Un'entità unica e caotica con le proprie regole e dinamiche. In un passato abbastanza remoto, era un'isola felice di tre abitanti: Matteo, Paolo ed il sottoscritto. Il tempo scorreva lento, i timer erano silenziosi ed i pranzi meno diversificati: pollo fritto e kebab. Matteo, sei stato per me un fratello maggiore, perchè già sapevi tutto, e sei per me ora un amico di quelli che incontri all'asilo mentre rovisti nella scatola dei Lego. Meno male che ci sei. Paolo, sei per me una creatura leggendaria, e mi manchi molto. Dalla nostra isola ci hai insegnato a commentare in maniera molto alfa tutte le navi che passavano. Siamo partiti scarsi assieme per poi raggiungere ognuno i suoi traguardi. Non posso fare altro che ringraziarvi per tutte le risate, augurandovi buona fortuna per le avventure che avete davanti a voi.

A onore del vero, l'isola felice di pochi abitanti era spesso malfunzionante e poco oliata. Come d'altronde ci si aspetta da una densità elevata di cromosomi Y. Quel passato prevedeva, da protocollo, un numero di sei mani per fare un gel di agarosio per poi elegantemente sbagliarlo tra l'incredulità degli artefici. Tra i partecipanti c'era anche Ruben, guascone olandese. Una persona a cui non si può che volere bene, hai reso anche una semplice piadina arrotolata male un'emozione giornaliera. Spero che tu te la cavi.

L'isola è poi stata invasa da un trio scoppiettante composto da Gaia, Greta e Vale, nello stupore generale dei tre naufraghi uomini. Traendo ispirazione dal vostro desktop, siete state le Charlies Angels del laboratorio per tutto il periodo della tesi. Ognuna a vostro modo, avete portato allegria, spensieratezza e tanti mostrini alle giornate lavorative. In periodi di pandemia, mi sono sentito fortunato a condividere con voi tanto tempo. Pur essendo stato per molto tempo vostro tutor, sento di aver imparato tantissimo da voi e non solo a livello lavorativo.

In tutto questo, non cambiano solo gli abitanti dell'isola ma anche le loro abitazioni. Nell'ultimo periodo, la disposizione delle nuove postazioni ha avuto, ahimè, un

risvolto sfavorevole per fare spazio ai nuovi arrivi. Dal giorno alla notte, ecco l'ingresso in laboratorio di due figure uniche nel loro genere. Trovandomi io nel mezzo, alla destra non mi sono ritrovato Gesù, ma una Adriana Lima che per arrotondare la borsa di dottorato, le sere d'estate serve Bacardi all'Aquasplash di Ospitaletto. Fonte d'ispirazione per la stesura del Galateo dei buon costumi seduti a tavola, aspirante regina d'Inghilterra, Silvia hai da subito travolto tutti con la tua espansività e quella sfrontatezza che sembra rendere tutto semplice. Pota. Non cambiare mai.

Alla sinistra non lo spirito santo, ma Christina Aguilera che a carnevale ha deciso di travestirsi da velociraptor. Sulla carta d'identità del dinosauro un distratto burocrate ha confuso Vizzolo Predabissi con Harlem, Manhattan. Se Miley Cirus si può comprare i fiori da sola e Bruno Mars lascerà per sempre la porta aperta, io ricordo ancora cosa ho pensato quando ti ho aperto il giorno della tua prova: ACCIDENTACCIO. Già avevo capito che quelli che stavano per entrare non erano ciò che pensavo essere tanti guai in veste di studentessa di tesi, ma una persona speciale nella mia vita. Grazie per non avermi ancora fatto a fettine in un congelatore. Le lavatrici a gettoni americane ne sanno molto più di me.

Recentemente altri abitanti hanno preso parte alla vita isolana, ed è impossibile non citarli. Ringrazio Jack per la calma che riesce a trasmettere, anche quando gli cadono provette di sangue, oltre che ad essere il miglior segugio di offerte e promozioni che io conosca. I tre babies Marika, J e Fra per avermi fatto ridere di gusto non poche volte, la bravura con cui hanno sostenuto i fallimenti e poi i successi che ne derivano, sostenendosi sempre a vicenda. Siete un esempio di amicizia che abbiamo visto sbocciare, e anche sboccare a dirla tutta.

Un grazie sincero va inevitabilmente a Viviana, Ben e Giulio per avermi accolto nel loro mondo americano e avermi dato la loro piena fiducia. Per il momento credo sia solo un arrivederci.

Ben più vicini invece sono gli appartenenti al gruppo TB, dirimpettai che mi hanno sempre offerto consigli ed asilo politico quando cercavo un po' di pace.

La mia riconoscenza va anche alla stanza del tempo nota anche come BL3. Luogo di estrema sicurezza e rifugio durante le bufere che imperversavano, ne ho sempre apprezzato l'esistenza per due motivi: la totale assenza di oggetti taglienti e/o contundenti potenzialmente utilizzabili per commettere delitti e la presenza al suo interno di bombe biologiche ben più mansuete di quelle subito al suo esterno.

Fuori dal lab tante altre persone hanno contribuito alla mia integrità e sanità: i miei amici, Pocciafava e non, per avermi sostenuto anche quando ero irraggiungibile. Alle uscite in montagna con Effe, alle discussioni (sempre vinte) con gli energetici Dani e Michi e agli ultimi quindici anni di conoscenza con tutti gli altri. Alla Perla Nera!

I miei genitori, perchè a loro devo tutto, così come alle mie due sorelle maggiori e ai miei nonni. I loro successi e i loro esempi positivi mi hanno sempre spronato a sentirmi all'altezza di chi mi ha preceduto. Prima ancora che iniziassi questo percorso, ho conosciuto una persona che mi ha accompagnato per molti anni e a cui devo tanto. Grazie Cate. Infine, un pensiero a chi ci ha lasciati da poco e chi invece è arrivato da poco, ricordandoci sempre che tutto ciò che sta nel mezzo è un viaggio bellissimo.

Chapter 7 – Bibliography

1. UNAIDS. Global HIV Statistics. *Fact Sheet 2021* 1–3 (2021).

2. Centers for Disease Control. Morbidity and Mortality Weekly Report: June 5, 1981. *Morb. Mortal. Wkly. Rep.* **30**, 1–3 (1981).

3. Update: Mortality Attributable to HIV Infection/AIDS Among Persons Aged 25-44 Years - United States, 1990-1991. *MMWR Surveillance Summaries* vol. 70 481–486 (1993).

4. Sharp, P. M. & Hahn, B. H. The evolution of HIV-1 and the origin of AIDS. *Philos. Trans. R. Soc. B Biol. Sci.* **365**, 2487–2494 (2010).

5. Barré-Sinoussi, F. *et al.* Isolation of a T-lymphotropic retrovirus from a patient at risk for acquired immune deficiency syndrome (AIDS). *Science (80-.).* **220**, 868–871 (1983).

6. Clavel, F. *et al.* Isolation of a New Human Retrovirus from West African Patients with AIDS. *Science (80-.).* **233**, 343–346 (1986).

7. Ayouba, A. *et al.* Evidence for continuing cross-species transmission of SIVsmm to humans: Characterization of a new HIV-2 lineage in rural Côte d'Ivoire. *Aids* **27**, 2488–2491 (2013).

8. Campbell-Yesufu, O. T. & Gandhi, R. T. Update on human immunodeficiency virus (HIV)-2 infection. *Clin. Infect. Dis.* **52**, 780–787 (2011).

9. Guyader, M. reille *et al.* Genome organization and transactivation of the human immunodeficiency virus type 2. *Nature* **326**, 662–669 (1987).

10. Neil, S. J. D., Zang, T. & Bieniasz, P. D. Tetherin inhibits retrovirus release and is antagonized by HIV-1 Vpu. *Nature* **451**, 425–430 (2008).

11. Laguette, N. *et al.* SAMHD1 is the dendritic- and myeloid-cell-specific HIV-1 restriction factor counteracted by Vpx. *Nature* **474**, 654–657 (2011).

12. Manel, N. *et al.* A cryptic sensor for HIV-1 activates antiviral innate immunity in dendritic cells. *Nature* **467**, 214–217 (2010).

13. Hrecka, K. *et al.* Vpx relieves inhibition of HIV-1 infection of macrophages mediated by the SAMHD1 protein. *Nature* **474**, 658–661 (2011).

14. Faria, N. R. *et al.* The early spread and epidemic ignition of HIV-1 in human populations. *Science (80-.).* **346**, 56–61 (2014).

15. Worobey, M. *et al.* 1970s and 'Patient 0' HIV-1 genomes illuminate early HIV/AIDS history in North America. *Nature* **539**, 98–101 (2016).

16. Hütter, G. *et al.* Long-term control of HIV by CCR5 Delta32/Delta32 stem-cell transplantation. *N. Engl. J. Med.* **360**, 692–8 (2009).

17. Gupta, R. K. *et al.* HIV-1 remission following CCR5Δ32/Δ32 haematopoietic stem-cell transplantation. *Nature* **568**, 244–248 (2019).

18. Gupta, R. K. *et al.* Evidence for HIV-1 cure after CCR5Δ32/Δ32 allogeneic haemopoietic stem-cell transplantation 30 months post analytical treatment interruption: a case report. *Lancet HIV* **7**, e340–e347 (2020).

19. Jensen, B.-E. O. *et al.* In-depth virological and immunological characterization of HIV-1 cure after CCR5Δ32/Δ32 allogeneic hematopoietic stem cell transplantation. *Nat. Med.* (2023) doi:10.1038/s41591-023-02213-x.

20. Davey, R. T. *et al.* HIV-1 and T cell dynamics after interruption of highly active antiretroviral therapy (HAART) in patients with a history of sustained viral suppression. *Proc. Natl. Acad. Sci. U. S. A.* **96**, 15109–15114 (1999).

21. Chun, T. W. *et al.* In vivo fate of HIV-1-infected T cells: Quantitative analysis of the transition to stable latency. *Nat. Med.* **1**, 1284–1290 (1995).

22. Chun, T. W. *et al.* Presence of an inducible HIV-1 latent reservoir during highly active antiretroviral therapy. *Proc. Natl. Acad. Sci. U. S. A.* **94**, 13193–13197 (1997).

23. Elsheikh, M. M., Tang, Y., Li, D. & Jiang, G. Deep latency: A new insight into a functional HIV cure. *EBioMedicine* **45**, 624–629 (2019).

24. Ait-Ammar, A. *et al.* Current Status of Latency Reversing Agents Facing the Heterogeneity of HIV-1 Cellular and Tissue Reservoirs. *Front. Microbiol.* **10**, (2020).

25. Abner, E. & Jordan, A. HIV "shock and kill" therapy: In need of revision. *Antiviral Res.* **166**, 19–34 (2019).

26. Kim, Y., Anderson, J. L. & Lewin, S. R. Getting the "Kill" into "Shock and Kill": Strategies to Eliminate Latent HIV. *Cell Host Microbe* **23**, 14–26 (2018).

27. Jimmy Yeh, Y. H. & Ho, Y. C. Shock-and-kill versus block-and-lock: Targeting the fluctuating and heterogeneous HIV-1 gene expression. *Proc. Natl. Acad. Sci. U. S. A.* **118**, 16–18 (2021).

28. Deeks, S. G. *et al.* Research priorities for an HIV cure: International AIDS Society Global Scientific Strategy 2021. *Nat. Med.* (2021) doi:10.1038/s41591-021-01590-5.

29. Body Fluids That Transmit HIV | HIV Transmission | HIV Basics | HIV/AIDS | CDC. https://www.cdc.gov/hiv/basics/hiv-transmission/body-fluids.html.

30. *UNAIDS Report On The Global IADS Epidemic*. *Urban Research & Practice* vol. 3 (2010).

31. David, D. H. *et al.* Rapid turnover of plasma virions and CD4 lymphocytes in HIV-1 Infection. *Nature* vol. 373 123–6 (1995).

32. Geijtenbeek, T. B. H. *et al.* Identification of DC-SIGN, a novel dendritic cell-

specific ICAM-3 receptor that supports primary immune responses. *Cell* **100**, 575–585 (2000).

33. Geijtenbeek, T. B. H. *et al.* DC-SIGN, a dendritic cell-specific HIV-1-binding protein that enhances trans-infection of T cells. *Cell* **100**, 587–597 (2000).

34. Wu, L. & KewalRamani, V. N. Dendritic-cell interactions with HIV: Infection and viral dissemination. *Nat. Rev. Immunol.* **6**, 859–868 (2006).

35. Joseph, S. B., Swanstrom, R., Kashuba, A. D. M. & Cohen, M. S. Bottlenecks in HIV-1 transmission: Insights from the study of founder viruses. *Nat. Rev. Microbiol.* **13**, 414–425 (2015).

36. Fiebig, E. W. *et al.* Dynamics of HIV viremia and antibody seroconversion in plasma donors. *Aids* **17**, 1871–1879 (2003).

37. Myron, C. S., Shaw, G. M., McMichael, A. J. & Haynes, B. F. Acute HIV-1 Infection. *N. Engl. J. Med.* 1943–1954 (2011).

38. Lyles, R. H. *et al.* Natural history of human immunodeficiency virus type 1 viremia after seroconversion and proximal to AIDS in a large cohort of homosexual men. *J. Infect. Dis.* **181**, 872–880 (2000).

39. Fletcher, C. V. *et al.* Persistent HIV-1 replication is associated with lower antiretroviral drug concentrations in lymphatic tissues. *Proc. Natl. Acad. Sci. U. S. A.* **111**, 2307–2312 (2014).

40. Gulick, R.M., Mellors, J.W., Havlir, D., Eron, J.J., Gonzalez, C., McMahon, D., Richman, D.D., Valentine, F.T., Jonas, L., Meibohm, A. and Emini, E. A. Treatment with indinavir, zidovudine, and lamivudine in adults with human immunodeficiency virus infection and prior antiretroviral therapy. *New Eng J Med* 734–739 (1997).

41. Larder, B. a, Darby, G. & Richman, D. D. HIV with Reduced Sensitivity to Zidovudine (AZT) Isolated During Prolonged Therpy. *Science (80-.).* **243**,

1731–1734 (1989).

42. Richman, D. D. Susceptibility to nucleoside analogues of zidovudine-resistant isolates of human immunodeficiency virus. *Am. J. Med.* **88**, 8–10 (1990).

43. Fischl, M. A. *et al.* The efficacy of azidothymidine (AZT) in the treatment of patients with AIDS and AIDS-related complex. A double-blind, placebo-controlled trial. *N. Engl. J. Med.* **317**, 185–91 (1987).

44. FDA-Approved HIV Medicines | NIH. https://hivinfo.nih.gov/understanding-hiv/fact-sheets/fda-approved-hiv-medicines.

45. Rodger, A. J. *et al.* Risk of HIV transmission through condomless sex in serodifferent gay couples with the HIV-positive partner taking suppressive antiretroviral therapy (PARTNER): final results of a multicentre, prospective, observational study. *Lancet* **393**, 2428–2438 (2019).

46. Kwong, P. D. *et al.* Structures of HIV-1 gp120 Envelope Glycoproteins from Laboratory-Adapted and Primary Isolates. *Structure* **8**, 1329–1339 (2000).

47. Hill, C. P., Worthylake, D., Bancroft, D. P., Christensen, A. M. & Sundquist, W. I. Crystal structures of the trimeric human immunodeficiency virus type 1 matrix protein: Implications for membrane association and assembly. *Proc. Natl. Acad. Sci. U. S. A.* **93**, 3099–3104 (1996).

48. Zhao, G. *et al.* Mature HIV-1 capsid structure by cryo-electron microscopy and all-atom molecular dynamics. *Nature* **497**, 643–646 (2013).

49. Pornillos, O. *et al.* X-Ray Structures of the Hexameric Building Block of the HIV Capsid. *Cell* vol. 137 1282–1292 (2009).

50. Pornillos, O., Ganser-Pornillos, B. K. & Yeager, M. Atomic-level modelling of the HIV capsid. *Nature* **469**, 424–427 (2011).

51. Alcover, J. A. *et al.* Characterization of ribosomal frameshifting in HIV-1 gag-pol expression. *Nature* **331**, 10 (1988).

52. Moore, J. P., Mckeating, J. A., Weiss, R. A. & Sattentau, Q. J. Dissociation of gp120 from HIV-1 Virions Induced by Soluble CD4. *Science (80-.).* **250**, 1139–1142 (1990).

53. Behrens, A. J. *et al.* Composition and Antigenic Effects of Individual Glycan Sites of a Trimeric HIV-1 Envelope Glycoprotein. *Cell Rep.* **14**, 2695–2706 (2016).

54. Strebel, K. HIV accessory proteins versus host restriction factors. *Curr. Opin. Virol.* **3**, 692–699 (2013).

55. Mehle, A. *et al.* Vif Overcomes the Innate Antiviral Activity of APOBEC3G by Promoting Its Degradation in the Ubiquitin-Proteasome Pathway. *J. Biol. Chem.* **279**, 7792–7798 (2004).

56. Lama, J. The Physiological Relevance of CD4 Receptor Down-Modulation During HIV Infection. *Curr. HIV Res.* **1**, 167–184 (2003).

57. Mariani, R. & Skowronski, J. CD4 down-regulation by nef alleles isolated from human immunodeficiency virus type 1-infected individuals. *Proc. Natl. Acad. Sci. U. S. A.* **90**, 5549–5553 (1993).

58. Das, S. R. & Jameel, S. Biology of the HIV Nef protein. *Indian J. Med. Res.* **121**, 315–332 (2005).

59. Pizzato, M. *et al.* Dynamin 2 is required for the enhancement of HIV-1 infectivity by Nef. *Proc. Natl. Acad. Sci. U. S. A.* **104**, 6812–6817 (2007).

60. Rosa, A. *et al.* HIV-1 Nef promotes infection by excluding SERINC5 from virion incorporation. *Nature* **526**, 212–217 (2015).

61. Usami, Y., Wu, Y. & Göttlinger, H. G. SERINC3 and SERINC5 restrict HIV-1

infectivity and are counteracted by Nef. *Nature* **526**, 218–223 (2015).

62. Inuzuka, M., Hayakawa, M. & Ingi, T. Serine, an activity-regulated protein family, incorporates serine into membrane lipid synthesis. *J. Biol. Chem.* **280**, 35776–35783 (2005).

63. Planelles, V. *et al.* Vpr-induced cell cycle arrest is conserved among primate lentiviruses. *J. Virol.* **70**, 2516–2524 (1996).

64. He, J. *et al.* Human immunodeficiency virus type 1 viral protein R (Vpr) arrests cells in the G2 phase of the cell cycle by inhibiting p34cdc2 activity. *J. Virol.* **69**, 6705–6711 (1995).

65. Laguette, N. *et al.* Premature activation of the slx4 complex by vpr promotes g2/m arrest and escape from innate immune sensing. *Cell* **156**, 134–145 (2014).

66. Klimkait, T., Strebel, K., Hoggan, M. D., Martin, M. A. & Orenstein, J. M. The human immunodeficiency virus type 1-specific protein vpu is required for efficient virus maturation and release. *J. Virol.* **64**, 621–629 (1990).

67. Saphire, A. C. S., Bobardt, M. D., Zhang, Z., David, G. & Gallay, P. A. Syndecans Serve as Attachment Receptors for Human Immunodeficiency Virus Type 1 on Macrophages. *J. Virol.* **75**, 9187–9200 (2001).

68. Mondor, I., Ugolini, S. & Sattentau, Q. J. Human Immunodeficiency Virus Type 1 Attachment to HeLa CD4 Cells Is CD4 Independent and gp120 Dependent and Requires Cell Surface Heparans. *J. Virol.* **72**, 3623–3634 (1998).

69. Stein, B. S. *et al.* pH-independent HIV entry into CD4-positive T cells via virus envelope fusion to the plasma membrane. *Cell* **49**, 659–668 (1987).

70. Maddon, P. J. *et al.* HIV infection does not require endocytosis of its receptor, CD4. *Cell* **54**, 865–874 (1988).

71. Permanyer, M., Ballana, E. & Esté, J. A. Endocytosis of HIV: Anything goes.

Trends Microbiol. **18**, 543–551 (2010).

72. Hung, C.-S., Vander Heyden, N. & Ratner, L. Analysis of the Critical Domain in the V3 Loop of Human Immunodeficiency Virus Type 1 gp120 Involved in CCR5 Utilization. *J. Virol.* **73**, 8216–8226 (1999).

73. Mild, M. *et al.* Differences in molecular evolution between switch (R5 to R5X4/X4-tropic) and non-switch (R5-tropic only) HIV-1 populations during infection. *Infect. Genet. Evol.* **10**, 356–364 (2010).

74. Samson, M. *et al.* Resistance to HIV-1 infection in caucasian individuals bearing mutant alleles of the CCR-5 chemokine receptor gene. *Nature* vol. 382 722–726 (1996).

75. Novembre, J., Galvani, A. P. & Slatkin, M. The geographic spread of the CCR5 Δ32 HIV-resistance allele. *PLoS Biol.* **3**, 1954–1962 (2005).

76. Von Appen, A. *et al.* In situ structural analysis of the human nuclear pore complex. *Nature* **526**, 140–143 (2015).

77. Zila, V. *et al.* Cone-shaped HIV-1 capsids are transported through intact nuclear pores. *Cell* **184**, 1032-1046.e18 (2021).

78. Burdick, R. C. *et al.* HIV-1 uncoats in the nucleus near sites of integration. *Proc. Natl. Acad. Sci. U. S. A.* **117**, 5486–5493 (2020).

79. Fernandez, J. *et al.* Microtubule-associated proteins 1 (MAP1) promote human immunodeficiency virus type I (HIV-1) intracytoplasmic routing to the nucleus. *J. Biol. Chem.* **290**, 4631–4646 (2015).

80. Francis, A. C. & Melikyan, G. B. Single HIV-1 Imaging Reveals Progression of Infection through CA-Dependent Steps of Docking at the Nuclear Pore, Uncoating, and Nuclear Transport. *Cell Host Microbe* **23**, 536-548.e6 (2018).

81. Selyutina, A., Persaud, M., Lee, K., KewalRamani, V. & Diaz-Griffero, F.

Nuclear Import of the HIV-1 Core Precedes Reverse Transcription and Uncoating. *Cell Rep.* **32**, 108201 (2020).

82. Dharan, A., Bachmann, N., Talley, S., Zwikelmaier, V. & Campbell, E. M. Nuclear pore blockade reveals that HIV-1 completes reverse transcription and uncoating in the nucleus. *Nat. Microbiol.* **5**, 1088–1095 (2020).

83. Suzuki, Y. & Craigie, R. The road to chromatin - Nuclear entry of retroviruses. *Nat. Rev. Microbiol.* **5**, 187–196 (2007).

84. Guedán, A., Caroe, E. R., Barr, G. C. R. & Bishop, K. N. The role of capsid in hiv-1 nuclear entry. *Viruses* **13**, 1–14 (2021).

85. Shen, Q., Wu, C., Freniere, C., Tripler, T. N. & Xiong, Y. Nuclear import of hiv-1. *Viruses* **13**, 1–14 (2021).

86. Fernandez, J. *et al.* Transportin-1 binds to the HIV-1 capsid via a nuclear localization signal and triggers uncoating. *Nat. Microbiol.* **4**, 1840–1850 (2019).

87. Kane, M. *et al.* Nuclear pore heterogeneity influences HIV-1 infection and the antiviral activity of MX2. *Elife* **7**, 1–44 (2018).

88. Nunzio, F. Di *et al.* Human Nucleoporins Promote HIV-1 Docking at the Nuclear Pore , Nuclear Import and Integration. *PLoS One* **7**, (2012).

89. Brass, A. L. *et al.* Identification of host proteins required for HIV infection through a functional genomic screen. *Pediatrics* **122**, 921–926 (2008).

90. Schaller, T. *et al.* HIV-1 capsid-cyclophilin interactions determine nuclear import pathway, integration targeting and replication efficiency. *PLoS Pathog.* **7**, (2011).

91. Lin, D. H., Zimmermann, S., Stuwe, T., Stuwe, E. & Hoelz, A. Structural and functional analysis of the C-terminal domain of Nup358/RanBP2. *J. Mol. Biol.* **425**, 1318–1329 (2013).

92. Matreyek, K. A. & Engelman, A. The Requirement for Nucleoporin NUP153 during Human Immunodeficiency Virus Type 1 Infection Is Determined by the Viral Capsid. *J. Virol.* **85**, 7818–7827 (2011).

93. Price, A. J. *et al.* Host Cofactors and Pharmacologic Ligands Share an Essential Interface in HIV-1 Capsid That Is Lost upon Disassembly. *PLoS Pathog.* **10**, (2014).

94. Li, L. *et al.* Role of the non-homologous DNA end joining pathway in the early steps of retroviral infection. **20**, (2001).

95. Chen, J. C. H. *et al.* Crystal structure of the HIV-1 integrase catalytic core and C-terminal domains: A model for viral DNA binding. *Proc. Natl. Acad. Sci. U. S. A.* **97**, 8233–8238 (2000).

96. Krishnan, L. *et al.* Structure-based modeling of the functional HIV-1 intasome and its inhibition. *Proc. Natl. Acad. Sci. U. S. A.* **107**, 15910–15915 (2010).

97. Craigie, R. & Bushman, F. D. HIV DNA integration. *Cold Spring Harb. Perspect. Med.* **2**, 1–18 (2012).

98. Mansharamani, M. *et al.* Barrier-to-Autointegration Factor BAF Binds p55 Gagand Matrix and Is a Host Component of Human ImmunodeficiencyVirus Type 1Virions. *J. Virol.* **77**, 13084–13092 (2003).

99. Skoko, D. *et al.* Barrier-to-autointegration factor (BAF) condenses DNA by looping. *Proc. Natl. Acad. Sci. U. S. A.* **106**, 16610–16615 (2009).

100. Sowd, G. A. *et al.* A critical role for alternative polyadenylation factor CPSF6 in targeting HIV-1 integration to transcriptionally active chromatin. *Proc. Natl. Acad. Sci. U. S. A.* **113**, E1054–E1063 (2016).

101. Kvaratskhelia, M., Sharma, A., Larue, R. C., Serrao, E. & Engelman, A. Molecular mechanisms of retroviral integration site selection. *Nucleic Acids Res.* **42**, 10209–10225 (2014).

102. Ciuffi, A. *et al.* A role for LEDGF/p75 in targeting HIV DNA integration. *Nat. Med.* **11**, 1287–1289 (2005).

103. Cereseto, A. *et al.* Acetylation of HIV-1 integrase by p300 regulates viral integration. *EMBO J.* **24**, 3070–3081 (2005).

104. Manganaro, L. *et al.* Concerted action of cellular JNK and Pin1 restricts HIV-1 genome integration to activated CD4+ T lymphocytes. *Nat. Med.* **16**, 329–333 (2010).

105. Bushman, F. *et al.* Genome-wide analysis of retroviral DNA integration. *Nat. Rev. Microbiol.* **3**, 848–858 (2005).

106. Lusic, M. & Siliciano, R. F. Nuclear landscape of HIV-1 infection and integration. *Nature Reviews Microbiology* (2017) doi:10.1038/nrmicro.2016.162.

107. Schroder, A. R. W. *et al.* HIV-1 Integration in the Human Genome Favors Active Genes and Local Hotspots. *Cell* **110**, 521–529 (2002).

108. Demeulemeester, J., De Rijck, J., Gijsbers, R. & Debyser, Z. Retroviral integration: Site matters. Mechanisms and consequences of retroviral integration site selection. *BioEssays* **37**, 1202–1214 (2015).

109. Wu, X., Li, Y., Crise, B. & Burgess, S. M. Transcription start regions in the human genome are favored targets for MLV integration. *Science (80-.).* **300**, 1749–1751 (2003).

110. Ikeda, T., Shibata, J., Yoshimura, K., Koito, A. & Matsushita, S. Recurrent HIV-1 integration at the BACH2 locus in resting CD4+ T cell populations during effective highly active antiretroviral therapy. *J. Infect. Dis.* **195**, 716–725 (2007).

111. Liu, H. *et al.* Integration of Human Immunodeficiency Virus Type 1 in Untreated Infection Occurs Preferentially within Genes. *J. Virol.* **80**, 7765–7768 (2006).

112. Marini, B. *et al.* Nuclear architecture dictates HIV-1 integration site selection. *Nature* **521**, 227–231 (2015).

113. Klaver, B. & Berkhout, B. Comparison of 5′ and 3′ long terminal repeat promoter function in human immunodeficiency virus. *J. Virol.* **68**, 3830–3840 (1994).

114. Cary, D. C., Fujinaga, K. & Matija Peterlin, B. Molecular mechanisms of HIV latency. *J Clin Invest* **126**, 448–454 (2016).

115. Duh, E. J., Maury, W. J., Folks, T. M., Fauci, A. S. & Rabson, A. B. Tumor necrosis factor α activates human immunodeficiency virus type 1 through induction of nuclear factor binding to the NF-κB sites in the long terminal repeat. *Proc. Natl. Acad. Sci. U. S. A.* **86**, 5974–5978 (1989).

116. Granowitz, E. V., Saget, B. M., Wang, M. Z., Dinarello, C. A. & Skolnik, P. R. Interleukin 1 induces HIV-1 expression in chronically infected U1 cells: Blockade by interleukin 1 receptor antagonist and tumor necrosis factor binding protein type 1. *Mol. Med.* **1**, 667–677 (1995).

117. Siekevitz, M. *et al.* Activation of the HlV-1 LTR by T cell mitogens and the trans-activator protein of HTLV-I. *Science (80-.).* **238**, 1575–1578 (1987).

118. Pereira, L. A., Bentley, K., Peeters, A., Churchill, M. J. & Deacon, N. J. A compilation of cellular transcription factor interactions with the HIV-1 LTR promoter. *Nucleic Acids Res.* **28**, 663–668 (2000).

119. Berkhout, B., Silverman, R. H. & Jeang, K. T. Tat trans-activates the human immunodeficiency virus through a nascent RNA target. *Cell* **59**, 273–282 (1989).

120. Shukla, A., Ramirez, N. P. & Orso, I. D. HIV-1 Proviral Transcription and Latency in the New Era. 1–40 (2020) doi:10.3390/v12050555.

121. Fujinaga, K., Huang, F. & Peterlin, B. M. P-TEFb: The master regulator of

transcription elongation. *Mol. Cell* **83**, 393–403 (2023).

122. Herrmann, C. H. & Rice, A. P. Specific interaction of the human immunodeficiency virus Tat proteins with a cellular protein kinase. *Virology* vol. 197 601–608 (1993).

123. Mancebo, H. S. Y. *et al.* P-TEFb kinase is required for HIV Tat transcriptional activation in vivo and in vitro. *Genes Dev.* **11**, 2633–2644 (1997).

124. Zhu, Y. *et al.* Transcription elongation factor P-TEFb is required for HIV-1 Tat transactivation in vitro. *Genes Dev.* **11**, 2622–2632 (1997).

125. Wei, P., Garber, M. E., Fang, S. M., Fischer, W. H. & Jones, K. A. A novel CDK9-associated C-type cyclin interacts directly with HIV-1 Tat and mediates its high-affinity, loop-specific binding to TAR RNA. *Cell* (1998) doi:10.1016/S0092-8674(00)80939-3.

126. Kao, S. Y., Calman, A. F., Luciw, P. A. & Peterlin, B. M. Anti-termination of transcription within the long terminal repeat of HIV-1 by tat gene product. *Nature* **330**, 489–493 (1987).

127. Donahue, D. A., Kuhl, B. D., Sloan, R. D. & Wainberg, M. A. The Viral Protein Tat Can Inhibit the Establishment of HIV-1 Latency. *J. Virol.* **86**, 3253–3263 (2012).

128. Pomerantz, R. J., Seshamma, T. & Trono, D. Efficient replication of human immunodeficiency virus type 1 requires a threshold level of Rev: potential implications for latency. *J. Virol.* **66**, 1809–1813 (1992).

129. Cron, R. Q. *et al.* NFAT1 enhances HIV-1 gene expression in primary human CD4 T cells. *Clin. Immunol.* **94**, 179–191 (2000).

130. Nabel, G. & Baltimore, D. An inducible transcription factor activates expression of human immunodeficiency virus in T cells. *Nature* (1987) doi:10.1038/326711a0.

131. Bielinska, A., Krasnow, S. & Nabel, G. J. NF-kappa B-mediated activation of the human immunodeficiency virus enhancer: site of transcriptional initiation is independent of the TATA box. *J. Virol.* (1989) doi:10.1128/jvi.63.9.4097-4100.1989.

132. Liu, T., Zhang, L., Joo, D. & Sun, S. C. NF-κB signaling in inflammation. *Signal Transduct. Target. Ther.* **2**, (2017).

133. Sen, R. & Baltimore, D. Inducibility of κ immunoglobulin enhancer-binding protein NF-κB by a posttranslational mechanism. *Cell* **47**, 921–928 (1986).

134. Hayden, M. S. & Ghosh, S. NF-κB in immunobiology. *Cell Res.* **21**, 223–244 (2011).

135. Alcamí, J. *et al.* Absolute dependence on kappa B responsive elements for initiation and Tat-mediated amplification of HIV transcription in blood CD4 T lymphocytes. *EMBO J.* **14**, 1552–60 (1995).

136. Hiscott, J., Kwon, H. & Génin, P. Hostile takeovers: Viral appropriation of the NF-κB pathway. *J. Clin. Invest.* **107**, 143–151 (2001).

137. Oeckinghaus, A. & Ghosh, S. The NF-kappaB family of transcription factors and its regulation. *Cold Spring Harb. Perspect. Biol.* **1**, 1–14 (2009).

138. Chen, F. E., Huang, D. Bin, Chen, Y. Q. & Ghosh, G. Crystal structure of p50/p65 heterodimer of transcription factor NF-κb bound to DNA. *Nature* **391**, 410–412 (1998).

139. Zhong, H., May, M. J., Jimi, E. & Ghosh, S. The phosphorylation status of nuclear NF-κB determines its association with CBP/p300 or HDAC-1. *Mol. Cell* **9**, 625–636 (2002).

140. Pahl, H. L. Activators and target genes of Rel/NF-κB transcription factors. *Oncogene* **18**, 6853–6866 (1999).

141. Hu, H. *et al.* OTUD7B controls non-canonical NF-κB activation through deubiquitination of TRAF3. *Nature* **494**, 371–374 (2013).

142. Shao-Cong Sun. The non-canonical NF-κB pathway in immunity and inflammation. *Nat. Rev. Immunol.* **17**, 545–558 (2017).

143. Gheysen, D. *et al.* Assembly and release of HIV-1 precursor Pr55gag virus-like particles from recombinant baculovirus-infected insect cells. *Cell* **59**, 103–112 (1989).

144. Chen, J. *et al.* High efficiency of HIV-1 genomic RNA packaging and heterozygote formation revealed by single virion analysis. *Proc. Natl. Acad. Sci. U. S. A.* **106**, 13535–13540 (2009).

145. Darlix, J. L., Gabus, C., Nugeyre, M. T., Clavel, F. & Barré-Sinoussi, F. Cis elements and Trans-acting factors involved in the RNA dimerization of the human immunodeficiency virus HIV-1. *J. Mol. Biol.* **216**, 689–699 (1990).

146. Freed, E. O. HIV-1 assembly, release and maturation. *Nat. Rev. Microbiol.* **13**, 484–496 (2015).

147. Ndung'u, T., McCune, J. M. & Deeks, S. G. Why and where an HIV cure is needed and how it might be achieved. *Nature* **576**, 397–405 (2019).

148. Perelson, A. S. *et al.* Decay characteristics of HIV-1-infected compartments during combination therapy. *Nature* vol. 387 188–191 (1997).

149. Crooks, A. M. *et al.* Precise quantitation of the latent HIV-1 reservoir: Implications for eradication strategies. *J. Infect. Dis.* (2015) doi:10.1093/infdis/jiv218.

150. Finzi, D. *et al.* Latent infection of CD4+ T cells provides a mechanism for lifelong persistence of HIV-1, even in patients on effective combination therapy. *Nat. Med.* **5**, 512–517 (1999).

151. Siliciano, J. D. *et al.* Long-term follow-up studies confirm the stability of the latent reservoir for HIV-1 in resting CD4+ T cells. *Nat. Med.* **9**, 727–728 (2003).

152. Ho, Y. C. *et al.* Replication-competent noninduced proviruses in the latent reservoir increase barrier to HIV-1 cure. *Cell* **155**, 540 (2013).

153. Chun, T.-W. *et al.* Quantification of latent tissue reservoirs and total body viral load in HIV-1 infection. *Nature* **387**, 183–188 (1997).

154. Finzi, D. *et al.* Identification of a reservoir for HIV-1 in patients on highly active antiretroviral therapy. **278**, 1295–1300 (1997).

155. Blankson, J. N., Persaud, D. & Siliciano, R. F. The challenge of viral reservoirs in hiv-1 infection. *Annu. Rev. Med.* **53**, 557–593 (2002).

156. Ho, D. D., Rota, T. R. & Hirsch, M. S. Infection of Monocyte / Macrophages by Human T Lymphotropic Virus Type III. *J. Clin. Invest.* **77**, 1712–1715 (1986).

157. Saleh, S. *et al.* CCR7 ligands CCL19 and CCL21 increase permissiveness of resting memory CD4+ T cells to HIV-1 infection: A novel model of HIV-1 latency. *Blood* **110**, 4161–4164 (2007).

158. Dornadula, G. *et al.* Residual HIV-1 RNA in blood plasma of patients taking suppressive highly active antiretroviral therapy. *Biomed. Pharmacother.* **55**, 7–15 (2001).

159. Palmer, S. *et al.* Low-level viremia persists for at least 7 years in patients on suppressive antiretroviral therapy. *Proc. Natl. Acad. Sci. U. S. A.* **105**, 3879–3884 (2008).

160. Lorenzo-Redondo, R. *et al.* Persistent HIV-1 replication maintains the tissue reservoir during therapy. *Nature* **530**, 51–56 (2016).

161. Jenabian, M. A. *et al.* Immune tolerance properties of the testicular tissue as a viral sanctuary site in ART-treated HIV-infected adults. *Aids* **30**, 2777–2786

(2016).

162. J Buzón, M. *et al.* HIV-1 replication and immune dynamics are affected by raltegravir intensification of HAART-suppressed subjects. *Nat. Med.* **16**, 460–465 (2010).

163. Evering, T. H. *et al.* Absence of HIV-1 evolution in the gut-associated lymphoid tissue from patients on combination antiviral therapy initiated during primary infection. *PLoS Pathog.* **8**, (2012).

164. Dinoso, J. B. *et al.* Treatment intensification does not reduce residual HIV-1 viremia in patients on highly active antiretroviral therapy. *Proc. Natl. Acad. Sci. U. S. A.* **106**, 9403–9408 (2009).

165. Wong, J. K. *et al.* Recovery of Replication-Competent HIV Despite Prolonged Suppression of Plasma Viremia. *Sci. Reports* **278**, 1291–1295 (1997).

166. Shan, L. *et al.* Transcriptional Reprogramming during Effector-to-Memory Transition Renders CD4+ T Cells Permissive for Latent HIV-1 Infection. *Immunity* **47**, 766-775.e3 (2017).

167. Perng, G. C. & Jones, C. Towards an understanding of the herpes simplex virus type 1 latency-reactivation cycle. *Interdiscip. Perspect. Infect. Dis.* **2010**, (2010).

168. Eisele, E. & Siliciano, R. F. Redefining the Viral Reservoirs that Prevent HIV-1 Eradication. *Immunity* **37**, 377–388 (2012).

169. Kwon, K. J. & Siliciano, R. F. HIV persistence: Clonal expansion of cells in the latent reservoir. *Journal of Clinical Investigation* (2017) doi:10.1172/JCI95329.

170. Simonetti, F. R. *et al.* Clonally expanded CD4+ T cells can produce infectious HIV-1 in vivo. *Proc. Natl. Acad. Sci. U. S. A.* (2016) doi:10.1073/pnas.1522675113.

171. Hosmane, N. N. *et al.* Proliferation of latently infected CD4+ T cells carrying replication-competent HIV-1: Potential role in latent reservoir dynamics. *J. Exp. Med* **214**, 959–972 (2017).

172. Wagner, T. A. *et al.* Proliferation of cells with HIV integrated into cancer genes contributes to persistent infection. *Science (80-.).* **345**, 570–573 (2014).

173. Cohn, L. B., Chomont, N. & Deeks, S. G. The Biology of the HIV-1 Latent Reservoir and Implications for Cure Strategies. *Cell Host Microbe* **27**, 519–530 (2020).

174. Maldarelli, F. *et al.* Specific HIV integration sites are linked to clonal expansion and persistence of infected cells. *Science (80-.).* **345**, 179–183 (2014).

175. Cesana, D. *et al.* HIV-1-mediated insertional activation of STAT5B and BACH2 trigger viral reservoir in T regulatory cells. *Nat. Commun.* **8**, (2017).

176. Surh, C. D. & Sprent, J. Homeostasis of Naive and Memory T Cells. *Immunity* **29**, 848–862 (2008).

177. Chomont, N. *et al.* HIV reservoir size and persistence are driven by T cell survival and homeostatic proliferation. *Nat. Med.* (2009) doi:10.1038/nm.1972.

178. Bosque, A., Famiglietti, M., Weyrich, A. S., Goulston, C. & Planelles, V. Homeostatic proliferation fails to efficiently reactivate HIV-1 latently infected central memory CD4+ T cells. *PLoS Pathog.* (2011) doi:10.1371/journal.ppat.1002288.

179. Douek, D. C. *et al.* A Novel Approach to the Analysis of Specificity, Clonality, and Frequency of HIV-Specific T Cell Responses Reveals a Potential Mechanism for Control of Viral Escape. *J. Immunol.* **168**, 3099–3104 (2002).

180. Henrich, T. J. *et al.* Human immunodeficiency virus type 1 persistence following systemic chemotherapy for malignancy. *J. Infect. Dis.* **216**, 254–262 (2017).

181. Murray, A. J., Kwon, K. J., Farber, D. L. & Siliciano, R. F. The Latent Reservoir for HIV-1: How Immunologic Memory and Clonal Expansion Contribute to HIV-1 Persistence. *J. Immunol.* (2016) doi:10.4049/jimmunol.1600343.

182. Chun, T. W. *et al.* Early establishment of a pool of latently infected, resting CD4+ T cells during primary HIV-1 infection. *Proc. Natl. Acad. Sci. U. S. A.* **95**, 8869–8873 (1998).

183. Whitney, J. B. *et al.* Rapid seeding of the viral reservoir prior to SIV viraemia in rhesus monkeys. *Nature* **512**, 74–77 (2014).

184. Okoye, A. A. *et al.* Early antiretroviral therapy limits SIV reservoir establishment to delay or prevent post-treatment viral rebound. *Nat. Med.* **24**, 1430–1440 (2018).

185. Henrich, T. J. *et al.* HIV-1 persistence following extremely early initiation of antiretroviral therapy (ART) during acute HIV-1 infection: An observational study. *PLoS Med.* **14**, 1–22 (2017).

186. Ananworanich, J. *et al.* HIV DNA Set Point is Rapidly Established in Acute HIV Infection and Dramatically Reduced by Early ART. *EBioMedicine* **11**, 68–72 (2016).

187. Colby, D. J. *et al.* Rapid HIV RNA rebound after antiretroviral treatment interruption in persons durably suppressed in Fiebig i acute HIV infection brief-communication. *Nat. Med.* **24**, 923–926 (2018).

188. Garcia-Broncano, P. *et al.* Early antiretroviral therapy in neonates with HIV-1 infection restricts viral reservoir size and induces a distinct innate immune profile. *Sci. Transl. Med.* **11**, (2019).

189. Restifo, N. P. & Gattinoni, L. Lineage relationship of effector and memory T cells. *Curr Opin Immunol.* **25**, 1–7 (2013).

190. Burke, B. *et al.* Primary Cell Model for Activation-Inducible Human

Immunodeficiency Virus. *J. Virol.* **81**, 7424–7434 (2007).

191. Swiggard, W. J. *et al.* Human Immunodeficiency Virus Type 1 Can Establish Latent Infection in Resting CD4 + T Cells in the Absence of Activating Stimuli . *J. Virol.* **79**, 14179–14188 (2005).

192. Wong, M. E., Jaworowski, A. & Hearps, A. C. The HIV reservoir in monocytes and macrophages. *Front. Immunol.* **10**, (2019).

193. Cameron, P. U. *et al.* Establishment of HIV-1 latency in resting CD4+ T cells depends on chemokine-induced changes in the actin cytoskeleton. *Proc. Natl. Acad. Sci. U. S. A.* **107**, 16934–16939 (2010).

194. Manganaro, L. *et al.* IL-15 regulates susceptibility of CD4+ T cells to HIV infection. *Proc. Natl. Acad. Sci. U. S. A.* **115**, E9659–E9667 (2018).

195. McBrien, J. B. *et al.* Robust and persistent reactivation of SIV and HIV by N-803 and depletion of CD8+ cells. *Nature* **578**, 154–159 (2020).

196. Zhang, X., Sun, S., Hwang, I., Tough, D. F. & Sprent, J. Potent and selective stimulation of memory-phenotype CD8+ T cells in vivo by IL-15. *Immunity* **8**, 591–599 (1998).

197. Ku, C. C., Murakami, M., Sakamoto, A., Kappler, J. & Marrack, P. Control of homeostasis of CD8+ memory T cells by opposing cytokines. *Science* **288**, 675–8 (2000).

198. Fehniger, T. A. & Caligiuri, M. A. Interleukin 15: Biology and relevance to human disease. *Blood* **97**, 14–32 (2001).

199. Cieri, N. *et al.* IL-7 and IL-15 instruct the generation of human memory stem T cells from naive precursors. *Blood* **121**, 573–584 (2013).

200. Budagian, V., Bulanova, E., Paus, R., Bulfone-paus, S. & Lu, D.-. IL-15 / IL-15 receptor biology : A guided tour through an expanding universe. *Cytokine*

Growth Factor Rev. **17**, 259–280 (2006).

201. Swaminathan, S. *et al.* Interleukin-15 (Il-15) strongly correlates with increasing HIV-1 viremia and markers of inflammation. *PLoS One* **11**, 4–11 (2016).

202. Stacey, A. R. *et al.* Induction of a Striking Systemic Cytokine Cascade prior to Peak Viremia in Acute Human Immunodeficiency Virus Type 1 Infection, in Contrast to More Modest and Delayed Responses in Acute Hepatitis B and C Virus Infections. *J. Virol.* (2009) doi:10.1128/jvi.01844-08.

203. Baldauf, H. M. *et al.* SAMHD1 restricts HIV-1 infection in resting CD4 + T cells. *Nat. Med.* **18**, 1682–1687 (2012).

204. Wu, L. SAMHD1: a new contributor to HIV-1 restriction in resting CD4+ T-cells. *Retrovirology* **9**, 1–5 (2012).

205. Lahouassa, H. *et al.* SAMHD1 restricts HIV-1 by reducing the intracellular pool of deoxynucleotide triphosphates. **13**, 223–228 (2013).

206. Cribier, A., Descours, B., Valadão, A. L. C., Laguette, N. & Benkirane, M. Phosphorylation of SAMHD1 by Cyclin A2/CDK1 Regulates Its Restriction Activity toward HIV-1. *Cell Rep.* (2013) doi:10.1016/j.celrep.2013.03.017.

207. White, T. E. *et al.* The retroviral restriction ability of SAMHD1, but not its deoxynucleotide triphosphohydrolase activity, is regulated by phosphorylation. *Cell Host Microbe* (2013) doi:10.1016/j.chom.2013.03.005.

208. Kandathil, A. J., Sugawara, S. & Balagopal, A. Are T cells the only HIV-1 reservoir? *Retrovirology* **13**, 1–10 (2016).

209. García, M., Buzón, M. J., Benito, J. M. & Rallón, N. Peering into the HIV reservoir. *Rev. Med. Virol.* **28**, 1–26 (2018).

210. Honeycutt, J. B. *et al.* HIV persistence in tissue macrophages of humanized myeloid-only mice during antiretroviral therapy. *Nat. Med.* **23**, 638–643 (2017).

211. Chun, T. W. *et al.* Decay of the HIV reservoir in patients receiving antiretroviral therapy for extended periods: Implications for eradication of virus. *J. Infect. Dis.* **195**, 1762–1764 (2007).

212. Estes, J. D. *et al.* Defining total-body AIDS-virus burden with implications for curative strategies. *Nat. Med.* **23**, 1271–1276 (2017).

213. Chaillon, A. *et al.* HIV persists throughout deep tissues with repopulation from multiple anatomical sources. *J. Clin. Invest.* **130**, 1699–1712 (2020).

214. Cossarizza, A. *et al.* CD45 isoforms expression on CD4 + and CD8 + T cells throughout life, from newborns to centenarians: implications for T cell memory. *Mech. Ageing Dev.* **86**, 173–195 (1996).

215. Sallusto, F., Lenig, D., Förster, R., Lipp, M. & Lanzavecchia, A. Two subsets of memory T lymphocytes with distinct homing potentials and effector functions. *Nature* **401**, 708–712 (1999).

216. Mahnke, Y. D., Brodie, T. M., Sallusto, F., Roederer, M. & Lugli, E. The who's who of T-cell differentiation: Human memory T-cell subsets. *European Journal of Immunology* (2013) doi:10.1002/eji.201343751.

217. Sanders, M. E. *et al.* Human Memory T Lymphocytes Express Increased Levels of Three Production. *J. Immunol.* 1401–1407 (1988).

218. Michie, C. A., Mclean, A., Alcock, C. & Beverley, P. C. L. Lifespan of human lymphocyte subsets defined by CD45 isoforms. *Nature* **359**, 710–713 (1992).

219. Sallusto, F., Geginat, J. & Lanzavecchia, A. Central memory and effector memory T cell subsets: Function , Generation , and Maintenance. *Annu. Rev. Immunol.* (2004) doi:10.1146/annurev.immunol.22.012703.104702.

220. Okada, R., Kondo, T., Matsuki, F., Takata, H. & Takiguchi, M. Phenotypic classification of human CD4 1 T cell subsets and their differentiation. *Int. Immunol.* **20**, 1189–1199 (2008).

221. Masopust, D., Vezys, V., Marzo, A. L. & Lefrancois, L. Preferential localization of effector memory cells in nonlymphoid tissue. *Sci. Reports* **291**, 2413–2417 (2001).

222. Amyes, E. *et al.* Characterization of the CD4+ T cell response to epstein-barr virus during primary and persistent infection. *J. Exp. Med.* **198**, 903–911 (2003).

223. Fritsch, R. D. *et al.* Stepwise Differentiation of CD4 Memory T Cells Defined by Expression of CCR7 and CD27. *J. Immunol.* (2022) doi:10.4049/jimmunol.175.10.6489.

224. Gattinoni, L. *et al.* A human memory T cell subset with stem cell – like properties. *Nat. Med.* (2011) doi:10.1038/nm.2446.

225. Zhang, Y., Joe, G., Hexner, E., Zhu, J. & Emerson, S. G. Host-reactive CD8+ memory stem cells in graft-versus- host disease. *Nat. Med.* **11**, 1299–1305 (2005).

226. Gattinoni, L. *et al.* Wnt signaling arrests effector T cell differentiation and generates CD8+ memory stem cells. *Nat. Med.* **15**, 808–813 (2009).

227. del Amo, P. C. *et al.* Human TSCM cell dynamics in vivo are compatible with long-lived immunological memory and stemness. *PLoS Biol.* **16**, 1–22 (2018).

228. Scholz, G. *et al.* Modulation of mTOR Signalling Triggers the Formation of Stem Cell-like Memory T Cells. *EBIOM* **4**, 50–61 (2016).

229. Lugli, E. *et al.* Superior T memory stem cell persistence supports long-lived T cell memory. *J. Clin. Biochem. Nutr.* **23**, 85–93 (1997).

230. Fuertes Marraco, S. A. *et al.* Long-lasting stem cell-like memory CD8+ T cells with a naïve-like profile upon yellow fever vaccination. *Sci. Transl. Med.* **7**, (2015).

231. Jung, S. *et al.* The generation of stem cell-like memory cells early after

BNT162b2 vaccination is associated with durability of memory CD8+ T cell responses. *Cell Rep.* **40**, 111138 (2022).

232. Guerrera, G. *et al.* BNT162b2 vaccination induces durable SARS-CoV-2–specific T cells with a stem cell memory phenotype. *Sci. Immunol.* **6**, 1–13 (2021).

233. Jung, J. H. *et al.* SARS-CoV-2-specific T cell memory is sustained in COVID-19 convalescent patients for 10 months with successful development of stem cell-like memory T cells. *Nat. Commun.* **12**, 1–12 (2021).

234. Buzon, M. J. *et al.* HIV-1 persistence in CD4+ T cells with stem cell-like properties. *Nat. Med.* (2014) doi:10.1038/nm.3445.

235. Cartwright, E. K. *et al.* Divergent CD4 + T Memory Stem Cell Dynamics in Pathogenic and Nonpathogenic Simian Immunodeficiency Virus Infections . *J. Immunol.* **192**, 4666–4673 (2014).

236. Jaafoura, S. *et al.* Progressive contraction of the latent HIV reservoir around a core of less-differentiated CD4 + memory T cells. *Nat. Commun.* (2014) doi:10.1038/ncomms6407.

237. Harari, A., Vallelian, F. & Pantaleo, G. Phenotypic heterogeneity of antigen-specific CD4 T cells under different conditions of antigen persistence and antigen load. *Eur. J. Immunol.* 3525–3533 (2004) doi:10.1002/eji.200425324.

238. Henson, S. M., Riddell, N. E. & Akbar, A. N. Properties of end-stage human T cells defined by CD45RA re-expression. *Curr. Opin. Immunol.* **24**, 476–481 (2012).

239. Tian, Y. *et al.* Unique phenotypes and clonal expansions of human CD4 effector memory T cells re-expressing CD45RA. *Nat. Commun.* doi:10.1038/s41467-017-01728-5.

240. Pušnik, J. *et al.* Expansion of Stem Cell-Like CD4 + Memory T Cells during

Acute HIV-1 Infection Is Linked to Rapid Disease Progression . *J. Virol.* **93**, (2019).

241. Gálvez, C. *et al.* Atlas of the HIV-1 Reservoir in Peripheral CD4 T Cells of Individuals on Successful Antiretroviral Therapy. *MBio* **12**, 1–13 (2021).

242. Roche, M. *et al.* CXCR4-Using HIV Strains Predominate in Naive and Central Memory CD4 + T Cells in People Living with HIV on Antiretroviral Therapy: Implications for How Latency Is Established and Maintained . *J. Virol.* **94**, (2020).

243. Rullo, E. V., Cannon, L., Marilia Rita Pinzone Manuela Ceccarelli, G. N. & O'Doherty, U. Genetic Evidence That Naive T Cells Can Contribute Significantly to the Human Immunodeficiency Virus Intact Reservoir: Time to Re-evaluate Their Role. *Clin. Infect. Dis.* **69**, 2235–2236 (2019).

244. Zerbato, J. M., Mcmahon, D. K., Sobolewski, M. D., Mellors, J. W. & Sluis-cremer, N. Naive CD4 + T Cells Harbor a Large Inducible Reservoir of Latent , Replication-competent Human Immunodeficiency Virus Type 1. *Clin. Infect. Dis.* **69**, 1919–1925 (2019).

245. Soriano-Sarabia, N. *et al.* Quantitation of Replication-Competent HIV-1 in Populations of Resting CD4 + T Cells . *J. Virol.* **88**, 14070–14077 (2014).

246. Macallan, D. C. *et al.* Rapid turnover of effector-memory CD4+ T cells in healthy humans. *J. Exp. Med.* **200**, 255–260 (2004).

247. Horsburgh, B. A. *et al.* High levels of genetically-intact HIV in HLA-DR+ memory T-cells indicates their value for reservoir studies. *AIDS* **34**, 659–668 (2021).

248. Hermankova, M. *et al.* Analysis of Human Immunodeficiency Virus Type 1 Gene Expression in Latently Infected Resting CD4 + T Lymphocytes In Vivo . *J. Virol.* **77**, 7383–7392 (2003).

249. Telwatte, S. *et al.* Gut and blood differ in constitutive blocks to HIV transcription, suggesting tissue-specific differences in the mechanisms that govern HIV latency. *PLoS Pathog.* **14**, 1–28 (2018).

250. Yukl, S. A. *et al.* HIV latency in isolated patient CD4+ T cells may be due to blocks in HIV transcriptional elongation, completion, and splicing. *Physiol. Behav.* **176**, 139–148 (2017).

251. Lusic, M. & Giacca, M. Regulation of HIV-1 Latency by Chromatin Structure and Nuclear Architecture. *Journal of Molecular Biology* (2014) doi:10.1016/j.jmb.2014.07.022.

252. Van Damme, E., Laukens, K., Dang, T. H. & van Ostade, X. A manually curated network of the pml nuclear body interactome reveals an important role for PML-NBs in SUMOylation dynamics. *Int. J. Biol. Sci.* **6**, 51–67 (2010).

253. Bernardi, R. & Pandolfi, P. P. Structure, dynamics and functions of promyelocytic leukaemia nuclear bodies. *Nat. Rev. Mol. Cell Biol.* **8**, 1006–1016 (2007).

254. Everett, R. D. DNA viruses and viral proteins that interact with PML nuclear bodies. *Oncogene* **20**, 7266–7273 (2001).

255. Cohen, C. *et al.* Promyelocytic leukemia (PML) nuclear bodies (NBs) induce latent/quiescent HSV-1 genomes chromatinization through a PML NB/Histone H3.3/H3.3 Chaperone Axis. *PLoS Pathog.* **14**, e1007313 (2018).

256. Lusic, M. *et al.* Proximity to PML nuclear bodies regulates HIV-1 latency in CD4+ T cells. *Cell Host Microbe* **13**, 665–677 (2013).

257. Greger, I. H., Demarchi, F., Giacca, M. & Proudfoot, N. J. Transcriptional interference perturbs the binding of Sp1 to the HIV-1 promoter. *Nucleic Acids Res.* **26**, 1294–1300 (1998).

258. Lenasi, T., Contreras, X. & Peterlin, B. M. Transcriptional Interference

Antagonizes Proviral Gene Expression to Promote HIV Latency. *Cell Host Microbe* **4**, 123–133 (2008).

259. Lewinski, M. K. *et al.* Genome-Wide Analysis of Chromosomal Features Repressing Human Immunodeficiency Virus Transcription †. *J. Virol.* **79**, 6610–6619 (2005).

260. Tan, F. L. & Yin, J. Q. RNAi , a new therapeutic strategy against viral infection. *Cell Rev.* **14**, 460–466 (2004).

261. Bednarik, D. P. *et al.* DNA CpG methylation inhibits binding of NF-kappa B proteins to the HIV-1 long terminal repeat cognate DNA motifs. *New Biol.* **3**, 969—976 (1991).

262. Kauder, S. E., Bosque, A., Lindqvist, A., Planelles, V. & Verdin, E. Epigenetic regulation of HIV-1 latency by cytosine methylation. *PLoS Pathog.* **5**, (2009).

263. Blazkova, J. *et al.* Paucity of HIV DNA Methylation in Latently Infected, Resting CD4 + T Cells from Infected Individuals Receiving Antiretroviral Therapy . *J. Virol.* **86**, 5390–5392 (2012).

264. Imai, K., Togami, H. & Okamoto, T. Involvement of histone H3 lysine 9 (H3K9) methyltransferase G9a in the maintenance of HIV-1 latency and its reactivation by BIX01294. *J. Biol. Chem.* **285**, 16538–16545 (2010).

265. Chéné, I. Du *et al.* Suv39H1 and HP1γ are responsible for chromatin-mediated HIV-1 transcriptional silencing and post-integration latency. *EMBO J.* **26**, 424–435 (2007).

266. Pearson, R. *et al.* Epigenetic Silencing of Human Immunodeficiency Virus (HIV) Transcription by Formation of Restrictive Chromatin Structures at the Viral Long Terminal Repeat Drives the Progressive Entry of HIV into Latency. *J. Virol.* **82**, 12291–12303 (2008).

267. Verdin, E., Paras, P. & Van Lint, C. Chromatin disruption in the promoter of

human immunodeficiency virus type 1 during transcriptional activation. *EMBO J.* **12**, 3249–3259 (1993).

268. Van Lint, C., Emiliani, S., Ott, M. & Verdin, E. Transcriptional activation and chromatin remodeling of the HIV-I promoter in response to histone acetylation. *Chemtracts* **10**, 773–778 (1997).

269. Steger, D. J., Eberharter, A., John, S., Grant, P. A. & Workman, J. L. Purified histone acetyltransferase complexes stimulate HIV-1 transcription from preassembled nucleosomal arrays. *Proc. Natl. Acad. Sci. U. S. A.* **95**, 12924–12929 (1998).

270. Roth, S., Denu, J. & ALlis, C. D. Histone acetyltransferases. *Annu. Rev. Biochem* 81–120 (2001).

271. Marzio, G., Tyagi, M., Gutierrez, M. I. & Giacca, M. HIV-1 Tat transactivator recruits p300 and CREB-binding protein histone acetyltransferases to the viral promoter. *Proc. Natl. Acad. Sci. U. S. A.* **95**, 13519–13524 (1998).

272. Hottiger, M. O. & Nabel, G. J. Interaction of Human Immunodeficiency Virus Type 1 Tat with the Transcriptional Coactivators p300 and CREB Binding Protein. *J. Virol.* **72**, 8252–8256 (1998).

273. Benkirane, M. *et al.* Activation of integrated provirus requires histone acetyltransferase: p300 and P/CAF are coactivators for HIV-1 Tat. *J. Biol. Chem.* **273**, 24898–24905 (1998).

274. Lusic, M., Marcello, A., Cereseto, A. & Giacca, M. Regulation of HIV-1 gene expression by histone acetylation and factor recruitment at the LTR promoter. *EMBO J.* (2003) doi:10.1093/emboj/cdg631.

275. Williams, S. A. *et al.* NF-κB p50 promotes HIV latency through HDAC recruitment and repression of transcriptional initiation. *EMBO J.* **25**, 139–149 (2006).

276. Coull, J. J. *et al.* The Human Factors YY1 and LSF Repress the Human Immunodeficiency Virus Type 1 Long Terminal Repeat via Recruitment of Histone Deacetylase 1. *J. Virol.* **74**, 6790–6799 (2000).

277. Archin, N. M. *et al.* Administration of vorinostat disrupts HIV-1 latency in patients on antiretroviral therapy. *Nature* **487**, 482–485 (2012).

278. Rasmussen, T. A. *et al.* Panobinostat, a histone deacetylase inhibitor, for latent virus reactivation in HIV-infected patients on suppressive antiretroviral therapy: A phase 1/2, single group, clinical trial. *Lancet HIV* **1**, e13–e21 (2014).

279. Søgaard, O. S. *et al.* The Depsipeptide Romidepsin Reverses HIV-1 Latency In Vivo. *PLoS Pathog.* **11**, 1–22 (2015).

280. Pardons, M., Fromentin, R., Pagliuzza, A., Routy, J. P. & Chomont, N. Latency-Reversing Agents Induce Differential Responses in Distinct Memory CD4 T Cell Subsets in Individuals on Antiretroviral Therapy. *Cell Rep.* **29**, 2783-2795.e5 (2019).

281. Bullen, C. K., Laird, G. M., Durand, C. M., Siliciano, J. D. & Siliciano, R. F. New ex vivo approaches distinguish effective and ineffective single agents for reversing HIV-1 latency in vivo. *Nat. Med.* **20**, 425–429 (2014).

282. Korin, Y. D., Brooks, D. G., Brown, S., Korotzer, A. & Zack, J. A. Effects of Prostratin on T-Cell Activation and Human Immunodeficiency Virus Latency. *J. Virol.* **76**, 8118–8123 (2002).

283. Pache, L. *et al.* BIRC2/cIAP1 is a Negative Regulator of HIV-1 Transcription and Can Be Targeted by Smac Mimetics to Promote Reversal of Viral Latency. *Cell Host Microbe* **18**, 345–353 (2015).

284. Pache, L. *et al.* Pharmacological Activation of Non-canonical NF-κB Signaling Activates Latent HIV-1 Reservoirs In Vivo. *Cell Reports Med.* **1**, (2020).

285. Nixon, C. C. *et al.* Systemic HIV and SIV latency reversal via non-canonical

NF-κB signalling in vivo. *Nature* **578**, 160–165 (2020).

286. Tyagi, M., Pearson, R. J. & Karn, J. Establishment of HIV Latency in Primary CD4 + Cells Is due to Epigenetic Transcriptional Silencing and P-TEFb Restriction . *J. Virol.* **84**, 6425–6437 (2010).

287. Mousseau, G. *et al.* The tat inhibitor didehydro-cortistatin a prevents HIV-1 reactivation from latency. *MBio* **6**, (2015).

288. Banerjee, C. *et al.* BET bromodomain inhibition as a novel strategy for reactivation of HIV-1. *J. Leukoc. Biol.* **92**, 1147–1154 (2012).

289. Watson, D. C. *et al.* Treatment with native heterodimeric IL-15 increases cytotoxic lymphocytes and reduces SHIV RNA in lymph nodes. *PLoS Pathog.* **14**, 1–24 (2018).

290. Han, K. ping *et al.* IL-15:IL-15 receptor alpha superagonist complex: High-level co-expression in recombinant mammalian cells, purification and characterization. *Cytokine* **56**, 804–810 (2011).

291. Miller, J. S. *et al.* Safety and virologic impact of the IL-15 superagonist N-803 in people living with HIV: a phase 1 trial. *Nat. Med.* **28**, 392–400 (2022).

292. Kulpa, D. A. *et al.* Differentiation into an Effector Memory Phenotype Potentiates HIV-1 Latency Reversal in CD4+ T Cells. *J. Virol.* **93**, 1–23 (2019).

293. Sarabia, I., Huang, S.-H., Ward, A. R., Jones, R. B. & Bosque, A. The Intact Noninducible Latent HIV-1 Reservoir Is Established in an In Vitro Primary T CM Cell Model of Latency . *J. Virol.* **95**, 1–16 (2021).

294. Buck, M. D., O'Sullivan, D. & Pearce, E. L. T cell metabolism drives immunity. *J. Exp. Med.* **212**, 1345–1360 (2015).

295. Valle-Casuso, J. C. *et al.* Cellular Metabolism Is a Major Determinant of HIV-1 Reservoir Seeding in CD4 + T Cells and Offers an Opportunity to Tackle

Infection. *Cell Metab.* (2019) doi:10.1016/j.cmet.2018.11.015.

296. Shytaj, I. L. *et al.* Glycolysis downregulation is a hallmark of HIV-1 latency and sensitizes infected cells to oxidative stress. *EMBO Mol. Med.* **13**, 1–20 (2021).

297. Dahabieh, M. S., Ooms, M., Simon, V. & Sadowski, I. A Doubly Fluorescent HIV-1 Reporter Shows that the Majority of Integrated HIV-1 Is Latent Shortly after Infection. *J. Virol.* **87**, 4716–4727 (2013).

298. Calvanese, V., Chavez, L., Laurent, T., Ding, S. & Verdin, E. Dual-color HIV reporters trace a population of latently infected cells and enable their purification. *Virology* **446**, 283–292 (2013).

299. Battivelli, E. & Verdin, E. HIV-GKO: A Tool to Assess HIV-1 Latency Reversal Agents in Human Primary CD4+ T Cells. *Bio-Protocol* **8**, 1–14 (2018).

300. Kim, E. H. *et al.* Development of an HIV reporter virus that identifies latently infected CD4+ T cells. *Cell Reports Methods* **2**, 100238 (2022).

301. Salamango, D. J., Evans, D. A., Baluyot, M. F., Furlong, J. N. & Johnson, M. C. Recombination Can Lead to Spurious Results in Retroviral Transduction with Dually Fluorescent Reporter Genes. *J. Virol.* **87**, 13900–13903 (2013).

302. Battivelli, E. *et al.* Distinct chromatin functional states correlate with HIV latency reactivation in infected primary CD4+ T cells. *Elife* **7**, 1–22 (2018).

303. Kwon, K. J. *et al.* Different human resting memory CD4+ T cell subsets show similar low inducibility of latent HIV-1 proviruses. *Sci. Transl. Med.* **12**, 1–14 (2020).

304. Young, G. R. *et al.* HIV-1 Infection of Primary CD4+ T Cells Regulates the Expression of Specific Human Endogenous Retrovirus HERV-K (HML-2) Elements. *J. Virol.* **92**, 1–13 (2018).

305. Gao, F. *et al.* Molecular cloning and analysis of functional envelope genes from human immunodeficiency virus type 1 sequence subtypes A through G. The WHO and NIAID Networks for HIV Isolation and Characterization. *J. Virol.* **70**, 1651–1667 (1996).

306. Wain-hobson, A. S. *et al.* LAV Revisited : Origins of the Early HIV-1 Isolates from Institut Pasteur. 961–965 (1991).

307. Kim, Y., Cameron, P. U., Lewin, S. R. & Anderson, J. L. Limitations of dual-fluorescent HIV reporter viruses in a model of pre-activation latency. *J. Int. AIDS Soc.* **22**, 1–9 (2019).

308. Eberly, M. D. *et al.* Increased IL-15 Production Is Associated with Higher Susceptibility of Memory CD4 T Cells to Simian Immunodeficiency Virus during Acute Infection. *J. Immunol.* (2009) doi:10.4049/jimmunol.182.3.1439.

309. Fujinaga, K. *et al.* The Ability of Positive Transcription Elongation Factor b To Transactivate Human Immunodeficiency Virus Transcription Depends on a Functional Kinase Domain, Cyclin T1, and Tat. *J. Virol.* (1998) doi:10.1128/jvi.72.9.7154-7159.1998.

310. Rochman, Y., Spolski, R. & Leonard, W. J. New insights into the regulation of T cells by γc family cytokines. *Nat. Publ. Gr.* **9**, 480–490 (2009).

311. Amyes, E. *et al.* Six Phenotypically and Functionally Distinct Subsets. *J. Immunol.* (2022) doi:10.4049/jimmunol.175.9.5765.

312. Amir, E. A. D. *et al.* ViSNE enables visualization of high dimensional single-cell data and reveals phenotypic heterogeneity of leukemia. *Nat. Biotechnol.* (2013) doi:10.1038/nbt.2594.

313. Geginat, J., Sallusto, F. & Lanzavecchia, A. Cytokine-driven proliferation and differentiation of human naïve, central memory and effector memory CD4+ T cells. in *Journal of Experimental Medicine* (2001). doi:10.1016/S0369-

8114(03)00098-1.

314. Pierson, T. *et al.* Characterization of Chemokine Receptor Utilization of Viruses in the Latent Reservoir for Human Immunodeficiency Virus Type 1. *J. Virol.* **74**, 7824–7833 (2000).

315. Zhu, T. *et al.* Genotypic and phenotypic characterization of HIV-1 patients with primary infection. *Science* **261**, 1179–81 (1993).

316. Ramakrishnan, R., Dow, E. C. & Rice, A. P. Characterization of Cdk9 T-loop phosphorylation in resting and activated CD4 + T lymphocytes . *J. Leukoc. Biol.* **86**, 1345–1350 (2009).

317. Chiang, K., Sung, T.-L. & Rice, A. P. Regulation of Cyclin T1 and HIV-1 Replication by MicroRNAs in Resting CD4 + T Lymphocytes . *J. Virol.* **86**, 3244–3252 (2012).

318. Liou, L.-Y., Herrmann, C. H. & Rice, A. P. Transient Induction of Cyclin T1 during Human Macrophage Differentiation Regulates Human Immunodeficiency Virus Type 1 Tat Transactivation Function. *J. Virol.* **76**, 10579–10587 (2002).

319. Hoque, M., Shamanna, R. A., Guan, D., Pe'ery, T. & Mathews, M. B. HIV-1 replication and latency are regulated by translational control of cyclin T1. *J. Mol. Biol.* **410**, 917–932 (2011).

320. Chen, R., Yang, Z. & Zhou, Q. Phosphorylated Positive Transcription Elongation Factor b (P-TEFb) Is Tagged for Inhibition through Association with 7SK snRNA. *J. Biol. Chem.* (2004) doi:10.1074/jbc.M310044200.

321. Grau-Expósito, J. *et al.* Latency reversal agents affect differently the latent reservoir present in distinct CD4+ t subpopulations. *PLoS Pathog.* **15**, 1–23 (2019).

322. Pauls, E. *et al.* Cell Cycle Control and HIV-1 Susceptibility Are Linked by

CDK6-Dependent CDK2 Phosphorylation of SAMHD1 in Myeloid and Lymphoid Cells. *J. Immunol.* **193**, 1988–1997 (2014).

323. Fontenot, J. D., Rasmussen, J. P., Gavin, M. A. & Rudensky, A. Y. A function for interleukin 2 in Foxp3-expressing regulatory T cells. *Nat. Immunol.* **6**, 1142–1151 (2005).

324. Waldmann, T. A. The biology of interleukin-2 and interleukin-15: Implications for cancer therapy and vaccine design. *Nat. Rev. Immunol.* **6**, 595–601 (2006).

325. Wonderlich, E. R. *et al.* Effector memory differentiation increases detection of replication-competent HIV-l in resting CD4+ T cells from virally suppressed individuals. *PLoS Pathog.* **15**, (2019).

326. Rullo, E. V. *et al.* Persistence of an intact HIV reservoir in phenotypically naive T cells. *JCI Insight* **5**, 1–15 (2020).

327. Mavigner, M. *et al.* Simian Immunodeficiency Virus Persistence in Cellular and Anatomic Reservoirs in Antiretroviral Therapy-Suppressed Infant Rhesus Macaques. *J. Virol.* **93**, 1–18 (2019).

328. Obregon-Perko, V. *et al.* Simian-Human Immunodeficiency Virus SHIV.C.CH505 Persistence in ART-Suppressed Infant Macaques Is Characterized by Elevated SHIV RNA in the Gut and a High Abundance of Intact SHIV DNA in Naive CD4+ T Cells. *J. Virol.* **95**, (2020).

329. Klatt, N. R. *et al.* Limited HIV Infection of Central Memory and Stem Cell Memory CD4+ T Cells Is Associated with Lack of Progression in Viremic Individuals. *PLoS Pathog.* **10**, (2014).

330. Couturier, J. *et al.* Regulation of cyclin T1 during HIV replication and latency establishment in human memory CD4 T cells. *Virol. J.* (2019) doi:10.1186/s12985-019-1128-6.

331. Sabò, A., Lusic, M., Cereseto, A. & Giacca, M. Acetylation of Conserved Lysines in the Catalytic Core of Cyclin-Dependent Kinase 9 Inhibits Kinase Activity and Regulates Transcription. *Mol. Cell. Biol.* (2008) doi:10.1128/mcb.01557-07.

332. Fu, J., Yoon, H.-G., Qin, J. & Wong, J. Regulation of P-TEFb Elongation Complex Activity by CDK9 Acetylation. *Mol. Cell. Biol.* (2007) doi:10.1128/mcb.00857-06.

333. Kang, S., Tran, A., Grilli, M. & Lenardot, M. J. NF-KB Subunit Regulation in Nontransformed CD4 T Lymphocytes. *Science (80-.).* **256**, 1452–1456 (1991).

334. Ito, C. Y., Kazantsev, A. G. & Baldwin, A. S. Three NF-χB sites in the IχB-α promoter are required for induction of gene expression by TNFα. *Nucleic Acids Res.* **22**, 3787–3792 (1994).

335. Dutilleul, A., Rodari, A. & Van Lint, C. Depicting hiv-1 transcriptional mechanisms: A summary of what we know. *Viruses* **12**, 1–19 (2020).

336. Hermann-Kleiter, N. & Baier, G. NFAT pulls the strings during CD4+ T helper cell effector functions. *Blood* (2010) doi:10.1182/blood-2009-10-233585.

337. Lusic, M. & Giacca, M. Regulation of HIV-1 Latency by Chromatin Structure and Nuclear Architecture. *J. Mol. Biol.* **427**, 688–694 (2015).

338. Karn, J. & Mbonye, U. Control of HIV Latency by Epigenetic and Non-Epigenetic Mechanisms. *Curr. HIV Res.* (2011) doi:10.2174/157016211798998736.

339. Rawlings, J. S., Gatzka, M., Thomas, P. G. & Ihle, J. N. Chromatin condensation via the condensin II complex is required for peripheral T-cell quiescence. *EMBO J.* (2011) doi:10.1038/emboj.2010.314.

340. Crompton, J. G. *et al.* Lineage relationship of CD8+ T cell subsets is revealed by progressive changes in the epigenetic landscape. *Cell. Mol. Immunol.* (2016)

doi:10.1038/cmi.2015.32.

341. Aid, M. *et al.* Follicular CD4 T helper cells as a major HIV reservoir compartment: A molecular perspective. *Front. Immunol.* (2018) doi:10.3389/fimmu.2018.00895.

342. Paiardini, M. & Lichterfeld, M. Follicular T helper cells: Hotspots for HIV-1 persistence. *Nature Medicine* (2016) doi:10.1038/nm.4138.

343. Banga, R. *et al.* PD-1+ and follicular helper T cells are responsible for persistent HIV-1 transcription in treated aviremic individuals. *Nat. Med.* **22**, 754–761 (2016).

344. Perreau, M. *et al.* Follicular helper T cells serve as the major CD4 T cell compartment for HIV-1 infection, replication, and production. *J. Exp. Med.* **210**, 143–156 (2013).

345. Chun, T. *et al.* Persistence of HIV in Gut-Associated Lymphoid Tissue despite Long-Term Antiretroviral Therapy. **197**, (2008).

346. Evans, V. A. *et al.* Myeloid Dendritic Cells Induce HIV-1 Latency in Non-proliferating CD4+ T Cells. *PLoS Pathog.* **9**, 1–14 (2013).